EMULSION FORMATION MECHANISM FOR STEAM & SOLVENT-STEAM PROCESSES FOR BITUMEN RECOVERY

A Dissertation

by

TANIYA KAR

Submitted to the Office of Graduate and Professional Studies of
Texas A&M University
in partial fulfillment of the requirements for the degree of

DOCTOR OF PHILOSOPHY

Chair of Committee,	Berna Hascakir
Committee Members,	Walter Ayers
	Hadi Nasrabadi
	Yuefeng Sun
Head of Department,	A. Daniel Hill

August 2017

Major Subject: Petroleum Engineering

ABSTRACT

Hydrocarbon solvents are known to improve the overall oil recovery from oil sands when co-injected with steam, compared to steam injection alone in thermal enhanced oil recovery. However, the quality of the recovered oil is crucial in terms of water-oil emulsion complexity, especially due to the presence of significant asphaltene content in bitumen and water from steam processes. In addition, the type, chemical nature, and asphaltene solubility power of the hydrocarbon solvent injected, along with the reservoir clays, can either enhance or destabilize these emulsions. Moreover, crude oil itself has non-polar and polar fractions apart from asphaltenes, which have their own associations with these solvents, water, and reservoir clays. Emulsion formation is an interface phenomenon, and thus, the interactions between individual components in the obtained oil phase must be analyzed to understand it. In this study, steam and solvent-steam flooding, SAGD and Solvent-SAGD experiments were performed, and the obtained oils from these experiments were studied in terms of emulsion characterization, produced oil composition. Several correlations were inferred, depicting the interactions among these components.

Based on experimental results, the addition of either paraffinic or aromatic solvents improves the quality of produced oil, compared to steam injection alone, by lowering the amount of water carried with the oil. Kaolinite clay has a greater affinity towards water-phase compared to oil-phase. Mixtures of kaolinite and illite, on the other hand, interact more with the oil phase, along with water, thereby stabilizing emulsions via deposition at the interface. Lastly, presence of the aromatic solvent, toluene, generally lowers the

quality of the obtained oil by increasing the polarity and dispersion of asphaltenes in crude oil, consequently promoting water-oil and clay-oil associations.

DEDICATION

This dissertation is dedicated to my parents, Amar Kanti Kar and Tinku Kar. It is their unconditional love and care for me that has helped me overcome everything in life thus far, and I love and look up to them the most.

ACKNOWLEDGEMENTS

To begin with, I would like to thank my advisor, Dr. Berna Hascakir, for guiding and helping me in my research throughout my time here in this department, and always encouraging me to persevere and work harder to reach my goals.

I would like to thank my committee members, Professor Walter Ayers, Professor Hadi Nasrabadi, and Professor Yuefeng Sun, for their guidance and support throughout the course of this research.

I owe my heartfelt gratitude to all the members of the Heavy Oil, Oil shales, Oil sands, and Carbonate Analysis and Recovery Methods (HOCAM) research group for their help and support in my research. I would particularly like to thank Pedram Nezhad, Alwin Ng, Philipos Melake, and Abrar Al-Shaikh for helping me with measurements in the laboratory.

I sincerely thank my friends, colleagues, the department faculty, and staff of Petroleum Engineering for making my time at Texas A&M University a great experience.

Last, but not the least, I thank my family and friends for always supporting, loving, and inspiring me.

CONTRIBUTORS AND FUNDING SOURCES

Contributors

This work was supervised by a dissertation committee consisting of Professor Berna Hascakir, Professor Walter Ayers, and Professor Hadi Nasrabadi of the Department of Petroleum Engineering and Professor Yuefeng Sun of the Department of Geology and Geophysics.

All work conducted for the dissertation was completed by the student, independently.

Funding Sources

Graduate study was supported by a fellowship from Texas A&M University and a dissertation research fellowship from Dr. Berna Hascakir's research fund.

This work was made possible in part by Chevron Energy Technology Company.

NOMENCLATURE

AOSTRA	Alberta Oil Sands technology and Research Authority
API	American Petroleum Institute
Asp	Asphaltenes
ASTM	American Society for Testing and Materials
C3	propane
C5+	pentane plus
Clay1	kaolinite
Clay2	Mixture of kaolinite and illite
cP	centipoise
cSOR	cumulative Steam Oil Ratio
CSS	Cyclic Steam Stimulation
CWE	Cold Water Equivalent
DAO	Deasphalted Oil
E	Pore-Scale Displacement Efficiency
EOR	Enhanced Oil Recovery
ES-SAGD	Expanding-Solvent Steam-Assisted Gravity Drainage
FTIR	Fourier Transform Infrared Spectroscopy
GHG	Greenhouse Gas
ICP-MS	Inductively coupled plasma- mass spectrometry
IEA	International Energy Agency

MMP	Minimum Miscibility Pressure
nC4	n-butane
nC5	n-pentane
nC6	n-hexane
nC7	n-heptane
P-SAGD	Propane- Steam Assisted Gravity Drainage
P-SF	Propane- Steam Flooding
S-SAGD	Solvent- Steam Assisted Gravity Drainage
SAGD	Steam Assisted Gravity Drainage
SAGP	Steam and Gas Push
Soi	Initial oil saturation
Sor	Residual oil saturation
TGA-DTA	Thermogravimetric Analysis- Differential Thermal Analysis
TOT	Tetrahedron-Octahedron-Tetrahedron
vol%	volume percent
wt%	weight percent
XAS	X-ray Absorption Spectroscopy
XPS	X-ray Photoelectron Spectroscopy
XRD	X-ray Diffraction
1D	1 dimensional
2D	2 dimensional

TABLE OF CONTENTS

Page

LIST OF FIGURES

Page

LIST OF TABLES

Page

1. INTRODUCTION

As the world's demand for energy continues to rise and production from conventional oil reserves decreases, focus has increasingly shifted toward recovery from the huge unconventional petroleum reserves around the world. Heavy oil and bitumen are the significant alternative (unconventional) sources that are characterized by high density and viscosity. Oil sands are defined as unconsolidated sands that contain bitumen. Fig. 1.1 and 1.2 highlight the distribution of heavy oil and bitumen, respectively, around the world. South America and Middle East constitute 62% of the world's heavy oil, while natural bitumen is abundant (85%) in North and South America, specifically in Canada and Venezuela.

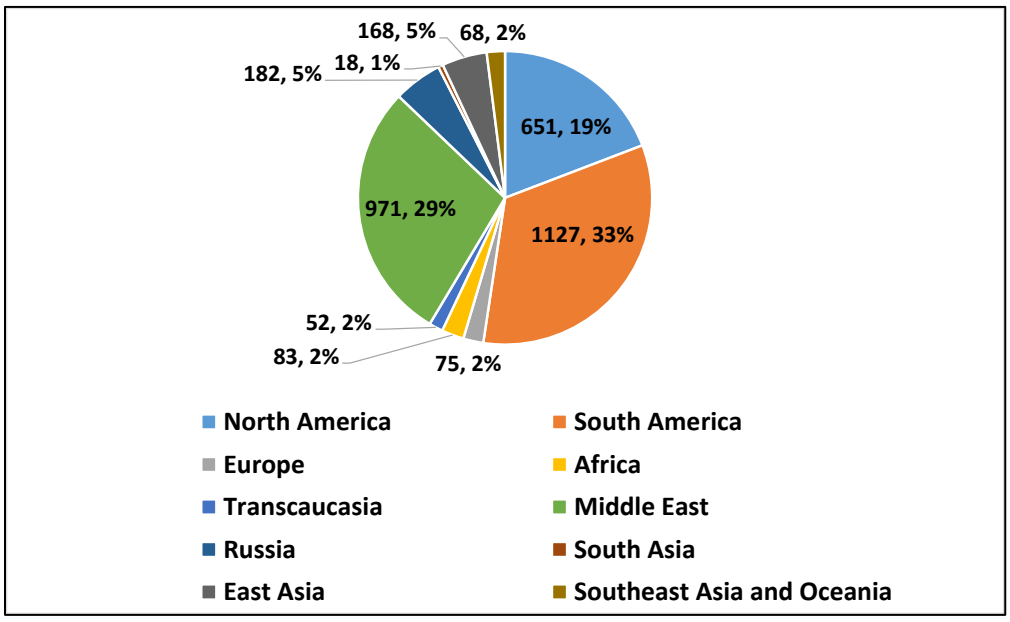

Fig. 1.1 - Geographic world distribution of heavy oil
(Reprinted from Meyer et al. 2007)

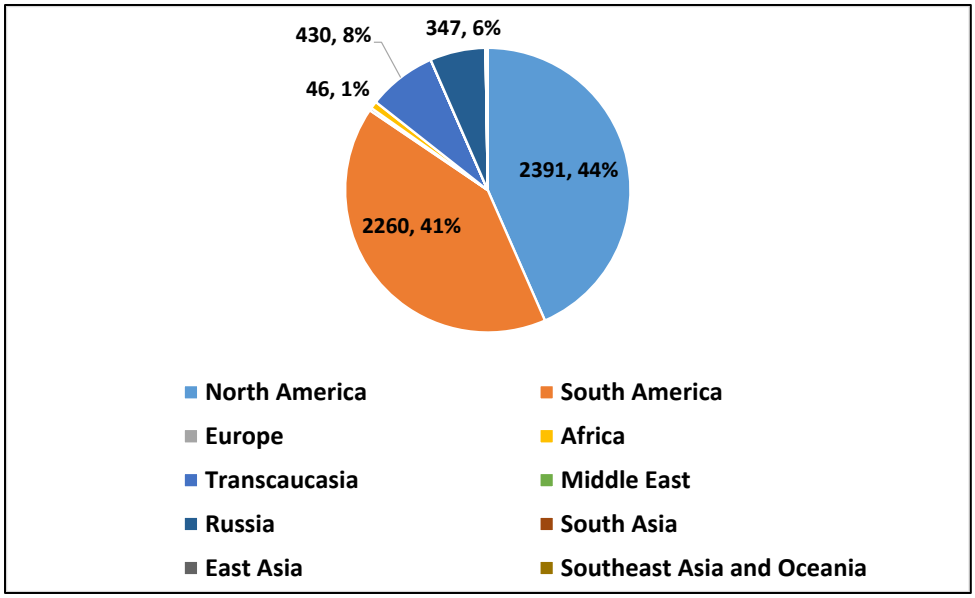

Fig. 1.2 - Geographic world distribution of bitumen
(Reprinted from Meyer et al. 2007)

Oil can be classified as conventional light oil (> 25 °API), medium oil (20 < °API < 25), heavy oil (10 < °API <= 20; viscosity > 100 cP), or natural bitumen (< 10 °API; viscosity > 10000 cP). Bitumen is termed as extra-heavy oil when it is in a moving state in the reservoir (Meyer et al. 2007). Low API gravity oils are untapped not only due to their high viscosity and low API gravity, but also because of their high hydrocarbon content. The heavy oil fractions of these types of hydrocarbons, namely resins and asphaltenes, are the fractions of crude oil with high metal (copper, nickel, vanadium) and non-metal (sulfur, nitrogen, oxygen) content (Meyer et al. 2007; Yen 1984).

The unfavorable physical and chemical properties of these vast resources allow only up to 30 to 40 percent of recovery through primary and secondary techniques. Thus, application of enhanced recovery techniques is essential. As defined by Saxman (1985), Enhanced Oil Recovery (EOR) refers to “Oilfield techniques that produce oil from mature

reservoirs, increase recovery beyond that obtainable using conventional techniques, or tap highly viscous or especially dense reservoirs." Some common EOR methods include gas injection (miscible or immiscible with reservoir hydrocarbons - carbon dioxide, nitrogen, gaseous hydrocarbons, flue gas), chemical flooding (polymers, surfactants, alkali), and thermal recovery (steam flooding, cyclic steam stimulation, in-situ combustion, steam-assisted gravity drainage) (Prats 1982; Green and Willhite 1998).

Due to the effective exponential reduction of bitumen viscosity with increase in temperature, thermal recovery via steam injection has proved to be successful in significant bitumen recovery (Prats 1982; Kovscek 2012). Steam injection processes usually favor reservoirs with depths lesser than 4500 ft, as there are chances of heat loss to the wellbore for reservoirs with greater depth, thereby converting the steam injection process to a hot water flood (Meyer et al 2007). Also, at certain depths, steam cannot be generated, due to high pressure of reservoirs it can be supercritical steam. According to the reservoir threshold criteria for application of thermal EOR techniques for heavy oil recovery (Taber, Martin and Seright, 1997 a,b), steam is favorable for heavy oil higher than 8 °API gravity, less than 200,000 cP viscosity, oil saturation higher than 40% pore volume, and net thickness higher than 20 ft. Steam injection is mostly applied to sandstone reservoirs, owing to tendency of heat loss in fractures for carbonate reservoirs. The commonly used thermal EOR techniques to recover heavy oil and bitumen from sandstone reservoirs include Cyclic Steam Stimulation (CSS), steam flooding, and Steam-Assisted Gravity Drainage (SAGD) (Alvarado and Manrique, 2010).

SAGD is a relatively new thermal EOR method involving two horizontal wells drilled at the base of the reservoir (Butler 1981; Butler 1982), injection of steam through the top well leading to the development of a steam chamber, and the effect of gravity to drain the mobilized oil and condensed steam down along the boundary of the steam chamber into the production wells. In spite of reports of pilot SAGD tests in U.S (Grills et al., 2002), Venezuela (Mendoza et al., 1999), and China (Li-qiang et al., 2006), SAGD has been commercially carried out only in Athabasca, Canada (Putnam and Christensen, 2004; Jimenez 2008). Hence, SAGD is a developing thermal EOR technique, with great future potential.

The three largest oil sand deposits in the world are Athabasca, Cold Lake, and Peace River; all are located in Canada. Steam recovery projects in Peace River date from 1979, when in-situ projects were initiated by Shell Canada Ltd. Later, Shell began SAGD projects in Peace River along with cyclic steam stimulation (Hamm and Ong, 1995). In the Athabasca region, Petro-Canada and Suncor have been active in developing oil sand projects and SAGD technology to recover oil from the vast bitumen reserves (Mattison et al, 2001).

Apart from the effective recovery, steam injection processes also include significant shortcomings, including the large amounts of fresh water and natural gas required for steam generation, steam quality produced by commercial steam generators, excessive greenhouse gases emissions, extensive treatment of produced water in downstream facilities, and surface footprint (Nasr et al 1991; Mukhametshina and Hascakir, 2014). To minimize these drawbacks, modified steam injection processes using

various additives of solvents (Rivero and Mamora, 2007), chemicals (Ovalles et al, 2001), foams (Mendez et al. 1992), or gases (Bagci and Gumrah, 2004) have been developed to improve the energy efficiency of the process and to further mobilize the oil via dilution (Zhu et al. 2016). Some solvent-steam co-injection processes tested at the pilot scale include Solvent-Aided Process (SAP), Liquid Addition to Steam for Enhancing Recovery (LASER) involving injection of pentane plus (C5+) hydrocarbons with steam in CSS tested in Cold Lake (Leaute 2002), and ES-SAGD (Expanding Solvent-SAGD) (Elliot and Kovscek, 2001; Stalder 2008). However, few of these pilot projects have been field tested (Alvarado and Manrique, 2010; Zhdanov et al 1996; Mbaba and Caballero, 1983).

Table A-1 (Appendix A) lists some of the steam and miscible gas (gaseous hydrocarbon) recovery projects in Alberta (Canada) as documented by Saxman 1985, along with API gravity of fields with heavy oil and bitumen deposits.

Although the hydrocarbon solvent additives proposed in steam injection processes improve oil recovery over conventional steam injection, detailed studies about the selection of solvent type for a reservoir, oil type are not available in literature. The phase of hydrocarbon solvent in reservoir conditions is an important consideration. It is known that these hydrocarbon solvents help mobilization of oil by reducing the interfacial tension; however, the effect of liquid and vapor phases of water on these interfacial forces are likely to depend on the phase and type of solvent. These interactions can be further influenced by the polar, heavy molecular weight fractions of crude oil, resins and asphaltenes (Zhao et al. 2009). Asphaltenes are known to be soluble in aromatic solvents but insoluble in paraffinic solvents (Speight 2014). Additionally, the asphaltene

solubilizing power of paraffinic solvents is known to increase with increasing carbon number (Mullins 2008; Shkalikov et al., 2010). This consideration is significant for oil sands since bitumen contains a high weight percent of asphaltenes in its composition (Meyer et al. 2007). More importantly, the quality of the obtained oil from steam and solvent-steam processes based on water-oil emulsion complexity is significant to determine the optimum solvent-steam combination for bitumen recovery.

Focus of this study was investigation of the emulsion formation mechanism for steam flooding, SAGD, solvent-steam flooding, and solvent-SAGD processes applied for the extraction of two bitumen samples from Alberta, Canada. In the first chapter, the emulsion quality of the obtained oil from steam and propane-steam flooding and SAGD experiments was analyzed on a general basis. The second chapter reports steam and solvent-steam flooding experiments conducted to generate water-oil emulsions. The solvents were selected on the basis of their phase at experimental conditions, chemical nature, and dissolving power of asphaltenes. Three sets of these experiments were performed, involving no clays, Clay1 consisting of kaolinite, and Clay2 consisting of a mixture of kaolinite and illite in the packing. Finally, in the last chapter we report results of in depth study of the generated emulsions, focusing on the mutual interactions between the crude oil fractions, water and clays. The affinities of clays towards water and oil phases were investigated. The impact of hydrocarbon solvent on oil quality and the effect of polarity and dispersion of asphaltenes on emulsion complexity were analyzed, also

2. EFFICIENCY OF SOLVENT-SAGD RELATIVE TO SAGD*

2.1 Overview

Solvent-Steam Assisted Gravity Drainage (S-SAGD) processes for bitumen extraction are proposed to reduce the environmental impact of steam injection. S-SAGD processes require more research due to the unknowns of solvent-bitumen interaction and the desire to reduce the cost of steam and solvent utilized. This study investigates propane-SAGD (P-SAGD) and propane-steam flooding (P-SF) performance for the recovery of an Alberta, Canada, bitumen with 9.6 API gravity, 290,500 cP viscosity (at 25 °C), and 21.7 wt% asphaltenes (n-pentane insoluble) content. Three two-dimensional SAGD experiments (one SAGD and two P-SAGD at two different propane doses) and three one-dimensional flooding experiments (propane, steam, and propane-steam) were conducted. By comparing 2D experiments with 1D, we were able to analyze the effect of continuous steam flow and steam chamber development on process performance in microscopic scale. Water and asphaltenes contents of produced oil were measured. The steam chamber development with propane co-injection enhanced the oil production; however, it led to delay in oil production compared to the steam flooding case. Thus, we also tested first steam injection until achieving communication between the injector and producer in SAGD configuration and then, switching to steam-propane co-injection. After allowing the steam-bitumen interaction first, propane injection did not result in severe water-in-oil emulsion formation. Moreover, lesser permeability reduction due to asphaltenes deposition was observed. The application of propane-SAGD as a follow up to SAGD

---

improved the process by the mobilization of trapped residual oil and enhanced the quality of produced oil by minimizing the formation of water-in-oil emulsions.

2.2 Introduction

Bitumen is one of the most abundant unconventional oil resources. The bulk production from global heavy oil and bitumen resources has been predicted to rise to approximately thrice as much in 2035, compared to 2010 (IEA, 2013). The challenge with extraction of bitumen is its extremely high viscosity (greater than 10000 cP), due to which, introduction of heat via steam has proved to be the most effective enhanced oil recovery (EOR) method (Speight, 1991). The common steam injection processes to mobilize the bitumen by greatly reducing its viscosity are cyclic steam stimulation (CSS) and steam-assisted gravity drainage (SAGD), with SAGD giving the highest recovery factor (50-70%) (IEA, 2013). SAGD was introduced by Dr. Roger Butler and his colleagues in 1979 (Butler et al., 1981; Butler, 1982). The process was tested at the Underground Test Facility Phase-A, beginning in 1987 by the Alberta Oil Sands Technology and Research Authority (AOSTRA) (O'Rourke et al., 1994).

In SAGD, steam is injected through the injector well, near the base of the reservoir. This allows the steam front to move upwards, forming a steam chamber and contacting much of the reservoir, warming and mobilizing the bitumen. While transfer of latent heat of condensation from steam to oil at the edge of the steam chamber boundary mobilizes the bitumen, gravity drains the mobilized oil and condensed steam down to the producer well(s) (Butler, 1998; Mukhametshina and Hascakir, 2014). The steam chamber growth in SAGD can be divided into Ceiling Drainage and Slope Drainage. Ceiling drainage

refers to the mobilization of bitumen from above the steam chamber and its flow down to the producer well, obstructed by the rising steam. Slope drainage refers to the bitumen and condensed steam flowing along the steam chamber boundary, owing to the heat conduction from the steam chamber (Edmunds, 2000; Sharma and Gates, 2011). SAGD has lower tendencies of coning and channeling issues since it is a low pressure process, mainly governed by growth of steam chamber influenced by gravity (Dusseault 2001). The process also helps to improve reservoir porosity and permeability due to dilation caused by thermally induced shearing (IEA, 2013). Thermal expansion creates a tensile stress on adjacent shale layers, thereby inducing vertical fractures (Dusseault 2001). However, SAGD entails significant drawbacks, owing to the huge amount of fresh water and natural gas required for steam generation, excessive greenhouse gas (GHG) emissions, and in the downstream facilities, extensive treatment of produced water and processing of produced oil (Mukhametshina et al., 2016).

To overcome these shortcomings, modified steam injection processes using hydrocarbon solvents have been developed (Ali and Abad, 1976) to improve the energy efficiency of the process and to aid in mobilizing the oil via chemical dissolution. Steam and Gas Push (SAGP) introduced by Butler (Butler, 1999; Jiang et al., 1998; Coelho et al., 2017) involves injection of a non-condensable gas with steam, allowing the gas to occupy the top of the steam chamber, thereby minimizing heat losses to the overburden and maintaining the steam temperature inside the chamber. In Expanding-Solvent SAGD (ES-SAGD), the hydrocarbon solvents travel with steam through the vapor chamber and condense with steam at the boundary, facilitating heat and mass transfer to the oil through

diffusion and convection (Nasr et al., 2003; Al-Murayri et al., 2016). It can be beneficial to select a solvent that has a vaporization temperature close to that of water to help simultaneous condensation of steam and solvent (Nasr et al., 2003; Mukhametshina and Hascakir, 2014). Another crucial consideration is the solubility of asphaltenes in solvents, because bitumen is high in asphaltene content (Speight, 1991). Asphaltenes are the polar and heavy molecular weight fractions of crude oil (Mojelsky et al., 1992; Akbarzadeh et al., 2007), which are soluble in aromatic solvents but insoluble in paraffinic solvents (Speight, 1991; Wiehe, 2012). Being polar in nature, asphaltenes have an affinity towards polar water molecules, thereby aggregating at the oil-water interface and stabilizing the water-in-oil emulsions (Jewell et al., 1972; Haghighat and Maini, 2010). Asphaltene precipitation in the reservoir and along the production lines occurs due to changes in temperature and pressure conditions, and composition of the crude oil (Leontaritis et al., 1994). Additionally, asphaltene precipitation in the reservoir and pipelines can cause plugging, reducing reservoir porosity and permeability, and consequently the sweep efficiency of the thermal EOR process. For this study, propane was selected as the solvent for Solvent-SAGD experiments. Previously, propane co-injection with steam was found to improve the efficiency of EOR processes, mainly due to the distillation of lighter components of crude oil in the presence of propane (Goite et al. 2001; Rivero and Mamora, 2005; Mamora et al. 2003). These distilled crude oil components travel with propane to untouched regions of the reservoir, getting miscible with crude oil in the process. This reduces the interfacial tension and viscosity of the oil, consequently improving oil recovery. Hence, injection of hydrocarbon solvents improve the amount of oil recovered

by providing chemical mobilization. But an important concern is the nature of obtained oil in terms of water-oil emulsion complexity. It is especially critical for steam injection processes in bitumen recovery due to the presence of considerable fraction of asphaltenes in bitumen, and water, which have a high affinity to each other, due to their similar polar nature. Moreover, co-injection of hydrocarbon solvents to improve the steam injection process can have an adverse effect on emulsion stability. To understand the emulsion mechanism, freshly produced emulsions should be analyzed, owing to the fact that emulsions are very unstable and change over time.

Since there are several unknowns associated to the oil quality produced from solvent-steam processes, this study investigated the effects of steam flooding, propane-steam flooding, SAGD, and propane-SAGD on the recovery of a Canadian bitumen. The efficiency of these processes was analyzed in terms of produced oil quality, emulsion characterization, water and asphaltene content, and delay in oil production.

2.3 Experimental Procedure

In this study, three core flooding experiments (propane, steam, and propane-steam co-injection) and three SAGD experiments (one SAGD and two propane-SAGD) were conducted on a bitumen sample, Oil1, with 9.6 °API gravity, 290,500 cP viscosity at room temperature, and 21.7 wt% asphaltenes content. Table 2.1 includes the nomenclature and experimental parameters (Kar et al. 2017).

Table 2.1 - Nomenclature and parameters for flooding and SAGD experiments

Experiment	Type	Steam flow rate (ml/min CWE)	Solvent flow rate (ml/min)
E1	Propane Flooding	-	500
E2	Steam Flooding	18	-
E3	Propane-Steam Flooding	18	2
E4	SAGD	18	-
E5	Propane-SAGD*	18	36
E6	Propane-SAGD**	18	36

CWE: Cold water equivalent. *E5: Initially, propane co-injected with steam, but change to only steam injection at 18 ml/min CWE after 4 hours due to delayed oil production. **E6: Initially steam injection, change to propane-steam co-injection after start of oil production at 92 minutes.

The flooding set of experiments consists of E1, E2, and E3. E1 involves propane flooding, since this was the first experiment conducted, the flow rate was at a testing stage to be used for the propane-steam flooding experiments. However, this experiment is included in the analysis to compare the quality of the produced oil via propane flooding alone, with those from steam and propane-steam flooding experiments. For the SAGD experiments, E4 is base SAGD involving only steam injection. E5 involves propane-steam co-injection since the beginning of the experimental time; however, there was a significant delay observed in oil production, which is believed to have been the result of production lines blockage by asphaltene deposition. Hence, parameters in the last experiment (E6) were modified, and propane co-injection with steam was initiated after start of oil production, when proper communication was established between injection and production wells. E6 is thus referred to as propane-SAGD as a follow-up to SAGD.

The experiments were performed at atmospheric pressure and steam temperature conditions. For the SAGD and propane-SAGD experiments, 1:1 mass flow rate of propane and steam was maintained. This was based on the density of water (liquid) and propane

(liquid) at room temperature conditions. In all experiments excluding E2 and E4, propane was co-injected with steam in gas phase.

For simplicity, the reservoir rock was prepared only with sand and no clays, to avoid additional pore-plugging and clay migration issues experienced in previous studies (Kar et al., 2015a; Kar et al., 2015b). Ottawa 20-40 mesh size sand was used to prepare 39.1% porosity laboratory-scale reservoir rock. The pore space was filled with 84 volume percent (vol%) of bitumen and 16 vol% of distilled water.

For the flooding experiments, a cylindrical core holder and for SAGD, a rectangular experimental set-up were used (Fig. 2.1). The holder has a height of 20 cm and internal diameter of 5.4 cm. In case of SAGD, the rectangular core holder represents one half of the reservoir, with the injection and production lines drilled at the base of one corner of the setup. Two perforated steel pipes were used as injection and production lines, with diameters of 0.25 and 0.5 inches, respectively. The length, width, and height of the setup are 10.25, 5, and 9.9 inches, respectively. The distance between the injector and producer wells is 1.9 inches.

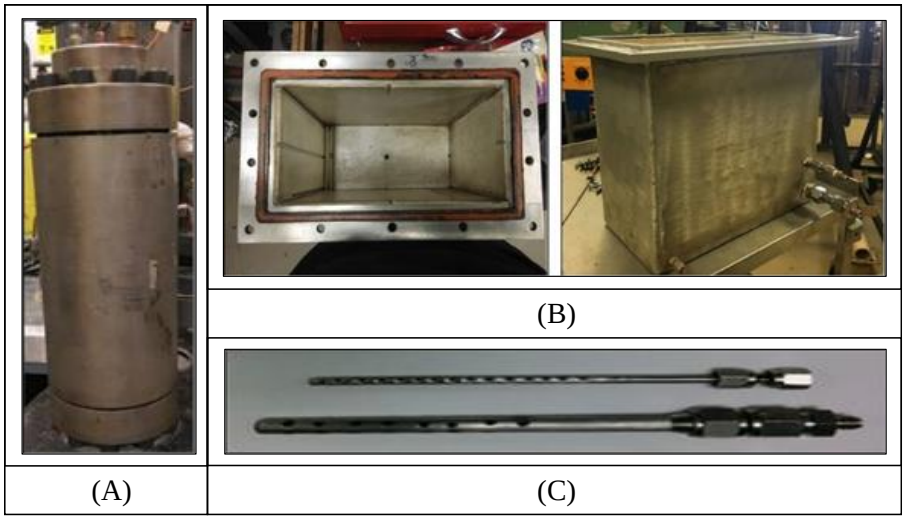

Fig. 2.1 - Experimental setup for experiments. (A) Core holder for flooding experiments (B) Core holder for SAGD experiments (C) Injector and producer wells for SAGD experiments

For SAGD, the injection and production wells are perforated and wrapped with stainless steel screen mesh to prevent sand production. Similarly, for flooding setup, a circular screen mesh is cut and inserted at the outlet, with the bottom cap of the setup. Glass wool, spiral pipe wrap, and insulation blankets are wrapped around the core holders as well as injection and production lines to prevent heat losses and condensation on the pipes. Additionally, for SAGD experiments, band heaters are wrapped around the core holder to maintain the steam temperature inside the setup. To monitor the temperature propagation during the experiments, thermowells are inserted into the core holders with thermocouples attached to them. The thermocouples are then connected via cables to a data acquisition system. The LabView software is used to record the temperature in real-time at each thermocouple position throughout the experimental time.

For both sets of experiments, the core holder is connected to the steam and solvent injection line and a separator to separate out the produced liquids from gases. The produced liquids are then collected in sampling bottles, while the produced gases are collected in a condenser. The condensable gases remain in the condenser and the non-condensable gases are vented out. Water is pumped into the steam generator using a syringe pump, while propane is pumped from a propane gas cylinder, with a calibrated flowmeter maintaining proper flow rate throughout the duration of the experiment. The flooding experiments are conducted for four hours and SAGD experiments for eight hours. The time of start of oil production is recorded for each experiment.

The water-in-oil emulsions in produced oil samples are visualized with high resolution optical microscopy (Meiji Techno MT9000). Asphaltenes from the produced oil are separated using ASTM standard D2007-11 method (ASTM 2011) using n-pentane as the asphaltene precipitating solvent. The water content in the produced oil samples is quantified using TGA-DTA (Thermogravimetric Analysis- Differential Thermal Analysis) (Chen et al., 2012; Kar and Hascakir, 2015). The residual oil is also determined thermally on spent rock samples via TGA-DTA, by observing the weight loss in the postmortem samples at original oil decomposition temperature (~550 °C) (Kar et al., 2016). Then, the displacement efficiency is calculated by using experimentally determined residual oil saturation values.

2.4 Experimental Results

As mentioned in the Experimental Procedure section, thermocouples placed at different locations inside the core holder were used to monitor the temperature growth

during the experiments in real-time. Fig. 2.2 illustrates the temperature propagation for the SAGD set of experiments, starting from two hours into the experiment till the end (8 hours). It can be seen that the steam chamber development is faster going from base SAGD (E4), to propane-SAGD (E5) to propane-SAGD as a follow-up to SAGD (E6) in ascending order, and temperature propagation is most uniform for E6. To understand the differences in temperature propagation for the SAGD experiments, we analyzed the obtained oil and spent rock that remained after the experiments.

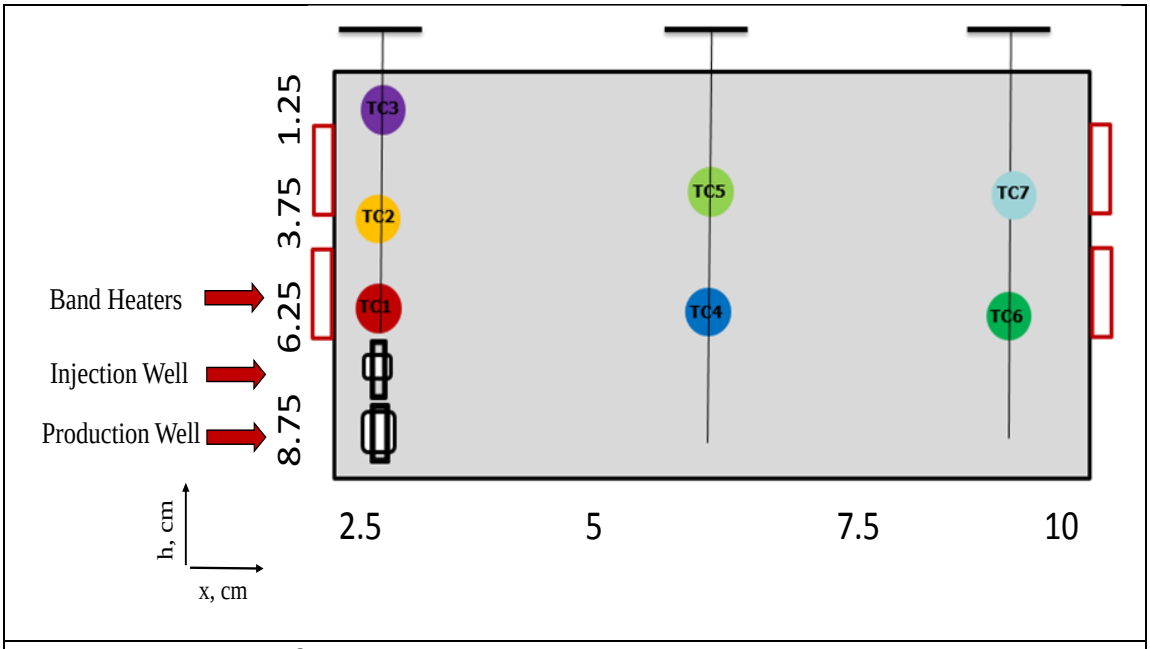

(A) Position of thermocouples placed inside the SAGD core holder setup

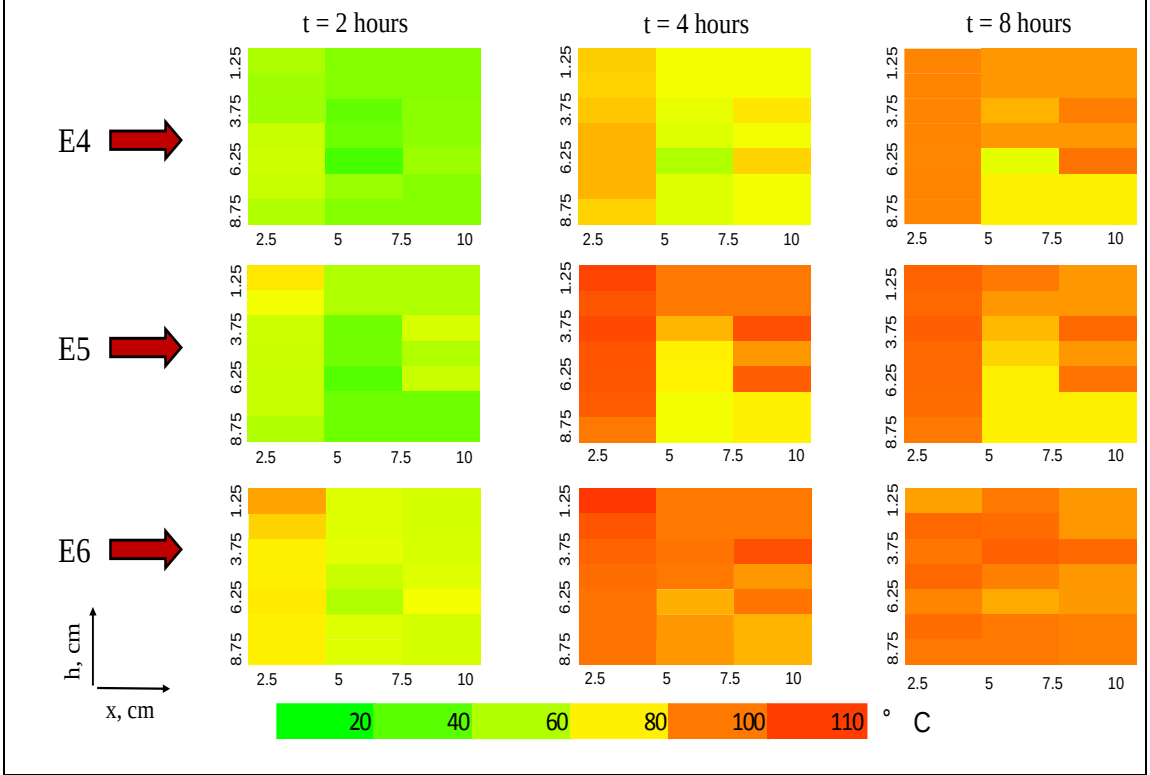

(B) Temperature propagation during SAGD experiments

Fig. 2.2 - Temperature profile for SAGD experiments (E4- Base SAGD, E5- Propane-SAGD, E6- Propane SAGD as a follow-up to SAGD)

The spent rock images for the flooding experiments and SAGD experiments are illustrated in Fig. 2.3 and Fig. 2.4, respectively.

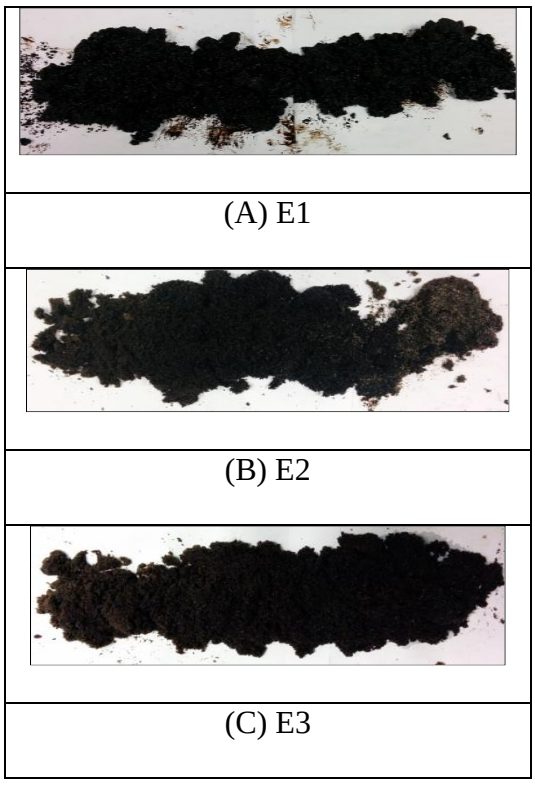

(A) E1

(B) E2

(C) E3

Fig. 2.3 - Spent rock images for flooding experiments (All images have been shown horizontally, injection from the left-hand side and production from the right side)

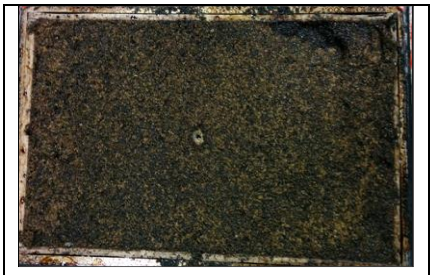

(A) E4

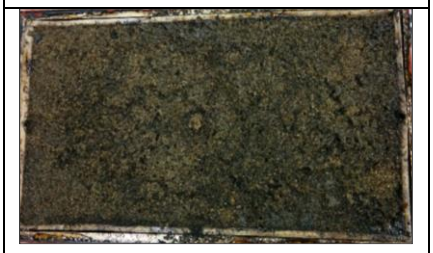

(B) E5

(C) E6

Fig. 2.4 - Spent rock images for SAGD experiments (All images have been shown from top-view; with injection and production wells in the bottom right corner)

The average initial oil saturation value for all experiments is 16.5 wt%. The spent rock is divided into two regions- inlet (injection side) and outlet (production side). The residual oil saturation is determined via TGA-DTA analysis of the spent rock. The TGA-DTA curves for spent rock are provided in Appendix C.

The asphaltene content in the residual oil is determined via solvent washing, using n-pentane and toluene solvents. Table 2.2 includes the residual oil saturation, along with the average asphaltene amount in the residual oil samples.

Table 2.2 -Residual oil saturation (based on initial oil saturation of 84 vol%) and asphaltene content in residual oil

Type of Enhanced Oil Recovery Method	Experiment	Residual Oil (vol%)			Avg. Asphaltene Content in Residual Oil (wt%)
		Inlet	Outlet	Avg.	
Flooding	E1	73.51	82.63	78.07	19.04
	E2	12.67	25.85	19.26	20.08
	E3	15.46	20.02	17.74	28.10
SAGD	E4	45.74	48.78	47.26	24.16
	E5	19.56	47.77	33.67	23.40
	E6	29.22	30.74	29.98	17.92

The graphs for cumulative oil production with respect to experimental time are provided in Appendix B (Fig. B-1, Fig. B-2). Experimental results indicate that among all flooding experiments, E3 (propane-steam flooding) yielded the best efficiency and among all SAGD experiments, E6 (propane-SAGD as a follow-up to SAGD) provided the best performance (Table 2.2). Experimental results were further evaluated to determine the pore-scale displacement efficiency by using the following formula;

$$E = \left\{\frac{S_{oi} - S_{or}}{S_{oi}}\right\} * 100$$

In where E = Pore-scale displacement efficiency

S_{oi} = Initial oil saturation

S_{or} = Residual oil saturation

The average value of residual oil saturation is then used to calculate pore-scale displacement efficiency. Furthermore, cumulative steam-oil ratio (cSOR) is calculated using the formula;

$$cSOR = \left\{\frac{Volume\ of\ steam\ injected}{Volume\ of\ oil\ produced}\right\}$$

Table 2.3 - Start of oil production and sweep efficiency for flooding and SAGD experiments

Type of Enhanced Oil Recovery Method	Experiment	Start of Oil Flow (min)	cSOR	Cumulative Oil Recovery (wt%)	E* (%)
Flooding	E1	48	11.26	-	7.19
	E2	12	9.86	75.32	77.04
	E3	15	10.19	57.4	78.87
SAGD	E4	104	9.92	11.19	43.75
	E5	160	10.6	8.76	59.92
	E6	92	10.31	7.82	64.26

*E- Pore-scale displacement efficiency, average values

For the flooding experiments (E1, E2, E3), propane-steam injection resulted in maximum pore-scale displacement efficiency, with similar time required to begin oil production compared to steam flooding. For propane flooding alone, due to absence of steam, oil production was delayed, and ultimately resulted in very low oil production. For SAGD experiments (E4, E5, E6), co-injection of propane with steam improved sweep efficiency compared to SAGD, however, there was a delay in oil production (E5). We infer that this is due to propane moving to colder parts of reservoir faster compared to steam, and depositing heavy oil fractions, which might block the flow of oil into

production lines. In E6, propane co-injection with steam was started only after oil production began, thereby minimizing blocking in the lines. This resulted in the earliest production of oil (92 min) and overall highest sweep efficiency. It should be noted that a delay in oil production observed for E5 can be verified with a non-uniform temperature growth after four hours for E5 (Fig. 2.2) which is believed to be related to blocking of lines due to uneven mobilization of bitumen. Co-injection of propane with steam after start of oil production helped in more uniform mobilization of trapped residual oil, thereby improving the efficiency of the solvent-SAGD process.

The higher cumulative oil recoveries as well as displacement efficiencies of the flooding experiments compared to SAGD experiments can be attributed to the difference in core holder (reservoir) sizes. The reservoir rock volumes for flooding and SAGD setup are 450.8 cc and 7750.2 cc, respectively. Hence, in terms of oil produced and oil displaced per unit reservoir volume, SAGD is clearly more efficient compared to flooding. As can be seen from Table 2.3, SAGD experiments ensued higher economic efficiency compared to flooding experiments, owing to their reduced cSOR. This means much lower amount of steam is required for SAGD experiments to produce the same amount of oil, than flooding. When extrapolated from pilot-scale to field-scale, the economic efficiency will increase considerably.

The microscopic images of produced oil obtained from the flooding and SAGD experiments indicated the presence of water-in-oil emulsions in produced oil samples (Fig. 2.5).

On comparing the images, E3 (Fig. 2.5C) and E6 (Fig. 2.5F) were found to have similar water-in-oil emulsion characteristics. Both E3 and E6 involved propane-steam co-injection. Comparatively, produced oil obtained from SAGD (Fig. 2.5D) showed more water droplets emulsified in oil, while in case of propane-SAGD (Fig. 2.5E and Fig. 2.5F), the water droplets are seen to be coalescing to form larger in size, but fewer in number, indicating less severe emulsions.

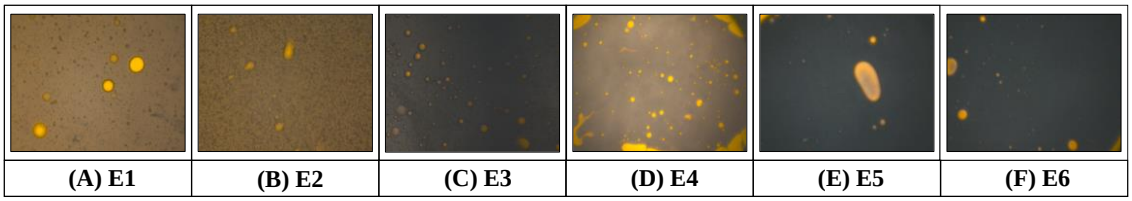

(A) E1	(B) E2	(C) E3	(D) E4	(E) E5	(F) E6

Fig. 2.5 - Microscopic images of produced oil for flooding and SAGD experiments (A) E1 (B) E2 (C) E3 (D) E4 (E) E5 (F) E6 (40X magnification)

After separation of the free water from the produced oil by heating, the produced oil was analyzed for asphaltene content via ASTM D2007-11 (ASTM, 2011), using n-pentane as the precipitating agent, and for water content in produced oil via TGA-DTA (Kar and Hascakir, 2015). The TGA-DTA curves for produced oil samples are in Appendix C. The bulk produced oil was divided into asphaltenes, deasphalted oil (DAO), and water (Fig. 2.6).

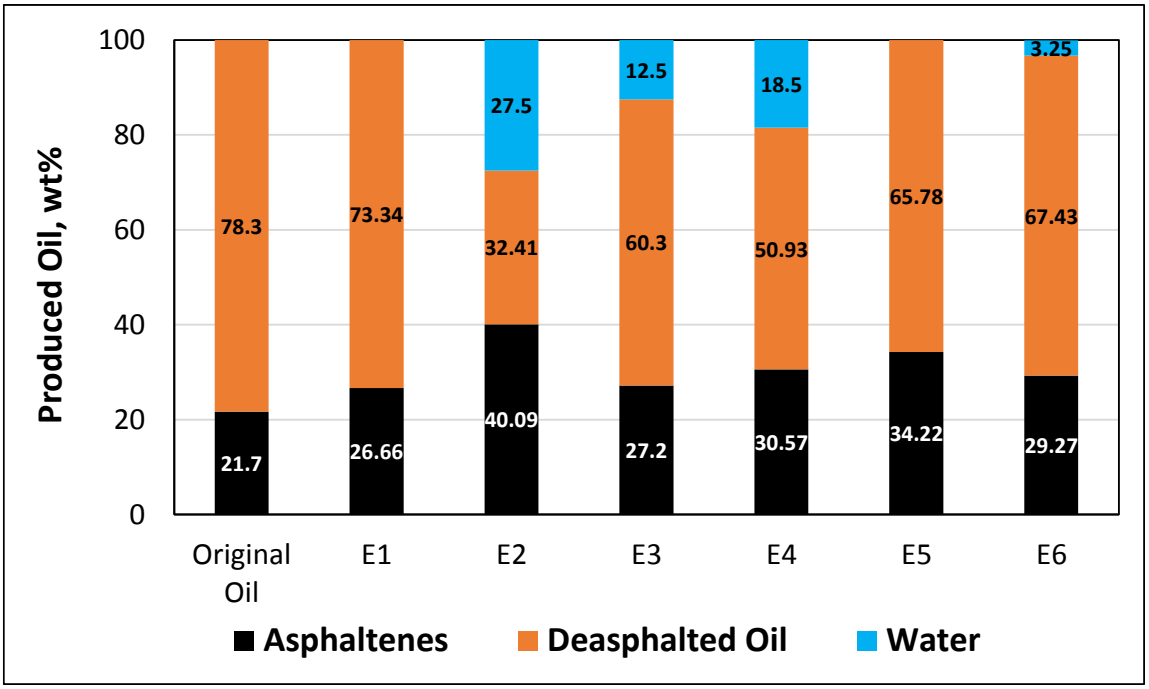

Fig. 2.6 - Components of bulk produced oil in terms of weight percent for flooding and SAGD experiments

For the flooding experiments, a greater amount of asphaltene content in produced oil led to a higher water concentration in the sample. This was observed for the steam flooding experiment (E2). With co-injection of propane with steam (E3), the water content in produced oil was reduced greatly, with negligible water content in case of propane flooding (E1). In case of SAGD experiments, a similar trend was observed. SAGD alone resulted in highest water content in bulk produced oil, compared to propane-SAGD experiments. Propane-SAGD as a follow-up to SAGD (E6) led to lowest asphaltenes content in produced oil. The reduced water content in produced oil through steam-propane co-injection correlated to the less emulsified water droplets visualized in the bulk oil (Fig. 2.5) for these cases.

2.5 Conclusions

In the flooding experiments, co-injection of propane with steam improved displacement efficiency and produced oil quality. For both sets of experiments, flooding and SAGD, propane co-injection with steam resulted in lower amount of water carried with the produced oil. Propane-SAGD as a follow-up to SAGD gave best performance in terms of highest oil recovery and lowest cSOR.

The improved performance of propane-SAGD as a follow-up to SAGD is believed to be due to the miscibility of oil in solvent, which reduces the interfacial tension between oil and propane in the presence of steam. Consequently, the trapped residual oil can be mobilized, improving the displacement efficiency.

In this study, co-injection of a gaseous phase paraffinic hydrocarbon solvent with steam led to improved oil recovery via better quality of produced oil. This refers to less complex emulsions due to lower amount of water carried into the bulk produced oil. However, in actual reservoirs, several other factors come into play, including the presence of reservoir clays, and their impact on water-oil emulsion complexity. Moreover, the co-injection of liquid hydrocarbon solvents can further influence these emulsions.

Future chapters, report a series of steam and solvent-steam flooding experiments that were conducted to generate water-oil emulsions and to analyze associated interfacial relations. For the solvent-steam experiments, a variety of hydrocarbon solvents were selected, based on their phase at reservoir conditions, solubility of asphaltenes in them, and their chemical nature.

3. STEAM AND SOLVENT-STEAM FLOODING

3.1 Overview

In this study, a series of steam and solvent-steam flooding experiments were conducted to generate water-oil emulsions in the produced oil. Three sets of experiments performed have seven experiments each, beginning with steam flooding, and solvent-steam flooding using propane, n-butane, n-pentane, n-hexane, and n-heptane as paraffinic solvents insoluble in asphaltenes, and toluene, which is a polar solvent soluble in asphaltenes. The first set excluded clays in core samples, to mainly focus on the impact of hydrocarbon solvents on emulsion quality. The second and third sets included kaolinite (Clay1) and a mixture of kaolinite and illite (Clay2), respectively, in the oil-sand packing, to analyze the contributions of clays towards emulsion complexity.

Progressing from Set 1 to Set3, the cumulative oil recovery decreased, with presence of Clay2 resulting in highest trapping of crude oil. As the carbon number of paraffinic solvent increased, greater amounts of asphaltenes were carried with the displaced residual oil left in the spent rock. In the presence of clays, this correlation gets disturbed, due to contribution of clay interactions with oil and water phases. Importantly, this chapter forms the basis for emulsion generation, which then is analyzed in detail in terms of intermolecular association among clays, water, and asphaltenes in the following chapter.

3.2 Introduction

Some common thermal EOR methods for bitumen recovery are hot water flooding, steam flooding, cyclic steam stimulation, in-situ combustion, and SAGD (Green and Willhite 1998). Steam is more effective compared to hot water, due to the higher heat content of steam than the same mass of hot water. This additional heat is stored in steam in the form of latent heat. Hence, for steam injection processes, steam quality generated by commercial steam generators is an important parameter, which is defined as the degree of dryness of steam. Steam flooding has been mainly applied to sandstone reservoirs because of their higher permeability than carbonates. In steam flooding, thermal energy is used for distillation of lighter fractions of crude oil which form a solvent bank (Prats 1982). This solvent bank helps in reducing trapped residual oil via miscibility. Additionally, the steam condenses to form a hot water bank, which acts as a secondary drive to push the crude oil towards production well.

There are numerous steam flooding projects listed in literature around the world for heavy oil and bitumen recovery, however, the significant amount of fresh water consumption, treatment of the produced water along with surface and air pollution caused by GHG emissions are among the pertinent drawbacks of the method. To improve the efficiency of steam flood, solvents are injected along with steam. These solvents are in gas phase, like carbon dioxide (Nejatian Daraei et al. 2015), propane (Rivero and Mamora, 2005), or liquid phase, like n-pentane (Souraki et al. 2016), n-hexane, etc. The purpose of adding solvents is to reduce the amount of steam required for the process, and chemical mobilization of the crude oil by reduction in interfacial tension. This is brought about by

miscibility of crude oil in hydrocarbon solvents. For gases, the solubility in solvents depends on the minimum miscibility pressure (MMP) (Luks et al. 1987). Selection of solvent should be done taking into consideration the phase of solvent at experimental conditions, solubility of asphaltenes in solvents, and effect of solvents on interfacial forces acting between polar crude oil components and water. It should be noted that asphaltenes are insoluble in paraffinic solvents but soluble in aromatic solvents (Speight 1999).

For both steam flooding and solvent-steam flooding techniques, the quality of the obtained oil should be analyzed in terms of water-in-oil emulsions and reservoir fines (clays) migrating into the produced oil (Evdokimov and Losev, 2014). Water-in-oil emulsions are stabilized by the polar crude oil components, resins and asphaltenes, which act as emulsifiers and due to their affinity towards polar water droplets, form a layer around the water drops, and prevent coalescence of the droplets. Aromatic solvents can increase the cumulative oil recovery, however, the higher amount of asphaltenes in the produced oil can deteriorate the oil quality. The migrated fines and water have to be separated from the oil to make it commercially viable. Moreover, asphaltenes precipitation occurring due to changing temperature, pressure, and oil composition can lower the pore-scale displacement efficiency of the process (Leontaritis et al. 1994).

Apart from asphaltene-water interactions, clays in the reservoir, commonly smectite, kaolinite, and illite (Czarnecka and Gillott, 1980) can cause significant issues in oil recovery and quality of the obtained oil. Kaolinite has hexagonal structures in its geometry, whereas illite has a filamentous and fibrous structure (Luffell et al. 1993; Pallatt et al. 1984). Smectite is a water-sensitive clay, and can reduce reservoir permeability

considerably during steam injection processes due to the presence of water (Bennion et al. 1992; Chappell et al. 2005). Non water-sensitive clays, mainly kaolinite and illite, which are widely documented in heavy oil and bitumen reservoirs, can also diminish reservoir permeability owing to their pore lining, pore bridging, and pore filling features (Nadeau 1998; Neasham 1977; Morris and Shepperd, 1982). This reduces the pore-scale displacement efficiency by trapping more hydrocarbon fluids in between the mineral layers and the pore spaces, thereby resulting in reduced oil recovery (Wilson and Pittman, 1977; Green and Willhite, 19998; Willhite 1986; Kar et al. 2015). Clays are known to associate with the polar fractions of crude oil, resins and asphaltenes, the degree of association depending on clay type, impurities in the polar crude oil fractions, etc. (Binner et al. 2014; Martinez-Palou et al. 2013). The adsorption of polar fractions of oil onto clays has been associated with surface properties of clays like surface area, cation exchange capacity, etc (Siffert et al. 1992). Clays can also cement the sand grains (Ahmed 2008), further reducing oil recovery. The high surface area of illite is especially found to be detrimental for bitumen recovery, as it promotes higher adsorption of organics onto its surface (Wallace et al. 2004; Mercier et al. 2008). Bantignies et al. (1997) compared the wettability contrasts in kaolinite and illite clays through X-ray powder diffraction (XRD), Fourier Transform Infrared Spectroscopy (FTIR), and X-ray Absorption Spectroscopy (XAS) and found kaolinite prefers to adsorb asphaltenes, whereas illite tends to be more water-wet, showing affinity for brine. Additionally, illite has been found to preferentially absorb nitrogen compounds over those of sulfur (Mercier et al. 1999).

The previous chapter included steam flooding and SAGD along with propane co-injection. This chapter expands solvent-steam flooding for bitumen recovery by incorporating multiple hydrocarbon solvents with increasing carbon number- propane and n-butane in gas phase, n-pentane, n-hexane, n-heptane, and toluene in liquid phase. Two types of clays are used in the reservoir packing- Clay1 (kaolinite) and Clay2 (mixture of kaolinite and illite). The mutual interactions between crude oil components, water, hydrocarbon solvents, and clays are analyzed to determine the optimum hydrocarbon solvent in solvent-steam flooding for a particular reservoir type.

3.3 Experimental Procedure

Three sets of steam and solvent-steam flooding experiments are conducted on a Peace River bitumen sample, Oil2, having viscosity of 54,000 cP, 8.8 °API gravity, and 34.4 wt% asphaltenes content. In the first set of experiments (Set1), the unconsolidated reservoir rock was prepared using Ottawa sand, Oil2, and distilled water; corresponding to a 39.1% porosity consisting of initial oil and water saturation of 84 vol% and 16 vol%, respectively. Experiments E1 and E2 were added from a previously conducted work (Coelho, 2016). For the second set (Set 2), the reservoir rock packing consisted of 85 wt% Ottawa sand and 15 wt% Clay1 (kaolinite). The resulting 32% porosity was filled with Oil2 and distilled water in the same proportion as for Set 1 (84:16 vol%). For the last set of experiments (Set 3), the components and initial saturations were exactly the same as for Set 2, except a different clay type, Clay2 (mixture of kaolinite and illite) was used in the packing. Data from experiments E15, E16, and E19 were incorporated from previously conducted experiments (Coelho 2016; Stape 2016). The oil-sand packing was then placed

in a cylindrical core holder (20 cm height, 5.4 cm internal diameter, 9.8 cm outer diameter). Table 3.1 lists the nomenclature for all three sets of experiments.

Table 3.1 - Nomenclature for steam and solvent-steam flooding experiments

Experiment Type	Experiment	Solvent Injected
Set 1-No Clay	E1*	none
	E2*	propane
	E3	n-butane
	E4	n-pentane
	E5	n-hexane
	E6	n-heptane
	E7	toluene
Set 2-Clay1	E8	none
	E9	propane
	E10	n-butane
	E11	n-pentane
	E12	n-hexane
	E13	n-heptane
	E14	toluene
Set 3-Clay2	E15*	none
	E16*	propane
	E17	n-butane
	E18	n-pentane
	E19**	n-hexane
	E20	n-heptane
	E21	toluene

*Coelho 2016, **Stape 2016

A circular screen mesh (size 210 µm) was inserted at the outlet of the core holder, with the bottom cap of the setup. Glass wool, spiral pipe wrap, and insulation blankets are wrapped around the core holder as well as injection and production lines to prevent heat losses and condensation on the pipes. To monitor the temperature propagation during the experiments, a thermowell is inserted into the center of the core holder with thermocouples attached to it. The thermocouples are then connected via cables to a data acquisition system. LabView software is used to record the temperature in real-time at each thermocouple position throughout the experimental time.

The core holder is connected to the steam and solvent injection line and a separator to separate out the produced liquids from gases. Water is pumped into the steam generator using TELEDYNE ISCO syringe pump at a constant rate of 18 ml/min cold water equivalent (CWE). For solvent-steam co-injection experiments, liquid solvents are pumped via BECKMAN continuous pump with a constant flow rate of 2 ml/min, while gaseous solvents are pumped from storage cylinders, via a calibrated flowmeter maintaining proper flow rate of 2 ml/min throughout the duration of the experiment. The produced liquids are then collected in sampling bottles, while the produced gases are collected in a condenser. The condensable gases remain in the condenser and the non-condensable gases are vented out. All experiments are conducted for a time period of four hours. Experimental temperature and pressure are maintained at 120-165 °C, and 75 psig.

After the collection of produced fluids, the sampling bottles are kept in oven at 60-70 °C to separate the free water and solvents from the produced oil samples. Finally, the produced oil is qualitatively and quantitatively analyzed. It should be noted that there might be trapped water and clay particles in the produced oil. The instantaneous produced fluids as well as the produced oil after separation of free water and solvents are visualized via optical microscopy. The spent rock left (postmortem) are divided into two parts- inlet (near injection) and outlet (near production), and residual oil is determined by thermal method (TGA-DTA analysis) (Chen et al. 2012; Kar et al., 2015a) and solvent washing method using n-pentane and toluene solvents (Amyx et al 1960; Kar et al. 2015a). Asphaltene content in residual oil is also determined using solvent washing method using

n-pentane and toluene solvents (Amyx et al., 1960; Kar et al. 2015), with n-pentane as the precipitating solvent.

3.4 Experimental Results

The cumulative oil production as well as oil production rate with respect to experimental time for all experiments are in Appendix B. Table 3.2 summarizes the net cumulative oil produced. For Set1 (no clay) experiments, solvent-steam flooding experiments improved oil production compared to steam flooding. This is due to the additional mobility of crude oil via chemical dilution due to the injection of hydrocarbon solvents. Steam flooding with toluene injection resulted in highest oil production, owing to the high solubility power of toluene. The general trend observed is the increase in bulk oil recovery with increase in carbon number of paraffinic solvent injected. Moreover, higher the molecular weight of the solvent, longer is the breakthrough period. The lighter solvents can travel through the core holder faster, causing faster mobilization of the oil via chemical dilution. As can be seen from the oil production rate graphs (Appendix B), experiments involving toluene injection with steam have considerable rate of oil production at a later period during the experiment, compared to other experiments.

For Set2 (Clay1) and Set3 (Clay2) experiments, the cumulative oil production was considerably lower, compared to Set1 experiments. This is due to the presence of clays in the oil-sand packing, which have an affinity towards the crude oil components, thereby trapping the oil and consequently, reducing the reservoir porosity and permeability. The lowest oil production values are obtained in Set3 experiments. This indicates the higher affinity of Clay2 (which is a mixture of kaolinite and illite) towards crude oil, compared

to Clay1 (only kaolinite). For Clay1 experiments, again the general trend is the increase in cumulative oil production with solvent-steam flooding, compared to only steam flooding. For the last set of experiments (Set3- Clay2), C3, nC6, and toluene solvents co-injected with steam gave better cumulative oil production results.

Table 3.2 - Cumulative oil production for steam and solvent-steam flooding experiments

Experiment Type	Experiment	Description	Cumulative Oil Production (wt%)
Set 1-No Clay	E1*	none	33.54
	E2*	propane	52.15
	E3	n-butane	40.17
	E4	n-pentane	38.23
	E5	n-hexane	46.40
	E6	n-heptane	48.22
	E7	toluene	71.31
Set 2- Clay1	E8	none	36.21
	E9	propane	37.94
	E10	n-butane	34.35
	E11	n-pentane	35.53
	E12	n-hexane	37.87
	E13	n-heptane	37.52
	E14	toluene	43.9
Set 3- Clay2	E15*	none	23.5
	E16*	propane	36.94
	E17	n-butane	22.65
	E18	n-pentane	19.27
	E19**	n-hexane	32.32
	E20	n-heptane	25.83
	E21	toluene	30.82

* Coelho 2016, ** Stape 2016

Fig. 3.1 represents the obtained images of spent rock left after the flooding experiments, the dark colored regions depict the residual oil left in the packing. For no clay experiments, the mixture is unconsolidated, with the color turning lighter with increase in carbon number of solvents, steam-toluene injection resulting in 100% displacement of oil (E7). For Set2, the spent rock mixture gets more consolidated due to the presence of kaolinite. Interestingly, the steam flooding experiment (E8) resulted in the

most consolidated spent rock compared to solvent-steam co-injection experiments. This indicates that for Clay1, co-injection of hydrocarbon solvents improved the sweep, with the exception of steam-n-pentane flooding (E11) which shows an uncharacteristically dark color in the middle region. These findings are also supported by the cumulative oil production values in Table 3.2. The poor performance of E11 might be due to the precipitation of asphaltenes initiated by n-pentane flooding, as the asphaltenes analyzed in this research are n-pentane insoluble asphaltenes. Finally, for Clay2 experiments, all the solvent-steam experiments appear highly consolidated, with steam-n-pentane flooding experiments again resulting in darkest color, implying highest residual oil (E18). Another observation made is that for the experiments with clay in the oil-sand packing (Set 2 and Set 3), the outlet side (right-hand side in the images) appear to have a better sweep (lighter color) compared to inlet side (injection side). For toluene co-injection with steam in the presence of Clay2 (E21), the spent rock is visually dark on the outside, however, the inner portions of the spent rock are significantly lighter in color, indicating the effective sweeping of crude oil via toluene. This indicates the displacement of the crude oil containing significant amount of asphaltenes towards the edges of the core holder. Toluene is a strong aromatic solvent with a high dissolving power for asphaltenes. The high asphaltene content near the edges and production side is believed to have led to asphaltene precipitation due to change in temperature near the outlet. It should be noted that the asphaltenes moved by the polar solvent toluene are very polar in nature. These precipitated asphaltenes were retained in the core holder due to their increased affinity towards Clay2.

This caused blocking of production lines and consequently, low cumulative oil production in sampling bottles in spite of effective displacement of oil inside the core holder.

Kaolinite is known to be more unstable at high temperatures and strong alkaline solutions and begins to dissolve in water, while illite is comparatively stable and is not prone to getting dissolved in water (Pang et al 2010). Additionally, in the sampling bottles, after removal of free water and solvent layer, clay-water slurry was observed at the bottom, for the Set 2 (Clay1) experiments. This indicates affinity of kaolinite towards produced water, similar findings were made in a previous study (Unal et al. 2015). Conversely, in the presence of kaolinite-illite mixture (Set 3- Clay2), there was significant delay in start of oil production (Appendix B), much lower cumulative oil recovery (Table 3.2), and migrated clays were found to be more dispersed within the produced oil, indicating affinity towards crude oil. This can be related to higher surface area of illite (Bantignies 1997), facilitating in greater interaction of illite with the polar oil fractions, and trapping higher amount of oil in the reservoir.

	
(E1)	(E2)
	
(E3)	(E4)
	
(E5)	(E6)
	
(E7)	(E8)
	
(E9)	(E10)
	
(E11)	(E12)

Fig. 3.1 - Spent rock images for all experiments

*All images are shown horizontally, injection from the left side and production from the right side

(E13)

(E14)

(E15)

(E16)

(E17)

(E18)

(E19)

(E20)

(E21)

(E21)

Fig. 3.1 Continued - Spent rock images for all experiments

*All images have been shown horizontally, injection from the left side and production from the right side

Table 3.3 lists the displacement efficiency (in terms of volume percent) for all three sets of experiments using TGA-DTA analysis. As discussed in a previous publication (Kar et al. 2016), TGA-DTA method is considered to be the more accurate estimation. The TGA-DTA curves for the spent rock samples are provided in Appendix C. The initial oil saturation in weight percent of oil-sand mixture for the three sets of experiments are – 16.66, 14.89, and 15.6 wt% respectively. The residual oil values are then converted into volume percent based on an initial oil saturation of 84 vol% in the oil-sand mixture (Table

3.3). For Set 1 (no clays), as expected, solvent-steam flooding improved the cumulative oil production compared to steam flooding alone.

For Set 2 (Clay1) experiments, it is observed that the addition of kaolinite clay in the oil-sand packing overpowers the effect of solvent injection in some cases and lowers the pore-scale displacement efficiency for solvent-steam flooding, compared to steam flooding alone. For propane and toluene injection cases, injection of solvents improved displacement efficiency of the flooding process. For Set 3 (Clay2), the cumulative oil production was much lower and residual oil volume significantly higher compared to the other two sets. Presence of Clay2 (mixture of kaolinite and illite) leads to trapping of much higher crude oil in the oil-sand packing, leading to cementation and consolidation of the whole mixture inside the core holder. These results correlate with previous findings in which, presence of 10-15 wt% of illite in Clay2 caused the cumulative oil production to decrease considerably when compared to Clay1 reservoir in SAGD recovery of bitumen (Mukhametshina et al. 2016).

As discussed in the Introduction section, asphaltenes are the heaviest, polar fractions of crude oil and a significant factor in determining sweep efficiency in reservoir and quality of recovered oil. Table 3.3 also includes the asphaltene content in the residual oil in the spent rock determined by solvent washing using n-pentane and toluene (Kar et al. 2015a).

For Set 1, with increase in carbon number of solvent injected, the average asphaltene amount in residual oil increases, this is directly related to increase in cumulative oil recovery (Table 3.2). With the exception of steam-nC5 experiment (E2),

displacement efficiency is generally found to improve with increase in carbon number of hydrocarbon solvent. However, when clays are introduced into the mixture (Set 2 and Set 3), there is no definite trend, due to the additional interaction of clays with crude oil, water, and hydrocarbon solvents. For Clay1 experiments, C3 (E9), nC6 (E12), and toluene (E14) are found to provide best performance for solvent-steam flooding, giving similar values of asphaltene content in the residual oil. For the last set of experiments with Clay2 (kaolinite-illite mixture), C3 (E16), nC6 (E19) and toluene (E21) resulted in comparatively higher displacement efficiency.

The highest value of asphaltene content in residual oil in spent rock was evaluated for steam-nC5 co-injection for both Clay1 and Clay2 experiments. This finding can be linked to the dark consolidated spent rock images observed for these two experiments in Figure 3.1 (E11 and E18).

Table 3.3 - Average displacement efficiency (based on initial oil saturation of 84 vol%) and asphaltene content in residual oil

Experiment Type	Experiment	Displacement Efficiency (vol%)			Avg Asphaltene content in Residual Oil (wt%)
		Inlet	Outlet	Average	
Set 1-No Clay	E1*	82.02	78.65	80.34	15.80
	E2*	84.27	82.02	83.15	5.50
	E3	85.59	80.19	82.89	10.22
	E4	90.10	91.6	90.85	14.90
	E5	88.78	81.51	85.14	33.41
	E6	96.57	97.46	97.02	35.49
	E7	100	100	100	-
Set 2- Clay1	E8	69.78	73.14	71.46	39.70
	E9	74.48	75.02	74.75	28.09
	E10	69.11	65.41	67.26	19.97
	E11	64.07	66.08	65.08	46.63
	E12	71.46	67.76	69.61	29.92
	E13	46.94	83.55	65.25	33.13
	E14	88.31	72.13	80.22	31.71
Set 3- Clay2	E15*	16.03	53.21	34.62	16.7
	E16*	55.77	74.36	65.06	19.4
	E17	29.49	44.23	36.86	6.39
	E18	14.74	25.0	19.87	40.65
	E19**	51.0	56.0	53.50	14.00
	E20	13.46	29.17	21.31	36.60
	E21	90.06	88.65	89.36	18.62

* Coelho 2016, ** Stape 2016

Based on the results from Table 3.3, the asphaltene content in residual oil is plotted with respect to carbon number of paraffinic solvent injected in Fig. 3.2. No value could be obtained for E7 as toluene co-injection had complete displacement. The residual oil is the oil moved or displaced in the reservoir, and could not be recovered. With increasing carbon number of injected solvent, the dissolving power of asphaltenes increases, hence the moved/displaced oil carries a higher proportion of asphaltenes with increasing carbon number of solvent.

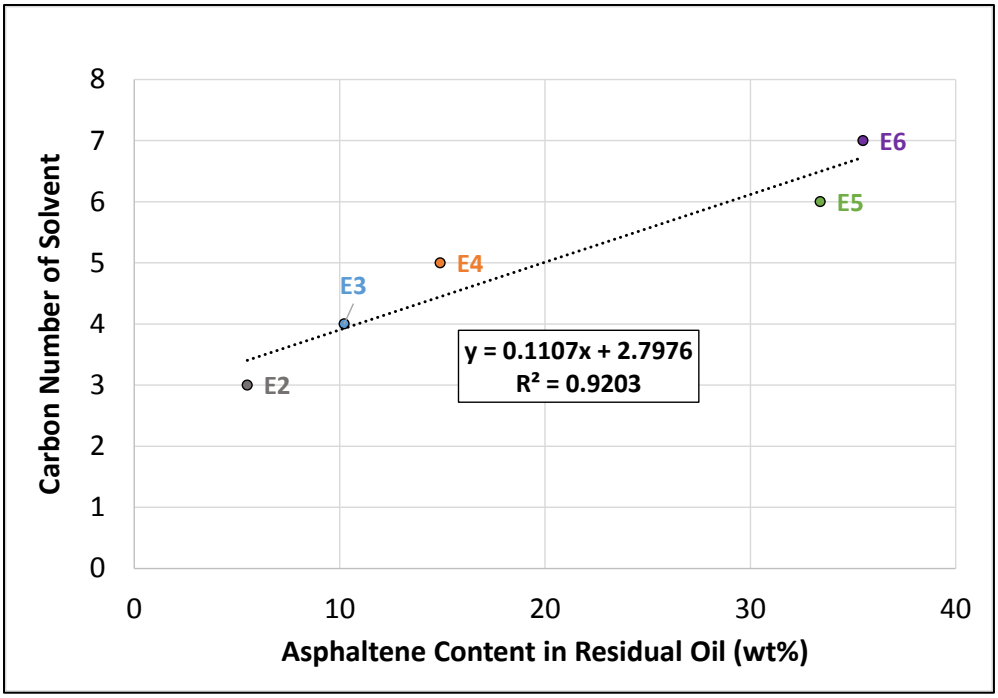

Fig. 3.2 - Asphaltenes in residual oil correlating with injected solvent (Set1-No Clay)

However, with the introduction of clays, the analysis gets more complicated and doesn't follow any general trend. This is due to the additional interaction between clays, crude oil fractions (mainly the polar asphaltenes and resins), and water. The wettability of clays can alter during the thermal EOR process, resulting in trapping of higher crude oil. Conversely, clays can migrate along with the produced fluid, with affinity towards either the water or oil phase. This can deteriorate the quality of the produced oil by stabilization of water-oil emulsions.

The next chapter discusses the quality of the bulk produced oil obtained from steam and solvent-steam flooding experiments in terms of water-oil emulsion severity, clay migration into the produced fluids, and the role of crude oil fractions, injected hydrocarbon solvents and clay type in the quality of the produced oil.

3.5 Conclusions

Based on the experimental results from steam and solvent-steam flooding experiments, we infer that co-injection of solvents improves the cumulative oil production, compared to steam flooding for experiments without clays. In the presence of clays, it is important to analyze the quality of the obtained oil, due to possibility of clay migration into produced oil. The presence of clays reduces the oil recovered, considerably, due to the trapping of crude oil with the clay-sands, thereby reducing the reservoir porosity and permeability.

The lowest recovery was obtained for experiments with a mixture of kaolinite and illite, indicating the strong affinity of illite towards crude oil. At steam conditions, the wettability of illite is believed to change towards more oil-wet compared to kaolinite, consequently trapping more amount of oil in the spent rock. With the co-injection of aromatic solvents, although the displacement efficiency improves, higher amount of asphaltenes carried with the displaced oil show greater plugging issues. Hence, in the presence of clays, aromatic solvents can be detrimental for the overall efficiency of the flooding process.

4. EMULSION CHARACTERIZATION FOR STEAM AND SOLVENT-STEAM FLOODING PROCESSES

4.1 Overview

Stability of emulsions is a function of positive interfacial tension, droplet size of dispersed phase, and presence of emulsifiers, which create an energy barrier and prevent the coalescence of the droplets. Commonly present emulsifiers in oil sand reservoirs are heavy oil components (asphaltenes, resins), clay fines, sands, etc. The solid emulsifiers at the interface in Pickering emulsions are generally biwettable (wetted partially by both oil and water phases). Reservoir clays are known to alter their wettability from water wet to oil wet, and if migrated into the oil phase, can be a significant factor in stabilizing water-oil emulsions. Additionally, the presence of hydrocarbon solvents in the produced oil obtained from solvent-steam injection processes can either promote or act as a barrier to the clay-oil interactions. This depends largely on the phase of the solvent and their solubilizing power of asphaltenes.

The objectives of this research is to fundamentally study the emulsion formation mechanism, and to determine the optimum solvent to minimize emulsion formation for solvent-steam injection processes for bitumen recovery.

4.2 Introduction

Formation of water-oil emulsions is a serious concern during steam injection in oil sands due to the presence of water and high content of asphaltenes in bitumen. Asphaltene-water interactions are due to their similar polar nature (Spiecker et al. 2003). Asphaltenes

consist of heteroatoms like nitrogen, sulfur, and oxygen in their composition which contribute to their polar nature (Groenzin and Mullins, 2000; Meyer et al. 2007). These nanoaggregates form a strong interfacial film at the oil-water interface, which is supported by resins, another polar fraction of crude oil (Goual and Firoozabadi, 2002). Water-oil emulsion problems have been persistent in the industry since long, regular water-in-oil emulsions observed during initial production in a steam injection project in Slocum Field, Anderson County, Texas (Hall and Bowman, 1973) were found to switch to reverse oil-in-water emulsions with rise in temperature. Mohammadzadeh et al. (2010) found in their pore-scale study of Steam-Assisted Gravity Drainage (SAGD) that emulsions are created due to trapping of water condensate droplets within the oil zone. Recently, Wang et al. (2016) concluded that for steam flooding, emulsion severity increases with temperature to a greater extent for heavy oil as compared to light oil.

Emulsions can be defined as a suspension of dispersed liquid phase droplets in a liquid dispersion medium (Kokal 2005; Kilpatrick 2012). It is a surface phenomenon, caused by the formation of an interface between two liquid phases, as explained by the Gibbs Model (Tadros 2013). The presence of emulsifiers stabilizes this interface, reducing the interfacial tension and increasing the interfacial area. Water-oil emulsions in the produced oil can be classified based on the droplet size, the dispersed phase (water-in-oil emulsions if water is the dispersed phase), and their complexity. Pickering emulsions are formed by the accumulation of solid particles at the oil-water interface, and these particles are generally biwettable in nature (Pickering 1907; Sztukowski and Yarranton, 2005). The principle forces in emulsions are the van der Waals intermolecular forces between the

molecules of the emulsified droplets, electrostatic repulsion caused due to the formation of an electrical double layer when ionic surfactants (emulsifiers) are present, and steric repulsion between the hydrophilic/hydrophobic parts of the non-ionic surfactants (Tadros 2013). Furthermore, for stable emulsions, the droplet size should be small enough for the Brownian motion of particles to overcome the van der Waals forces of attraction. When the attractive forces overcome the repulsive forces, breaking of emulsion occurs. The physical mechanisms involved in breaking of emulsions are creaming and sedimentation, flocculation, Ostwald ripening, and coalescence (Sarbar and Al-Jaziri, 1995).

The introduction of hydrocarbon solvents with steam in solvent-steam flooding and solvent-SAGD might promote or destabilize these water-oil emulsions. This depends on the chemical nature of solvent and their asphaltene solubility. The presence of solvents can affect the amount of water and clays migrating into the produced oil (Hascakir 2016). In SAGD, solvents in gaseous phase can diffuse into the oil phase, thereby mobilizing the oil and changing its chemical composition. Moreover, presence of paraffinic solvents induces asphaltene precipitation, while asphaltenes are soluble in aromatic solvents (Speight 2014).

Clays in the reservoir cause further complications in the bitumen recovery. Clays are defined as crystalline minerals composed of two-dimensional sheets of silicon-oxygen tetrahedra and two-dimensional sheets of aluminium/magnesium-oxygen-hydroxyl octahedra (van-Olphen and Hsu, 1978). The silicon and aluminium sites on the clay surface have a tendency to interact with the oil fractions (Bantignies et al 1997). Clay migration into the produced oil can stabilize water-oil emulsions. Crude oil can be divided

into four major components- non-polar fractions which are saturates and aromatics (Cho et al. 2012) and polar fractions resins and asphaltenes (Macko et al. 1988; Goual and Firoozabadi, 2002), known as SARA fractions. The mutual association of polar components of oil with the non-polar fractions also impact clay-water-oil interactions (Kar et al. 2016). The change in crude oil composition and their association with minerals also influence deposition issues during crude oil recovery (Carbognani et al. 1999). Clays are found to have a net negative surface charge (Swartzen-Allen and Matijevic, 1974; O'Carroll 2000), making them prone to adsorb organic material. This changes the clay wettability from water-wet to oil-wet and alters the surface properties of clays (Kotlyar et al. 1988). When these clay particles attached to the oil phase migrate into the produced oil, they can stabilize the oil-water emulsions by aggregating at the interface, forming Pickering emulsions (Pickering 1907; Levine et al. 1989).

While steam injection provides good efficiency for recovery of heavy oils with high asphaltene content, the interaction of clays and polar oil components with liquid and vapor forms of water are not very well documented in literature. Moreover, how these associations are affected by changing clay type are not well known. This research aims to study the emulsion formation mechanism during solvent-steam flooding in oil sands, in the presence of multiple emulsifiers (clays, asphaltenes) and the hydrocarbon solvents which might promote clay- asphaltene adsorption or form a barrier between the oil layer and clay particles.

4.3 Experimental Procedure

In the previous chapter, a series of steam and solvent-steam flooding experiments were conducted. This chapter expands on the qualitative and quantitative analyses of the composition of the obtained oil from these experiments. Table 4.1 lists the experiment nomenclature which will be followed throughout this chapter.

Table 4.1 - Nomenclature for steam and solvent-steam flooding experiments

Experiment Type	Experiment	Solvent Injected
Set 1-No Clay	E1*	none
	E2*	propane
	E3	n-butane
	E4	n-pentane
	E5	n-hexane
	E6	n-heptane
	E7	toluene
Set 2-Clay1	E8	none
	E9	propane
	E10	n-butane
	E11	n-pentane
	E12	n-hexane
	E13	n-heptane
	E14	toluene
Set 3- Clay2	E15*	none
	E16*	propane
	E17	n-butane
	E18	n-pentane
	E19**	n-hexane
	E20	n-heptane
	E21	toluene

* Coelho 2016; ** Stape 2016

Optical microscopy is used to visualize both the instantaneously produced oil as well as after separation of free water and solvents from the oil. Asphaltenes are separated from the bulk produced oil using ASTM standard D2007-11 filtration (ASTM 2011), using n-pentane as the precipitating solvent. The water content in the produced oil samples is quantified using TGA-DTA (Thermogravimetric Analysis- Differential Thermal Analysis) (Chen et al., 2012; Kar and Hascakir, 2015). The clay content of produced oil

samples was determined through filtration. This was done by first using a filter paper of pore size ~25 μm, which is greater than clay particle size, to allow clays to flow through with the crude oil, and then a filter paper of much lower pore size (~2 μm) to separate the clays from oil and to quantify them (Kar et al., 2015b).

The intermolecular interactions between clay particles, asphaltenes, and water have been analysed via Fourier Transform Infrared Spectroscopy (FTIR) measurements using Agilent FTIR. Lastly, the effect of the polarity of asphaltenes in the presence of hydrocarbon solvents and water has been quantified through dielectric constant measurements using a cylindrical capacitor (Punase and Hascakir 2016). The theoretical dielectric constant values for mixtures of asphaltenes, DAO (deasphalted oil), with hydrocarbon solvents in the presence and absence of water is measured through summation of volumetric contribution of dielectric constant values of individual components (Lowry 1927).

4.4 Experimental Results

Visualization of Produced Oil Samples

The generated bulk oil samples from the steam and solvent-steam flooding experiments are visualized with optical microscopy in Fig. 4.1. After removal of free water and solvents from the samples, the produced oil samples are again observed via microscope (Fig. 4.2). All images are with 40X magnification.

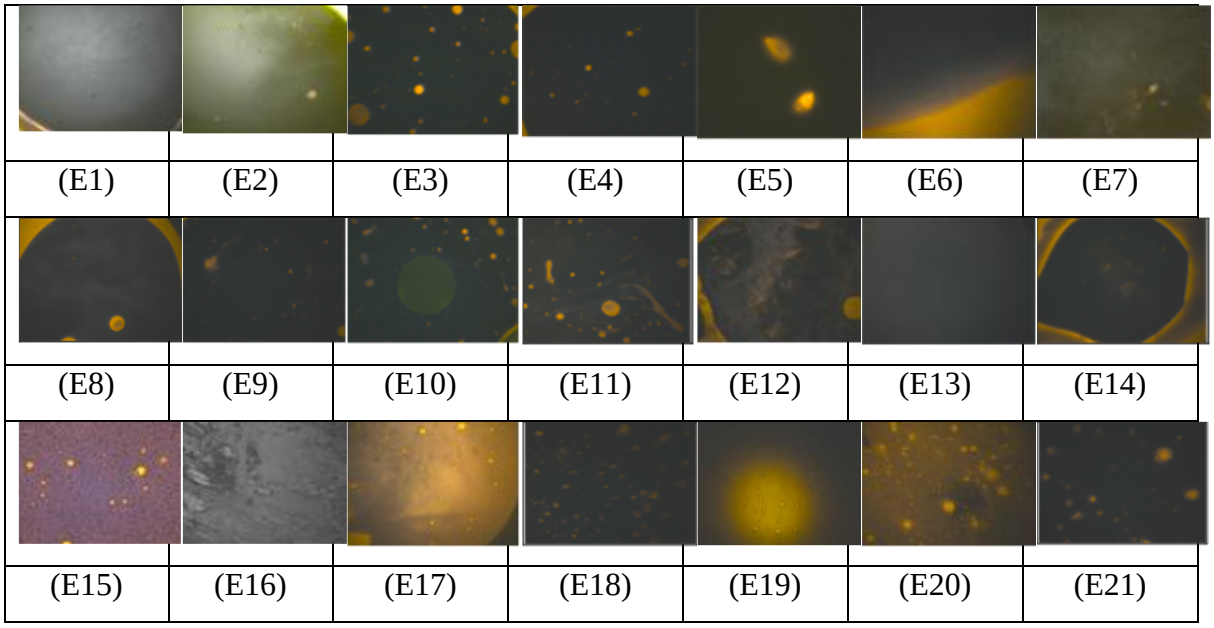

Fig. 4.1 - Microscopic images of generated emulsions in produced oil from all experiments

(40X Magnification)

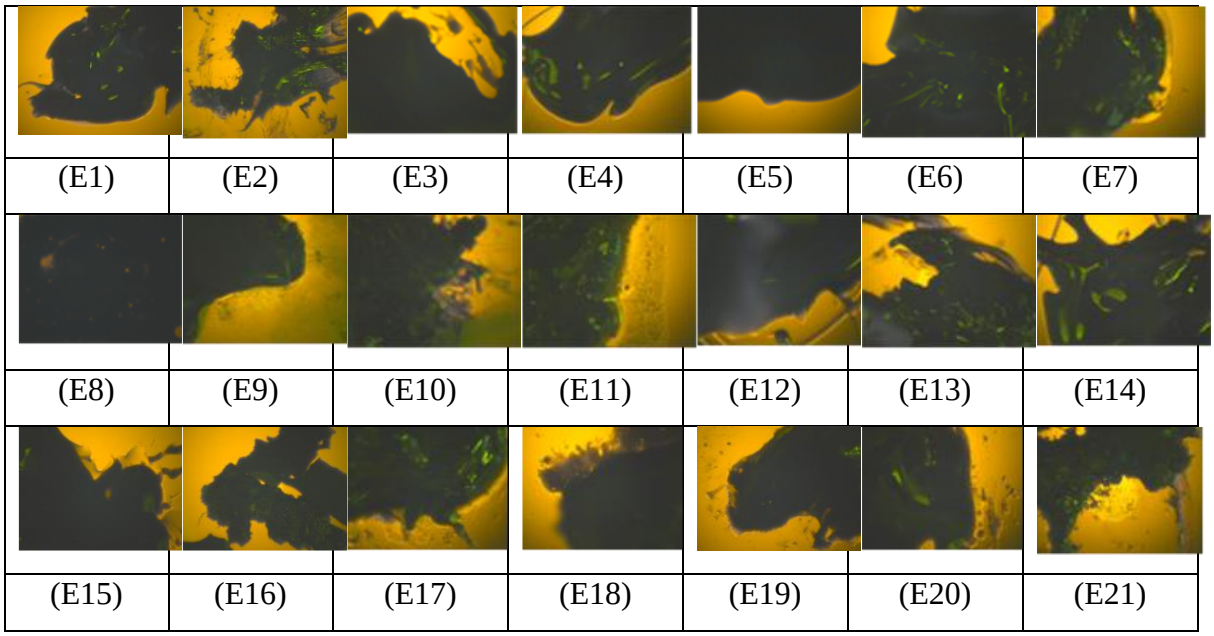

Fig. 4.2 - Microscopic images of produced oil after separation of free water and solvents

(40X Magnification)

Set 1 (No Clay) Experiments

The composition of bulk produced oil for Set1 (no clay) experiments are included in Fig. 4.3 in terms of asphaltenes, DAO, and water. Due to the absence of clays, the generated water-oil emulsions are not complex. Especially for E5 (nC6) and E6 (nC7), there are very few large coalescing water droplets observed in the instantaneous fluid, which get separated as free water. These can be linked to negligible water in the produced oil composition for E5 and E6 (Fig. 4.3). For E3 (C3) and E4 (nC4), the water droplets in the instantaneous emulsions are smaller in size and more dispersed throughout the oil, and are not completely separated as free water. However, the water layer can be seen to surround the oil layer after separation of free water (Fig. 4.2). E4 gave the highest asphaltene content in produced oil, which might be correlated to the small-sized numerous dispersed water droplets in the oil medium when viewed microscopically (Fig. 4.1). It should be noted that smaller the size of the dispersed phase, more stable are the emulsions. Asphaltenes are known to stabilize the water-oil emulsions by interacting with the polar water molecules and keeping them dispersed in the oil-phase. Water content in produced oil for solvent-steam flooding is found to be highest in steam-toluene co-injection (E7). Due to the presence of toluene, asphaltenes are believed to be more stable in the produced oil contributing to the preservation of asphaltene-water interaction in E7 owing to their similar polar nature. Moreover, there is no presence of clays to promote or demote these associations. It should be noted that the solvent-steam flooding processes improve the quality of the produced oil by lowering the amount of water carried into the bulk oil, as steam flooding (E1) is observed to have the highest water content.

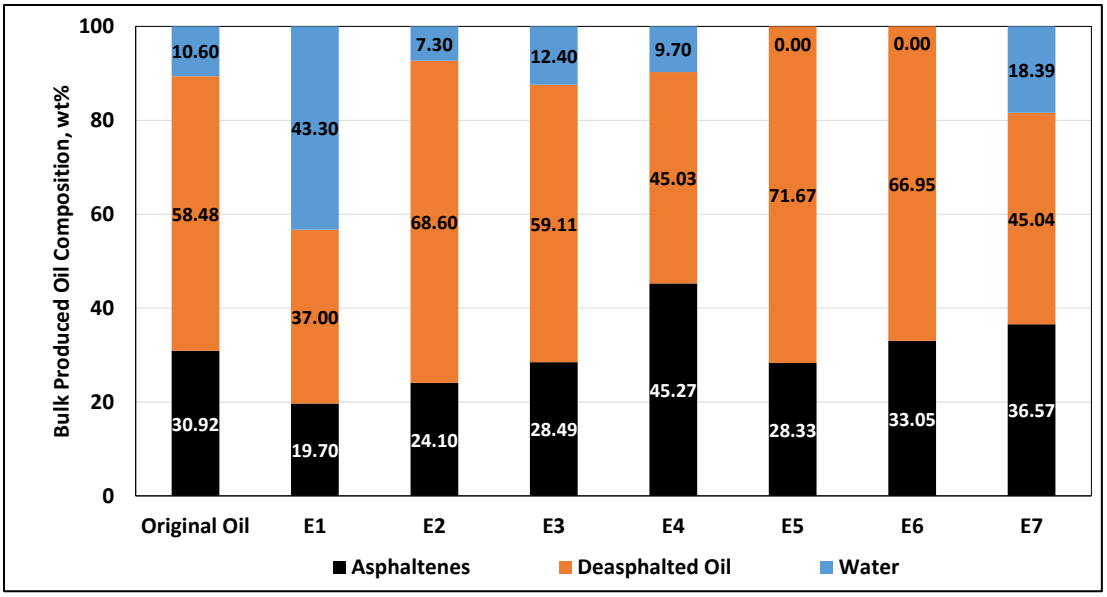

Fig. 4.3 - Bulk produced oil composition for Set 1 (No Clay) experiments

Based on the produced oil composition (Fig 4.3), the asphaltenes in produced oil have been plotted with respect to carbon number of injected hydrocarbon solvent in Fig. 4.4. [Note: Steam flooding alone has been assigned a number 0, while toluene has been assigned number 8 to denote highest polarity among injected solvents] From Fig. 4.4, it is observed that with increase in polarity of injected solvent with higher carbon number, the asphaltene content in produced oil increases. This follows an expected trend, since with increasing polarity of injected solvent, its asphaltene dissolving ability increases. It should be noted that n-pentane is used as the asphaltene precipitating solvent, and the experiment involving n-pentane co-injection with steam is observed as an outlier in Fig. 4.4. Not considering the data point for E4, the linear correlation improves considerably (R^2 = 0.9283).

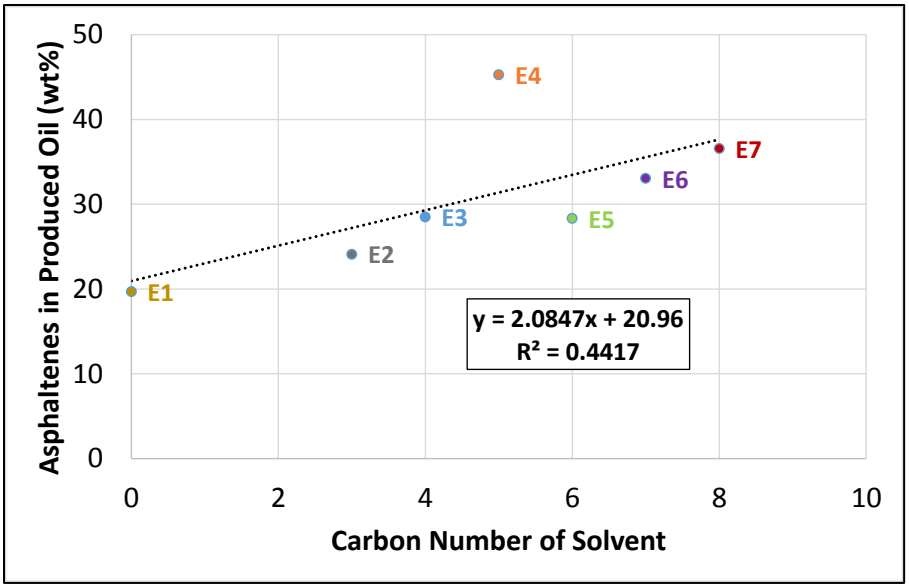

Fig. 4.4 - Carbon number of injected solvent to the asphaltenes content in produced oil (Set1-No Clay)

In addition to asphaltene content, the water content as well as the deasphalted oil (DAO) content in produced oil have been plotted with respect to carbon number of injected solvent, in Fig. 4.5 and Fig. 4.6, respectively. Water content and DAO content follow an opposite trend, with the lowest water amount and correspondingly highest DAO amount observed in E5 (steam+nC6) and E6 (steam+nC7). These are the produced oil samples with negligible (least complex) emulsions (Fig. 4.1). It can thus be inferred that these experiments had comparatively better quality of produced oil due to reduced water content, leading to reduced water-asphaltene polar interactions.

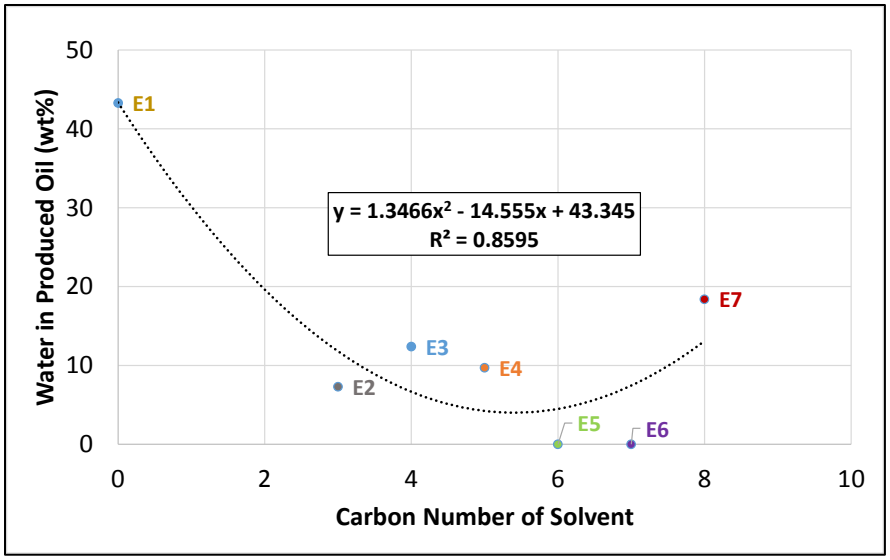

Fig. 4.5 - Carbon number of injected solvent to the water content in produced oil (Set1-No Clay)

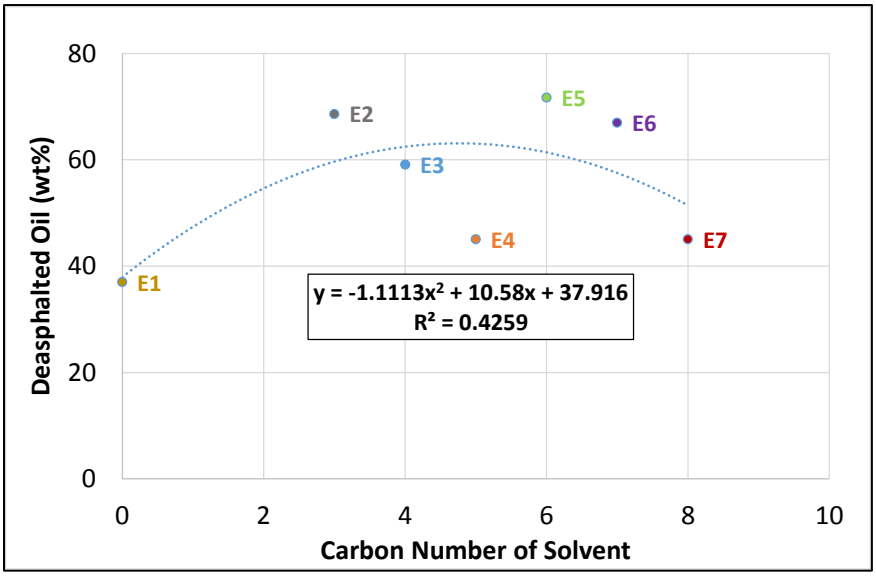

Fig. 4.6 - Carbon number of injected solvent to the deasphalted oil content in produced oil (Set1-No Clay)

Solvent co-injection with steam reduces the water migration into the produced oil considerably compared to steam flooding alone. Hence, solvent-steam flooding improves the quality of the produced oil.

Set 2 (Clay1) Experiments

Based on microscopic images of instantaneous emulsions, steam co-injection with C3 (E7), nC4 (E8), and nC5 (E9) gave the most stable emulsions, in terms of small-sized water droplets dispersed in the oil. However, after separation of free water and solvents, a separate clay-water layer can be observed clearly for these samples (Fig. 4.2), indicating affinity of migrated clay particles towards water, more than towards produced oil. It also displays that these emulsions, although more complex than Set1 emulsions, due to the presence of clays, are not very difficult to break, since clay-water layer can be separated from the obtained oil.

The breakdown of composition of bulk produced oil for Set2 experiments are provided in Fig. 4.7. Highest asphaltenes content is obtained in the produced oil resulting from steam-toluene co-injection (E12). This was expected, considering the solubility of asphaltenes in toluene.

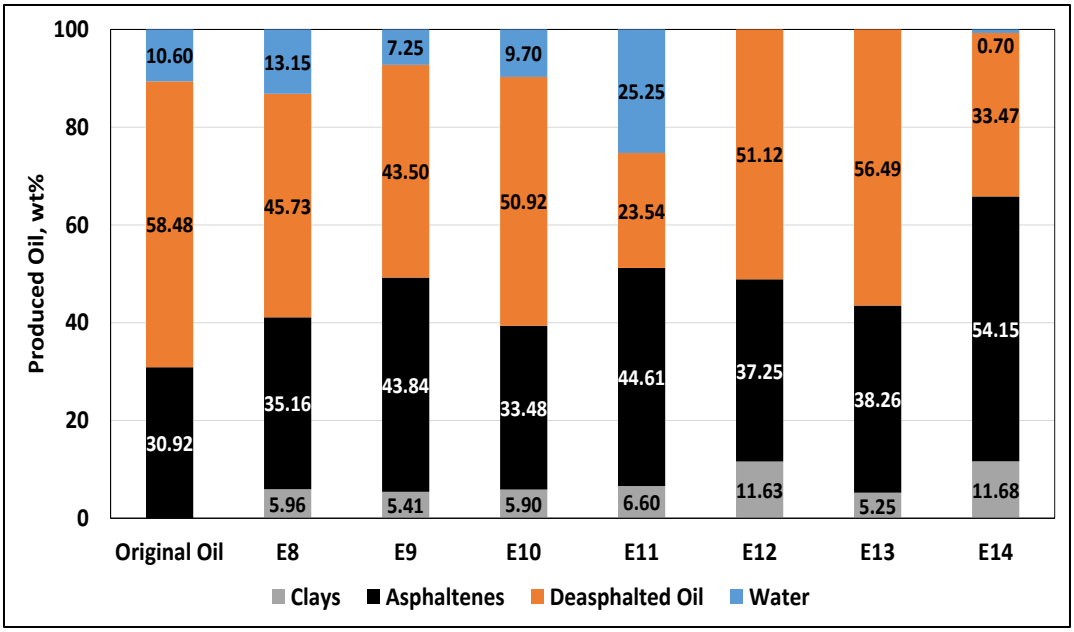

Fig. 4.7 - Bulk produced oil composition for Set 2 (Clay1) experiments

Due to the presence of migrated clay particles in the produced oil, the asphaltenes content and carbon number of injected solvent do not follow a definite linear trend. The relation between water and clay content with the asphaltenes have been tried to be analyzed further. Fig. 4.8 represents the net oil content with respect to migrated water-clay association in bulk produced oil.

The water-clay interaction is reduced with solvent co-injection and consequently, the net oil content is increased, except for n-pentane case (E11), which is supported by the water-oil emulsions observed in produced oil for E11 (Fig. 4.1). The best results are provided for n-hexane (E12), n-heptane (E13), and toluene (E14).

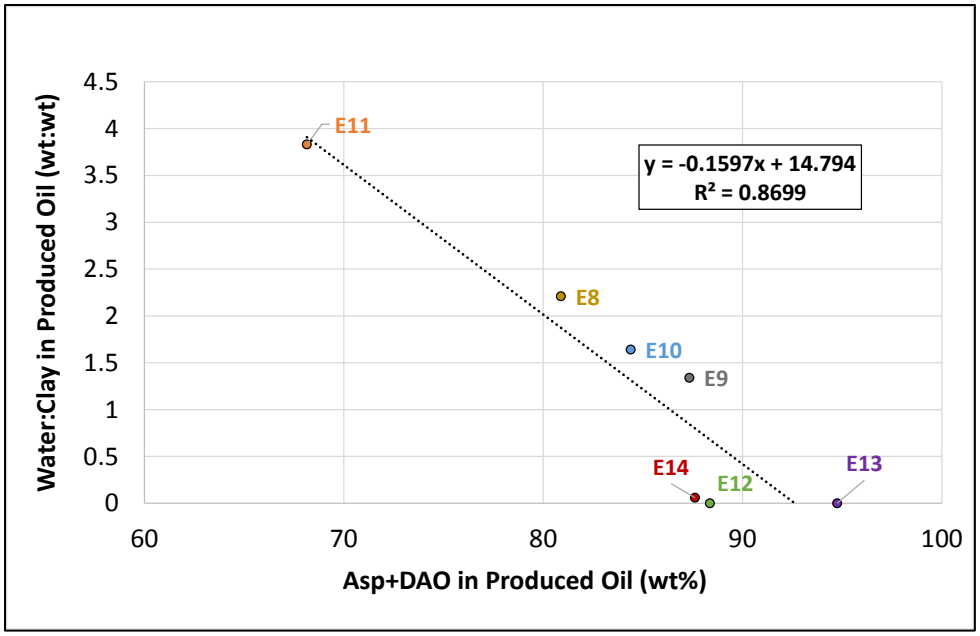

Fig. 4.8 - Net oil (asphaltenes and deasphalted oil) content with respect to water-clay interaction in bulk produced oil (Set2-Clay1)

This indicates the affinity of migrated Clay1 with the water, with E11 having the highest clay-water presence. This also explains the clay-water layer surrounding the oil, which is observed in the microscopic images of the produced oil samples (Fig. 4.2). In case of Set2 experiments, although there is fines migration into the bulk produced oil, the emulsions are not complex since the clays have a higher affinity towards water than towards the crude oil. The water-clay interaction is inversely related to the oil content in the bulk produced oil. The experiments with highest crude oil content and lowest amount of impurities in the form of water-clay interactions in the bulk produced oil are with propane (E9), n-hexane (E12), n-heptane (E13), and toluene (E14).

These relations strongly support the affinity of kaolinite towards the water phase in the bulk produced oil obtained from steam and solvent-steam flooding experiments.

Set 3 (Clay2) Experiments

For the produced oil samples from Clay2 experiments, all the instantaneous samples show significant water-in-oil emulsions (Fig. 4.1). In terms of produced oil composition, two trends are observed. Moving from low to high carbon number solvents and from paraffinic to aromatic solvents, there is an increase in asphaltenes content and decrease in water content (Fig. 4.9). Furthermore, all these samples are found to contain trapped water after separation of free water, thereby implying that the water-oil emulsions to be most severe for Set 3 (Clay2) compared to the other two sets of experiments.

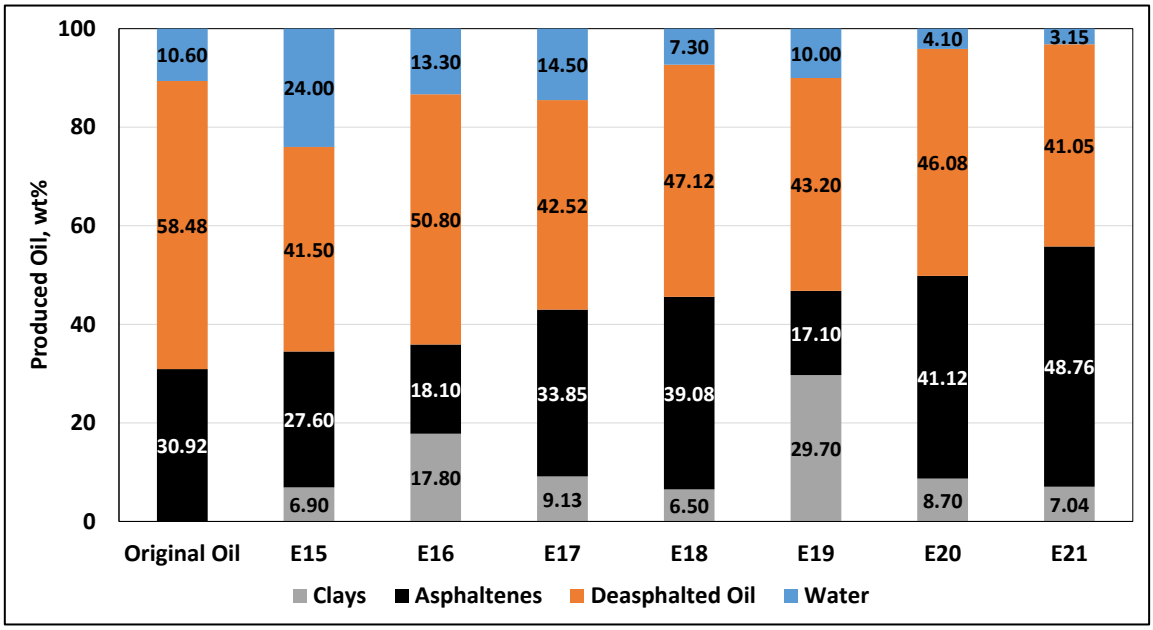

Fig. 4.9 - Bulk produced oil composition for Set 3 (Clay2) experiments

On the basis of the contribution of individual components in the bulk produced oil, the emulsion complexity has been tried to be analyzed. Similar to Set 2 analysis, the

asphaltenes in produced oil and carbon content of injected solvent fail to follow a specific trend.

A general observation made for all three sets of experiments is that the asphaltenes content in bulk produced oil for solvent-steam flooding experiments increases, moving from low to high carbon number paraffinic solvent, reaches a maxima for n-pentane-steam flooding, then decreases for higher carbon number solvents, and increases again for toluene-steam co-injection experiments (Fig. 4.3; Fig. 4.7; Fig. 4.9). It should be noted again that n-pentane has been used as the precipitating solvent for asphaltene content determination for all experiments. This has been done to minimize variations in controlling experimental parameters, such that all separated asphaltenes can be classified as n-pentane insoluble asphaltenes. The effect of asphaltene amount in oil on emulsion stability will be discussed in later sections.

Since asphaltenes are more polar, and presence of illite in Clay2 makes the clay more polar compared to Clay1, the focus on Set3 are asphaltenes-clay interactions in Fig. 4.10. The asphaltenes and water content in produced oil have also been correlated in Fig. 4.11. On comparing the clay and water amounts in bulk oil compared to asphaltenes content, it is observed that with increase in asphaltenes content, the clay and water content reduces. In particular, experiments E16 (steam+C3) and E19 (steam+nC6) are visualized to have less complex emulsions (Fig. 4.1), however, they have a high clay and water content. Consequently, to understand the emulsion formation and stabilization, the intermolecular forces of interaction between clays, asphaltenes, and water need to be studied.

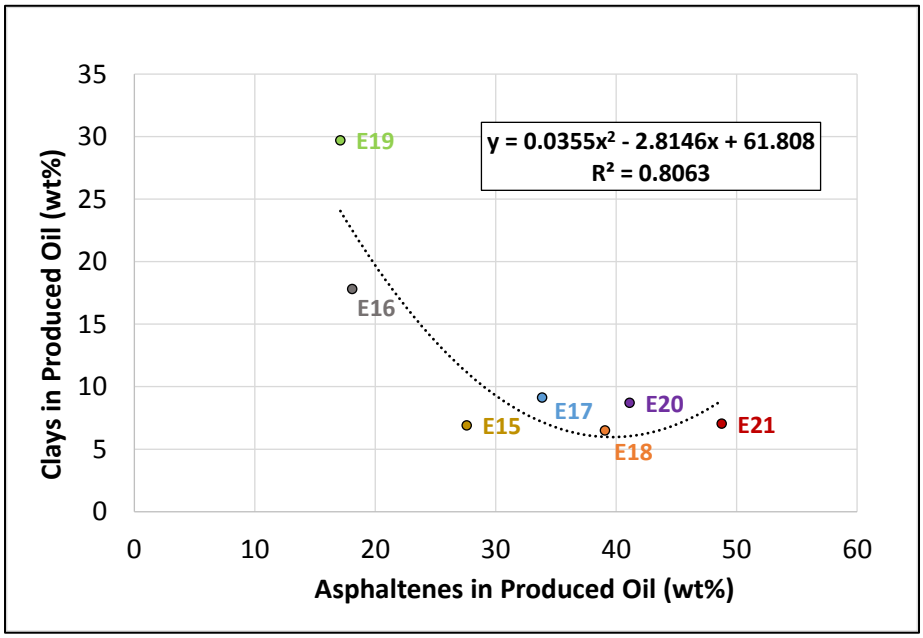

Fig. 4.10 - Asphaltenes with respect to clay content in bulk produced oil (Set3-Clay2)

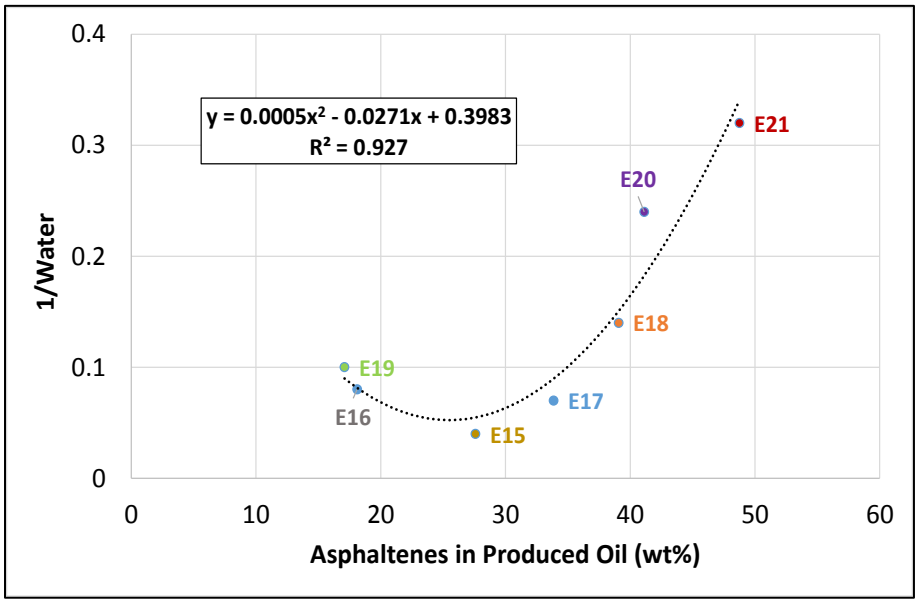

Fig. 4.11 - Asphaltenes with respect to water content in bulk produced oil (Set3-Clay2)

The following sections describe the structural arrangement of the clays, with the ionic charge concentration on clay surfaces. The intermolecular interactions between clay particles, water and asphaltenes have been analyzed via control experiments using FTIR measurements. The charge distribution on the asphaltenes surface determined using Inductively coupled plasma mass spectrometry (ICP-MS) has been tried to be compared with the elemental composition on clay surfaces through X-ray photoelectron spectroscopy (XPS) analysis. This has been performed to understand the nature and intensity of electrostatic forces of interactions between asphaltenes and clay particles. Finally, the changes in polarity and dispersion or aggregation of asphaltenes in the produced oil medium in the presence of different hydrocarbon solvents, and their impact on emulsion stability have been studied through dielectric constant measurements using an in-built capacitor.

Molecular Structure of Clays

Kaolinite is made up of tetrahedral sheets of silica attached to octahedral alumina sheets connected via oxygen atoms. Illite, on the other hand, is composed of an alumina octahedral sheet sandwiched between two silica tetrahedron sheets. Hence, it has a tetrahedron-octahedron-tetrahedron (TOT) structure (Grim, 1962). Due to differences in structure, illite has fewer hydroxyl groups at the grain surface compared to kaolinite. Fig. 4.12 represents the individual layered units for kaolinite and illite, adapted from Clay Mineralogy, University of Georgia.

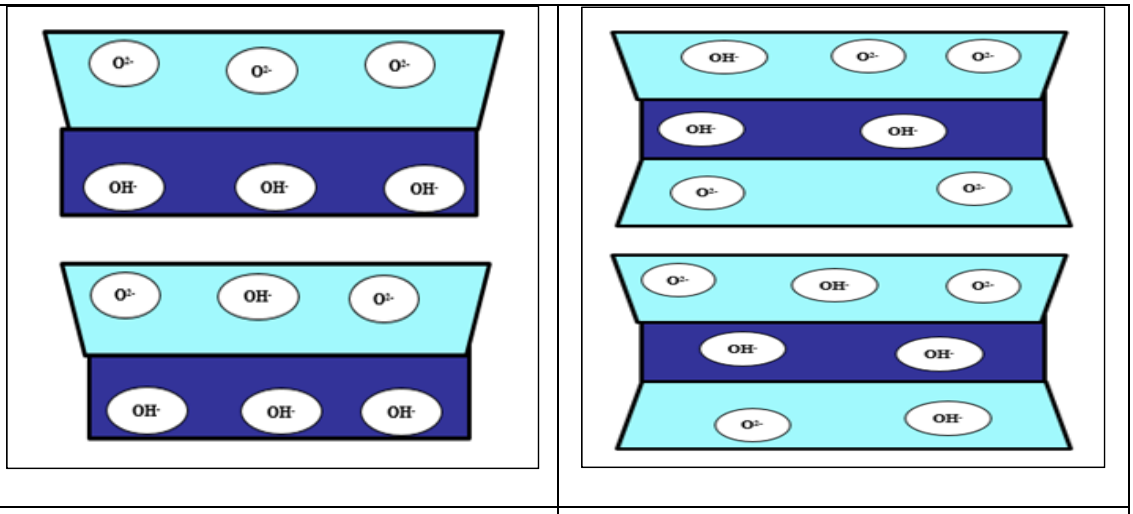

(A) Kaolinite unit | (B) Illite unit

Fig. 4.12 – Ion distribution in kaolinite and illite layered units

The silica layer (light blue layer) of kaolinite is concentrated with divalent oxygen ions at the edge, while the octahedral alumina layer (dark blue layer) consists mostly of hydroxyl (OH^-) ions. However, the divalent oxygen ions in the silica layer also have tendency of interacting with protons to form hydroxyls. This is represented by the following equation:

$$O^{2-} + H^+ = OH^-$$

Hence, the clay surfaces have an overall negative charge, with the charge intensity higher on the silica surface compared to alumina surface.

It should be noted that in this research, Clay1 constitutes of kaolinite, while Clay2 is a mixture of mostly kaolinite with some illite. Based on wettability changes, kaolinite is considered to be oil-wet, while illite has tendency to be water-wet. To understand the wettability behavior of clays, Bantignies et al. (1997) conducted FTIR measurements using asphaltenes precipitated from a heavy crude oil in Safaniya, Saudi Arabia. In the

presence of water, adsorption of asphaltenes on kaolinite was visualized by a drop in the FTIR spectrum corresponding to the inner and outer surface hydroxyl bond stretching. No such changes were observed in the illite spectrum in contact with asphaltenes, in the presence of water. Hence, kaolinite was classified as oil-wet and it was attributed to higher number of hydroxyl groups at the grain surface of kaolinite, compared to illite. However, it is known that clay behavior can differ depending on the nature of asphaltenes and the environmental conditions.

To analyze the interactions between clays, water, and asphaltenes specific to this research, control FTIR measurements were conducted by contacting Clay1 (kaolinite) and Clay2 (mixture of kaolinite and illite) with water, asphaltenes, and a mixture of water and asphaltenes. The results are provided in Fig. 4.13. The FTIR spectra are focused on the hydroxyl stretching zones on the clay surfaces. The absorbance stretches corresponding to wavenumbers 3622, 3655, and 3700 cm^{-1} represent the inner hydroxyl, inner surface, and inner surface as well as outer surface hydroxyl bonds, respectively (Bantignies et al. 1997).

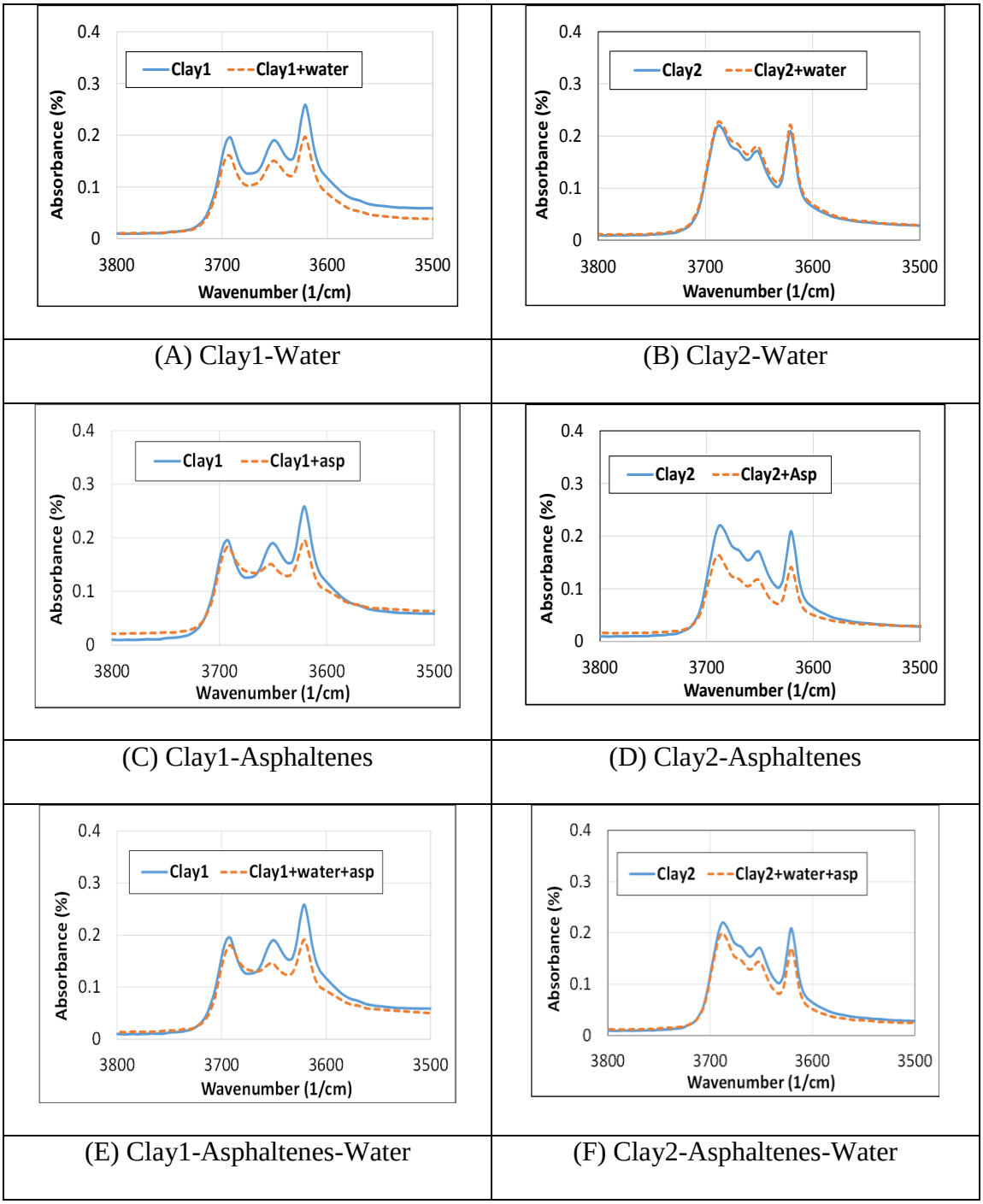

Fig. 4.13 - FTIR spectra of hydroxyl stretching regions on Clay surface during interaction with water, asphaltenes, and water-asphaltenes mixture

In the FTIR spectra, the amplitude of variations in the spectral lines depicts the intensity of forces of attraction between the components. Small variations indicate weak van der Waals forces of interactions. For clay-water interactions, it is observed that Clay1 has a higher affinity towards water compared to Clay2. This leads to the hypothesis that the water layer adsorption on Clay1 surface is more pronounced, thereby causing the Clay1 particles to mainly be coated by water, while Clay2 particles are mostly in the oil-phase, partially associated with the water droplets at the oil-water interface. The strong Clay1-water association can be correlated to the increasing emulsion complexity for Set2 (Clay1) produced oil samples with increase in clay-water interactions (Fig. 4.1; Fig. 4.8).

The intensity of asphaltene adsorption on clay surface is significantly higher for Clay2 compared to Clay1. It is inferred that for Clay2, both the inner and outer surface hydroxyl groups are contributing towards asphaltene adsorption, hence, Clay2 has a higher affinity towards asphaltenes, owing to stronger van der Waals forces of attraction. This supports the initial hypothesis of Clay2 particles to be more dispersed in the oil phase. Finally, when water is added to the clay-asphaltene mixture, there is no significant change in the hydroxyl stretching spectrum for Clay1 compared to the spectrum of Clay1-asphaltenes mixture (comparing Fig. 4.13C and Fig. 4.13E), but a reduced adsorption of asphaltenes on Clay2 surface is observed. This is denoted by a decrease in the amplitude of intermolecular forces of interaction between clay particles and asphaltenes, in the presence of water (comparing Fig. 4.13D and Fig. 4.13F). The structural arrangement of hydroxyl groups in Clay2 is believed to create an affinity towards both oil and water phases, indicating biwettable nature of Clay2.

The lipophilic nature of Clay2 is supported via a previously conducted study by Dubey and Waxman (1991), wherein tar-sand derived asphaltenes (using n-pentane as the precipitating solvent) were adsorbed on various mineral surfaces and the adsorbed asphaltene monolayer thickness on the clay surface was measured. Relative to this research, kaolin clay mineral was used which constituted mostly of kaolinite with around 15% illite. Its composition is similar to Clay2 used in this study. Among kaolin, kaolinite, and illite, the asphaltene monolayer thickness increased in terms of illite, kaolinite, and kaolin. In terms of weight of asphaltene monolayer per surface area of clay mineral, the reported values were 1.1, 2.0, and 2.2 mg/m^2 for illite, kaolinite, and kaolin, respectively. This can be linked to the favorable Clay2-asphaltenes association observed in this study.

Electrical Charges on Clay and Asphaltenes Surface

It is known that the negatively charged sites on clay surface are associated with the polar fractions of oil-phase, making them oil-wet (Al-Hadabi et al. 2016). Additionally, divalent cations in the environment have been found to have an affinity for ionic bond formation with clay minerals (Al-Hadabi et al. 2016). Hence, the elemental composition of the original oil (Oil2), and asphaltenes precipitated from Oil2 conducted via ICP-MS are compiled in Table 4.2 (Prakoso et al. 2016). The elemental atomic ratios for Clay1 and Clay2 are compared in Table 4.3, measured through XPS analysis (Ali 2015).

Table 4.2 - Metal composition of Oil2 and its asphaltenes
(Prakoso et al. 2016)

Metal (ppm)	Oil 2	Oil 2 Asphaltenes
Al	0	6.34
B	22.8	100
Ba	0	0
Ca	84.1	270
Cr	0	0
Cu	0	0
Fe	14.6	46.4
K	23	60
Mg	5.11	22.1
Mo	7.82	38.1
Na	235	1750
Ni	80.3	277
Pb	0	0
Si	7.49	41
Sn	1.5	12
Ti	3.18	14.3
V	218	775
Zn	5	9.01

Table 4.3 - Elemental atomic ratios based on XPS
(Ali 2015)

Element	Clay1	Clay2
Ca	0.225	0
Si	21.69	21.9
O	43.4	46.9
C	19.8	10.2
Fe	0.159	0.11
Al	20	20.39

The significant divalent cations present in the asphaltenes are reportedly calcium (Ca), iron (Fe), and magnesium (Mg). From Table 4.3, the Ca and Fe ions present on Clay1 are believed to reduce the net negative charge on the surface of Clay1, thereby reducing its affinity to oil-phase. These divalent cations cause repulsion forces between Clay1 particles and asphaltenes, thereby reducing the Clay1 dispersion in the oil-phase.

The elemental analyses of asphaltenes and clay surface further corroborates with the hypothesis of Clay1 particles covered with water layer, minimizing Clay1-asphaltene interactions, and Clay2 particles being more dispersed in the oil-phase, as well as in the oil-water interface (Fig. 4.14). The deposition of Clay2 particles at the oil-water interface leads to stabilization of emulsions through formation of Pickering emulsions (Pickering 1907).

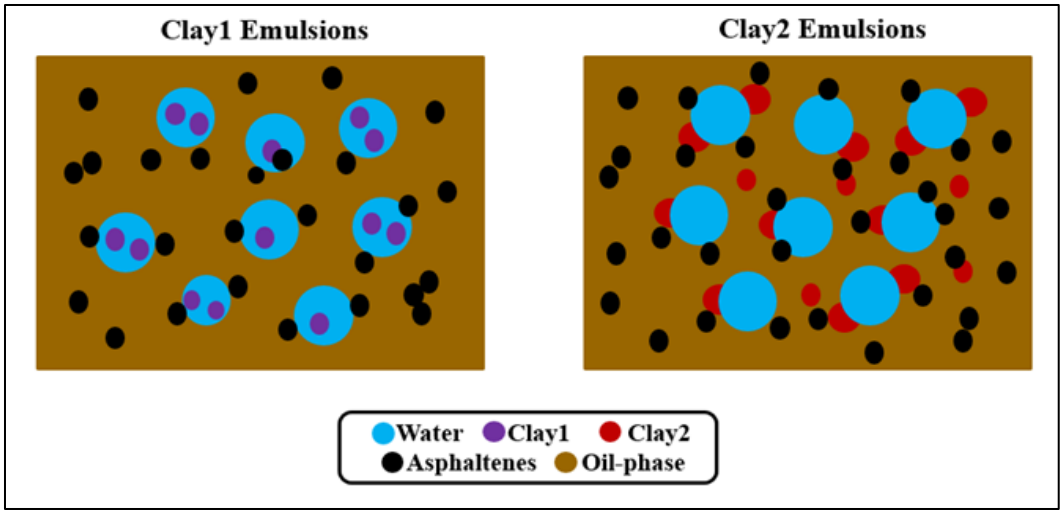

Fig. 4.14 - Hypothetical model of water-oil emulsions in presence of Clay1 and Clay2

After analyses of intermolecular interactions and elemental composition of clays and asphaltenes, the polarity of asphaltenes and its aggregation or dispersion in oil medium in the presence of solvents and water need to be investigated. The change in polarity of asphaltenes and their dispersion in different mixtures might have an impact on water-oil emulsion complexity.

Dielectric Constant Measurements

Dielectric constant measurements have been used to indirectly correlate with the polarity of a substance. If two or more substances are mixed together in volumetric proportions, the dielectric constant of the mixture should be equal to the summation of dielectric constant of the individual components in volumetric proportions, unless there are some impurities in the mixture or some components are interacting. In case of the steam and solvent-steam experiments, we have numerous components with varying degrees of polarity. The crude oil itself can be divided into non-polar fractions- saturates

and aromatics, and polar fractions- resins and asphaltenes. Saturates, aromatics, and resins are grouped together as maltenes or deasphalted oil (DAO). Among the hydrocarbon solvents, the paraffinic hydrocarbons- propane, n-butane, n-pentane, n-hexane, and n-heptane are non-polar, while the aromatic solvent toluene and water are polar in nature. Non-polar components are expected to be miscible with each other, meaning the DAO should favor paraffinic solvents. However, DAO also consists of resins, which are polar, though to a lesser degree than asphaltenes. Resins are expected to interact with the asphaltenes, polar solvents, and water. This makes the analysis of polarity of these mixtures complex.

In this study, the DAO component of the original bitumen sample has been mixed with hydrocarbon solvents, in the presence and absence of water, and the dielectric constant has been measured for the mixtures. The measured dielectric constants have been compared with the theoretical values obtained by summation of individual dielectric constants in a volumetric ratio (Lowry 1927). The measurements with n-pentane and liquid water are complicated as the n-pentane evaporates almost instantaneously owing to its low boiling point. Hence, measurements with n-pentane and water are difficult to analyze as the contribution of water in the dielectric constant of the mixture might be higher. Mixtures of asphaltenes with paraffinic solvents (nC5, nC6, nC7) have been not included in the measurements, since asphaltenes are insoluble, or soluble to a small degree in paraffinic solvents. Hence, homogeneous liquid mixture samples are difficult to be produced for measurements in the capacitor.

The density and dielectric constants for the individual components are provided in Appendix D. Table 4.4 includes the results.

Table 4.4 - Dielectric constant measurements for various mixtures of DAO of original bitumen, hydrocarbon solvents, and water

Mixture	ε Measured	ε Theoretical	% Difference
DAO+ nC5	2.14	1.78	20.47
DAO+nC6	2.15	1.82	18.38
DAO+nC7	2.10	1.84	14.35
DAO+Toluene	3.62	2.38	51.84
DAO+nC5+Water	14.15	6.91	104.57
DAO+nC6+Water	31.21	7.17	335.35
DAO+nC7+Water	20.10	7.40	171.56
DAO+Toluene+Water	54.35	9.19	491.62
Asp+Toluene	598.83	2.42	24645.04
Asp+Toluene+Water	96.67	10.20	847.75

For theoretical dielectric constant calculations of various mixtures, the following equation has been used, based on volumetric summation (Lowry 1927):

$$\epsilon_{\text{mix theoretical}} = \Sigma \epsilon_i y_i^f$$

where, $\epsilon_{\text{mix theoretical}}$ = Theoretical dielectric constant of mixture

ϵ_i = Theoretical dielectric constant of component i

y_i^f = Volumetric fraction of component i in mixture

Based on Table 4.4, it is observed that the lowest difference in measurements between measured and theoretical values are for the mixtures involving DAO and

paraffinic solvents (nC5, nC6, nC7). This is interpreted to be due to higher affinity of DAO towards paraffinic solvents because of their similar chemical nature. When water is added into the mixture, it theoretically increases the dielectric constant of the mixture considerably because of its high polarity. Mixtures involving DAO, hydrocarbon solvents, and liquid water are analyzed next. In case of paraffinic solvents, it is noted that the measured dielectric constant of the mixture increases from n-pentane to n-hexane, then decreases for n-heptane. Higher the mixture dielectric constant in presence of water, lower is the mutual interaction between the polar components in the mixture. N-hexane can thus be considered as an optimum paraffinic solvent which minimizes the polar interactions in the bulk crude oil, thereby reducing emulsion complexity.

Additional measurements have been conducted, by mixing asphaltenes of the original oil (Oil2) with toluene, in the presence and absence of water. The dielectric constant of the asphaltene-toluene mixture is found to increase by a significant value (Table 4.4). It is known that with increasing polarity of hydrocarbon solvent, asphaltenes are more dispersed in the medium (Dubey and Waxman 1991). The presence of toluene leads to summation of increased polarity of individual dispersed asphaltene particles, thereby increasing the overall dielectric constant considerably. Interestingly, in the presence of water, the mixture dielectric constant gets reduced. This is interpreted to be contributed by the polar-polar interactions between toluene and water which reduces the overall mixture polarity.

From Fig. 4.1, stable emulsions are observed for E21 (steam+toluene) experiment, in spite of low water and clay content in bulk produced oil (Fig. 4.10, Fig. 4.11). In the

presence of toluene, asphaltenes are more dispersed in the oil medium. As Clay2 particles have already been established to favor the oil-phase, the high amount and dispersion of asphaltenes in bulk produced oil promotes stabilization of water droplets in oil (E21), thereby leading to emulsion complexity.

Bitumen has been described to be composed of a high polarity micellar region, consisting of asphaltenes in the nucleus and less polar resins on the outer regions of the micelle. The micellae are surrounded by non-polar aliphatic fractions of crude oil, namely, saturates and aromatics. For any hydrocarbon solvent, the solvent power is defined as its ability to penetrate and dissolve the asphaltenes aggregates in the oil medium (Mitchell and Speight 1973). The energy required to counteract the association forces of the aggregates are contributed by the solvent's solution energy. More polar the solvent, higher is its solution energy. Hence, greater is its tendency to dissolve polar aggregates in crude oil. The lower solvent power of paraffinic solvent favors self-association, while the high solvent power of polar solvent favors dispersion forces.

From above analyses, it is inferred that the asphaltenes amount and aggregate form in bulk produced oil is an important parameter affecting water-oil emulsion stability. In presence of non-polar solvents, large asphaltene aggregates can provide an increased cluster size for association with clays. Conversely, with polar solvents, asphaltenes can get dispersed in the oil in the form of small-sized particles, resulting in higher surface area. This promotes higher tendency of small-sized water droplets to be dispersed throughout the oil phase, increasing emulsion stability in the produced oil.

Going back to the water-oil emulsions visualized in produced oil samples for Set3 (Clay2) experiments (Fig. 4.1), it can be implied that the dispersed water droplets observed for steam-toluene co-injection (E21) are a result of asphaltene dispersion in the crude oil. It can be interpreted as the amount of asphaltenes in the produced oil, and its aggregation or dispersion in the oil phase is a significant factor controlling emulsion stability.

Water and clay migration into produced oil are both unwanted impurities, and should be minimized to improve the cost economics in downstream treatment facilities. This is because water and clay particles have to be separated from the obtained oil to a degree which would be commercially acceptable. However, in terms of emulsion stability, the asphaltenes content and their dispersion in oil should also be considered, since these asphaltenes can stabilize the water droplets and lead to more rigorous methods of separating the water from oil. This will eventually increase the economics of the whole process. The migration of water and clays into the obtained oil is inevitable. Hence, an ideal solvent should be selected for solvent-steam flooding processes which would have an optimum asphaltene amount and dispersion in the oil medium, and thereby, minimized asphaltene-clay-water associations, leading to reduced water-oil emulsion complexity.

Specific to this research, liquid paraffinic solvents like n-hexane are suggested as better hydrocarbon solvents to be used in co-injection with steam for bitumen recovery, compared to aromatic solvents, to minimize emulsion stability.

4.5 Conclusions

In the absence of clays, co-injection of solvents along with steam improves the quality of produced oil by promoting less water migration into the bulk oil phase, hence reducing water-asphaltenes polar interactions.

Water-clay interactions are found to dominate in case of Clay1 (kaolinite) experiments, while asphaltene-clay associations are more severe in Clay2 (kaolinite-illite mixture) experiments. Clay1-water associations cause them to form a separate layer surrounding the oil phase, thereby proving to be easier to separate and result in less complex emulsions. On the other hand, Clay2 is more dispersed in the oil phase, having a strong affinity towards oil phase. The formation of Pickering emulsions due to deposition of Clay2 particles at the oil-water interface is believed to increase the complexity of water-oil emulsions for Set3 experiments. This is caused by the biwettable nature of Clay2, which is composed of mostly kaolinite with some illite.

The reduced negative charge on Clay1 surface due to the presence of divalent cations is believed to reduce the affinity of Clay1 towards oil-phase. Additionally, presence of polar solvents is found to increase the polarity and dispersion of asphaltenes in oil, leading to water-oil emulsion stability.

5. CONCLUSIONS

In this research, water-oil emulsion formation mechanism in the obtained oil for steam and solvent-steam flooding processes has been studied via intermolecular interactions between polar crude oil fractions (asphaltenes), water, and migrated clay particles. The wettability of clays has been analyzed via control FTIR measurements and elemental composition of clay surface and asphaltenes. Finally, the change in polarity and aggregation of apshaltenes in oil in the presence of various non-polar and polar hydrocarbon solvents, and its impact on emulsion stability have been studied.

Initially, propane-SAGD resulted in improved efficiency of SAGD process owing to miscibility of propane in crude oil, lowering the interfacial tension and mobilizing the oil. Additionally, it improved the produced oil quality by reducing water migration, hence resulting in less complex water-oil emulsions.

The impact of various hydrocarbon solvents on emulsion complexity during solvent-steam flooding processes is then analyzed by generation of fresh emulsions via a series of steam and solvent-steam flooding experiments, in the presence and absence of clays (kaolinite, mixtute of kaolinite and illite) in the core. The solubilizing power of asphaltenes with increase in carbon number of paraffinic solvent and going from non-polar paraffinic to polar aromatic solvent is seen to increase, in both the displaced residual oil, as well as the produced oil. However, in the presence of clays, the cumulative oil recovery decreases due to alteration of clay wettability during the thermal recovery process. Highest amount of oil trapping is observed for experiments with Clay2, indicating its affinity towards oil-phase.

In the absence of clays, paraffinic solvents result in reduced water-asphaltenes association and higher amount of deasphalted oil, thus improving the produced oil quality and minimizing water-oil emulsion tendency. Going from Clay1 to Clay2, water-oil emulsions are found to get more stabilized in oil medium. Intermolecular van der Waals forces of attraction are found to be higher between Clay1 and water, making it more water-wet. This is inferred to be caused by presence of divalent cations on Clay1 surface, reducing its net negative surface charge, and lowering its tendency to interact with the charged asphaltene particles. The presence of these cations on Clay1 surface promotes coating of water and leads to disturbance in emulsion stability due to tendency of coalescence of water droplets. On the contrary, Clay2 particles are found to have significant van der Waals forces of attraction with asphaltenes, which leads to Clay2 being dispersed in the oil-phase and at the oil-water interface, thereby stabilizing it by formation of Pickering emulsions. This results from the partially biwettable nature of Clay2 particles.

Lastly, the presence of polar solvent is found to increase the polarity and dispersion tendency of asphaltenes in the produced oil, leading to further stabilization of small water droplets in oil. Liquid paraffinic solvents are suggested to be optimum hydrocarbon solvents to minimize clay-water-asphaltene interactions, hence, lowering emulsion complexity in produced oil for bitumen recovery via solvent-steam flooding.

REFERENCES

Ahmed, W. 2008. Contrast in Clay Mineralogy and their Effect on Reservoir Properties in Sandstone Formations. *Bulletin of the Chemical Society of Ethiopia* **22** (01): 41-65. http://dx.doi.org/10.4314/bcse.v22i1.61333

Akbarzadeh, K., Hammami, A., Kharrat, A., Zhang, D., Allenson, S., Creek, J..., Mullins, O. C. 2007. Asphaltenes—Problematic but Rich in Potential. *Oilfield Review* **19** (02): 22-43.

Al Hadabi, I., Sasaki, K., and Sugai, Y. (2016). Effect of Kaolinite on Water-in-Oil Emulsion Formed by Steam Injection during Tertiary Oil Recovery: A Case Study of an Omani Heavy Oil Sandstone Reservoir with a High Kaolinite Sludge Content. Energy & Fuels, 30(12), 10917-10924. http://pubs.acs.org/doi/abs/10.1021/acs.energyfuels.6b01822

Al-Murayri, M. T., Maini, B. B., Harding, T. G., Oskouei, J. 2016. Cracked Naphtha Co-Injection in Steam-Assisted Gravity Drainage. *Energy & Fuels* **30**(07): 5330-5340. http://pubs.acs.org/doi/abs/10.1021/acs.energyfuels.5b02773

Ali, M. 2015. Produced Water Quality Based on Thermal Recovery Processes and After Interaction with Shale. MSc Thesis, Texas A&M University.

Ali, S. M.; Abad, B. 1976. Bitumen Recovery from Oil Sands, using Solvents in Conjunction with Steam. *Journal of Canadian Petroleum Technology* **15**(03). PETSOC-76-03-11-P. http://dx.doi.org/10.2118/76-03-11

Alvarado, V., Manrique, E. 2010. Enhanced Oil Recovery: An Update Review. *Energies* **3**(09): 1529-1575. http://dx.doi.org/10.3390/en3091529

Amyx, J. W., Bass, D. M., Whiting, R. L. 1960. Petroleum Reservoir Engineering, McGraw Hill, ISBN 07-001600-3: 103-104.

ASTM. 2011. D2007-11: Standard Test Method for Characteristic Groups in Rubber Extender and Processing Oils and Other Petroleum-Derived Oils by the Clay-Gel Absorption Chromatographic Method.

Bagci, A. S., Gumrah, F. 2004. Effects of CO2 and CH4 Addition to Steam on Recovery of West Kozluca Heavy Oil. Presented in SPE International Thermal Operations and Heavy Oil Symposium and Western Regional Meeting, 16-18 March, Bakersfield, California. Society of Petroleum Engineers. SPE-86953-MS. https://doi.org/10.2118/86953-MS

Bantignies, J. L., Moulin, C. C. D., Dexpert, H. 1997. Wettability Contrasts in Kaolinite and Illite Clays: Characterization by Infrared and X-ray Absorption Spectroscopies. *Le Journal de Physique IV* **7**(C2): C2-867- C2-869. https://doi.org/10.1051/jp4:1997261

Bennion, D. B., Thomas, F. B., Sheppard, D. A. 1992. Formation Damage Due to Mineral Alteration and Wettability Changes during Hot Water and Steam Injection in Clay Bearing Sandstone Reservoirs. Presented in SPE Formation Damage Control Symposium, 26-27 February, Lafayette, Louisiana. SPE-23783-MS. https://doi.org/10.2118/23783-MS

Binner, E. R., Robinson, J. P., Silvester, S. A., Kingman, S. W., Lester, E. H. 2014. Investigation into the Mechanisms by which Microwave Heating Enhances Separation of Water-in-Oil Emulsions. *Fuel* **116**: 516-521. https://doi.org/10.1016/j.fuel.2013.08.042

Butler, R. M., McNab, G. S., Lo, H. Y. 1981. Theoretical Studies on the Gravity Drainage of Heavy Oil during In-situ Steam Heating. *The Canadian Journal of Chemical Engineering* **59**(04): 455-460. http://onlinelibrary.wiley.com/doi/10.1002/cjce.5450590407/full

Butler, R. M. 1982. Method for Continuously Producing Viscous Hydrocarbons by Gravity Drainage While Injecting Heated Fluids. US Patent No. 4,344,485. Washington, DC: U.S. Patent and Trademark Office.

Butler, R. M. 1998. SAGD comes of Age! *Journal of Canadian Petroleum Technology* **37**(07). PETSOC-98-07-DA. http://dx.doi.org/10.2118/98-07-DA

Butler, R.M. (1999). Steam and Gas Push (SAGP). *Journal of Canadian Petroleum Technology* **38**(03). PETCOS-97-137-P. http://dx.doi.org/10.2118/99-03-05

Carbognani, L., Orea, M., Fonseca, M. 1999. Complex Nature of Separated Solid Phases from Crude Oils. *Energy & Fuels* **13**(02): 351-358. http://pubs.acs.org/doi/abs/10.1021/ef9801975

Chappell, M. A., Laird, D. A., Thompson, M. L., Li, H., Teppen, B. J., Aggarwal, V., Johnston, C. T., Boyd, S. A. 2005. Influence of Smectite Hydration and Swelling on Atrazine Sorption Behavior. *Environmental Science & Technology* **39**(09): 3150-3156. http://pubs.acs.org/doi/abs/10.1021/es048942h

Chen, K., Liu, H., Guo, A., Ge, D., Wang, Z. 2012. Study of the Thermal Performance and Interaction of Petroleum Residue Fractions during the Coking Process. *Energy & Fuels* **26**(10): 6343-6351. http://pubs.acs.org/doi/abs/10.1021/ef301378g

Cho, Y., Na, J. G., Nho, N. S., Kim, S., Kim, S. 2012. Application of Saturates, Aromatics, Resins, and Asphaltenes Crude Oil Fractionation for Detailed Chemical Characterization of Heavy Crude Oils by Fourier Transform Ion Cyclotron Resonance Mass Spectrometry Equipped with Atmospheric Pressure Photoionization. *Energy & Fuels* **26**(05): 2558-2565. http://pubs.acs.org/doi/abs/10.1021/ef201312m

Coelho, R.S.C. 2016. Microscopic Displacement of Bitumen During Solvent-Steam-Flooding: Effects of Reservoir Clays and Solvent Type. MSc Thesis, Texas A&M University.

Coelho, R.S.C., Ovalles, C., Benson, I.P., Hascakir, B. 2017. Clay-Asphaltene Interactions during Hybrid Solvent-Steam Injection into Bitumen Reservoirs, *Journal of Petroleum Science and Engineering* **150**: 203-207. http://dx.doi.org/10.1016/j.petrol.2016.12.006

Czarnecka, E., Gillott, J. E. 1980. Formation and Characterization of Clay Complexes with Bitumen from Athabasca Oil Sand. *Clays and Clay Minerals* **28**(03): 197-203.

Dubey, S. T., Waxman, M. H. 1991. Asphaltene Adsorption and Desorption from Mineral Surfaces. *SPE Reservoir Engineering* **6**(03): 389-395. https://doi.org/10.2118/18462-PA

Dusseault, M. B. 2001. Comparing Venezuelan and Canadian Heavy Oil and Tar Sands. Presented in Canadian International Petroleum Conference, 12-14 June, Calgary, Alberta. Petroleum Society of Canada. https://doi.org/10.2118/2001-061

Edmunds, N. 2000. Investigation of SAGD Steam Trap Control in Two and Three Dimensions. *Journal of Canadian Petroleum Technology* **39**(01). PETSOC-00-01-02. https://doi.org/10.2118/00-01-02

Elliot, K. T., Kovscek, A. R. 2001. A Numerical Analysis of the Single-well Steam Assisted Gravity Drainage Process (SW-SAGD). *Petroleum Science and Technology* 19(07-08): 733-760. http://www.tandfonline.com/doi/abs/10.1081/LFT-100106898

Evdokimov, I. N., Losev, A. P. 2014. Microwave Treatment of Crude Oil Emulsions: Effects of Water Content. Journal of Petroleum Science and Engineering, 115, 24-30. https://doi.org/10.1016/j.petrol.2014.02.006

Fingas, M. 2014. Water-in-Oil Emulsions: Formation and Prediction. *Journal of Petroleum Science Research* **3**(01): 38-49.

Goite, J. G., Mamora, D. D., Ferguson, M. A. 2001. Experimental Study of Morichal Heavy Oil Recovery Using Combined Steam and Propane Injection. Presented in SPE Latin American and Caribbean Petroleum Engineering Conference, 25-28 March, Buenos Aires, Argentina. Society of Petroleum Engineers. SPE-69566-MS. https://doi.org/10.2118/69566-MS

Goual, L., Firoozabadi, A. 2002. Measuring Asphaltenes and Resins, and Dipole Moment in Petroleum Fluids. *AIChE Journal* **48**(11): 2646-2663. http://onlinelibrary.wiley.com/doi/10.1002/aic.690481124/epdf

Green, D. W., Willhite, G. P. 1998. Enhanced Oil Recovery, Richardson, Tex.: Henry L. Doherty Memorial Fund of AIME, Society of Petroleum Engineers.

Grills, T. L., Vandal, B., Hallum, F., Trost, P. 2002. Case history: horizontal well SAGD technology is successfully applied to produce oil at LAK Ranch in Newcastle Wyoming. Presented in SPE International Thermal Operations and Heavy Oil Symposium and International Horizontal Well Technology Conference. Society of Petroleum Engineers. SPE-78964-MS. https://doi.org/10.2118/78964-MS

Grim, R. E. 1962. Clay Mineralogy. *Science* **135**(3507): 890-898.

Groenzin, H., Mullins, O. C. 2000. Molecular Size and Structure of Asphaltenes from Various Sources. *Energy & Fuels* **14**: 677. http://pubs.acs.org/doi/abs/10.1021/ef990225z

Haghighat, P., Maini, B. B. 2010. Role of Asphaltene Precipitation in VAPEX Process. *Journal of Canadian Petroleum Technology* **49**(03). SPE-134244-PA. http://dx.doi.org/10.2118/134244-PA

Hall, A. L., Bowman, R. W. 1973. Operation and Performance of the Slocum Thermal Recovery Project. *Journal of Petroleum Technology* **25**(04): 402-408. SPE-2843-PA. https://doi.org/10.2118/2843-PA

Hamm, R. A., Ong, T. S. 1995. Enhanced Steam-Assisted Gravity Drainage: A New Horizontal Well Recovery Process for Peace River, Canada. *Journal of Canadian Petroleum Technology* **34**(04). PETSOC-95-04-03. https://doi.org/10.2118/95-04-03

Hascakir, B. 2016. How to Select the Right Solvent for Solvent-Aided Steam Injection Processes. *Journal of Petroleum Science and Engineering* **146**: 746-751. https://doi.org/10.1016/j.petrol.2016.07.038

IEA 2013. Resources to Reserves: Oil, Gas and Coal Technologies for the Energy Markets of the Future. http://www.iea.org/publications/freepublications/publication/Resources2013.pdf

Jewell, D. M., Weber, J. H., Bunger, J. W., Plancher, H., Latham, D. R. 1972. Ion-Exchange, Coordination, and Adsorption Chromatographic Separation of Heavy-end Petroleum Distillates. *Analytical Chemistry* **44**(08): 1391-1395. http://pubs.acs.org/doi/abs/10.1021/ac60316a003

Jiang, Q., Butler, R., Yee, C.T. 1998. The Steam and Gas Push (SAGP) – 2: Mechanism Analysis and Physical Model Testing. Presented in 49th Annual Technical Meeting of The Petroleum Society, Calgary, Alberta, Canada. PETCOS 98-43. http://dx.doi.org/10.2118/98-43

Jimenez, J. 2008. The Field Performance of SAGD Projects in Canada. Presented in International Petroleum Technology Conference, 3-5 December, Kuala Lumpur, Malaysia. IPTC-12860-MS. https://doi.org/10.2523/IPTC-12860-MS

Kar, T., Hascakir, B. 2015. The Role of Resins, Asphaltenes, and Water in Water–Oil Emulsion Breaking with Microwave Heating. *Energy & Fuels* **29**(06): 3684-3690. http://pubs.acs.org/doi/abs/10.1021/acs.energyfuels.5b00662

Kar, T., Yeoh, J., Ovalles, C., Rogel, E., Benson, I. P., Hascakir, B. 2015a. The Impact of Asphaltene Precipitation and Clay Migration on Wettability Alteration for Steam Assisted Gravity Drainage (SAGD) and Expanding Solvent-SAGD (ES-SAGD). Presented in SPE Canada Heavy Oil Technical Conference. SPE-174439-MS. http://dx.doi.org/10.2118/174439-MS

Kar, T., Mukhametshina, A., Unal, Y., Hascakir, B. 2015b. The Effect of Clay Type on Steam Assisted Gravity Drainage Performance. *Journal of Canadian Petroleum Technology* **54**(06): 412-423. SPE-173795-PA. http://dx.doi.org/10.2118/173795-PA

Kar, T., Ovalles, C., Rogel, E., Vien, J., Hascakir, B. 2016. The Residual Oil Saturation Determination for Steam Assisted Gravity Drainage (SAGD) and Solvent-SAGD. *Fuel* **172**: 187-195. http://dx.doi.org/10.1016/j.fuel.2016.01.029

Kar, T., Nezhad, P. B., Ng, A. Z. Y., Ovalles, C., Benson, I. P., Hascakir, B. 2017. Mobilization of Trapped Residual Oil via Secondary SAGD with Propane. SPE-185684-MS. https://doi.org/10.2118/185684-MS

Kilpatrick, P. K. 2012. Water-in-Crude Oil Emulsion Stabilization: Review and Unanswered Questions. *Energy & Fuels* **26**(07): 4017-4026. http://pubs.acs.org/doi/abs/10.1021/ef3003262

Kokal, S. L. 2005. Crude Oil Emulsions: A State-of-the-art Review. *SPE Production & Facilities* **20**(01): 5-13. SPE 77497-PA. https://doi.org/10.2118/77497-PA

Kotlyar, L. S., Ripmeester, J. A., Sparks, B. D., Montgomery, D. S. 1988. Characterization of Organic-rich Solids Fractions Isolated from Athabasca Oil Sand using a Cold Water Agitation Test. *Fuel* **67**(02): 221-226. https://doi.org/10.1016/0016-2361(88)90267-0

Kovscek, A. 2012. Emerging Challenges and Potential Futures for Thermally Enhanced Oil Recovery. *Journal of Petroleum Science and Engineering* **98**: 130-143. https://doi.org/10.1016/j.petrol.2012.08.004v

Leaute, R. P. 2002. Liquid Addition to Steam for Enhancing Recovery (LASER) of Bitumen with CSS: Evolution of Technology from Research Concept to a Field Pilot at Cold Lake. Presented in SPE International Thermal Operations and Heavy Oil Symposium and International Horizontal Well Technology Conference, 4-7 November, Calgary, Alberta, Canada. Society of Petroleum Engineers. SPE-79011-MS. https://doi.org/10.2118/79011-MS

Lecture Notes for Clay Mineralogy, University of Georgia. http://clay.uga.edu/courses/8550/CM19.html

Leontaritis, K. J., Amaefule, J. O., Charles, R. E. 1994. A Systematic Approach for the Prevention and Treatment of Formation Damage caused by Asphaltene Deposition. *SPE Production & Facilities* **9**(03): 157-164. SPE-23810-PA. http://dx.doi.org/10.2118/23810-PA

Levine, S., Bowen, B. D., Partridge, S. J. 1989. Stabilization of Emulsions by Fine Particles I. Partitioning of Particles between Continuous Phase and Oil/Water Interface. *Colloids and Surfaces* **38**(02): 325-343. https://doi.org/10.1016/0166-6622(89)80271-9

Li-qiang, Y., Da-sheng, Z., Yu-huan, S. 2006. SAGD as Follow-Up to Cyclic Steam Stimulation in a Medium Deep and Extra Heavy-Oil Reservoir. In Proceedings of International Oil & Gas Conference and Exhibition, 5-7 December, Beijing, China. Society of Petroleum Engineers. SPE-104406-MS. https://doi.org/10.2118/104406-MS

Lowry, H. H. 1927. The Significance of the Dielectric Constant of a Mixture. *Journal of the Franklin Institute* **203**(03): 413-439. https://doi.org/10.1016/S0016-0032(27)91179-X

Luffel, D. L., Herrington, K. L., Walls, J. D. 1993. Effect of Drying on Travis Peak Cores Containing Fibrous Illite. *SPE Advanced Technology Series* **1**(01). SPE-20725-PA. https://doi.org/10.2118/20725-PA

Luks, K. D., Turek, E. A., Baker, L. E. 1987. Calculation of Minimum Miscibility Pressure. *SPE Reservoir Engineering* **2**(04): 501-506. SPE-14929-PA. https://doi.org/10.2118/14929-PA

Macko, S. A., Curry, D. J., Kiceniuk, J. W., Simpler, K. T. 1988. Variations in Geochemical Character of Asphaltenes from a Source Rock in Contact with an Oil Reservoir. *Organic Geochemistry* **13**(1-3): 273-281. https://doi.org/10.1016/0146-6380(88)90046-0

Mamora, D. D., Rivero, J. A., Hendroyono, A. 2003. Experimental and Simulation Studies of Steam-Propane Injection for the Hamaca and Duri Fields. In SPE Annual Technical Conference and Exhibition, 5-8 October, Denver, Colorado. Society of Petroleum Engineers. SPE-84201-MS. https://doi.org/10.2118/84201-MS

Martinez-Palou, R., Ceron-Camacho, R., Chavez, B., Vallejo, A. A., Villanueva-Negrete, D., Castellanos, J., Karamath, J., Reyes, J., Aburto, J. 2013. Demulsification of Heavy Crude Oil-in-Water Emulsions: A Comparative Study between Microwave and Thermal Heating. *Fuel* **113**: 407-414. https://doi.org/10.1016/j.fuel.2013.05.094

Mattison, B. W., King, B., Parry, D., Knight, J., Slevinsky, B. 2001. Petro-Canada's Mackay River In-Situ Oil Sands Project: Current Scope and Status. 201-206. http://www.cspg.org/documents/Conventions/Archives/Annual/2001/8-047.pdf

Mbaba, P. E., Caballero, E. P. 1983. Field Application of an Additive Containing Sodium Metasilicate during Steam Stimulation. Presented in SPE Annual Technical Conference and Exhibition, 5-8 October, San Francisco, California. Society of Petroleum Engineers. SPE-12058-MS. https://doi.org/10.2118/12058-MS

Mendez, Z., Alvarez, J. M., Escobar, E., Colonomos, P., Campos, E. 1992. Cyclic Steam Injection with Additives: Laboratory and Field Test Results of Steam/Foam and Steam/Solvent Processes. Presented in SPE Annual Technical Conference and Exhibition, 4-7 October, Washington, D.C. Society of Petroleum Engineers. SPE-24632-MS. https://doi.org/10.2118/24632-MS

Mendoza, H. A., Finol, J. J., Butler, R. M. 1999. SAGD, Pilot Test in Venezuela. Presented in Latin American and Caribbean Petroleum Engineering Conference,

21-23 April, Caracas, Venezuela. Society of Petroleum Engineers. SPE-53687-MS. https://doi.org/10.2118/53687-MS

Mercier, F., Toulhoat, N., Potocek, V., Trocellier, P. 1999. The Role of Nitrogen and Sulphur Bearing Compounds in the Wettability of Oil Reservoir Rocks: An Approach with Nuclear Microanalysis and Other Related Surface Techniques. *Nuclear Instruments and Methods in Physics Research Section B: Beam Interactions with Materials and Atoms* 152(01): 122-128. https://doi.org/10.1016/S0168-583X(98)00943-4

Mercier, P., Patarachao, B., Kung, J., Kingston, D., Woods, J., Sparks, B. D.,.., McCracken, T. 2008. X-ray Diffraction (XRD)-Derived Processability Markers for Oil Sands based on Clay Mineralogy and Crystallite Thickness Distributions. *Energy & Fuels* **22**(05): 3174-3193. http://pubs.acs.org/doi/abs/10.1021/ef8002203

Meyer, R. F., Attanasi, E. D., Freeman, P. A. 2007. Heavy Oil and Natural Bitumen Resources in Geological Basins of the World (No. 2007-1084). https://pubs.er.usgs.gov/publication/ofr20071084

Mitchell, D. L., Speight, J. G. 1973. The Solubility of Asphaltenes in Hydrocarbon Solvents. *Fuel* **52**(02): 149-152. https://doi.org/10.1016/0016-2361(73)90040-9

Mohammadzadeh, O., Rezaei, N., Chatzis, I. 2010. Pore-Level Investigation of Heavy Oil and Bitumen Recovery Using Solvent− Aided Steam Assisted Gravity Drainage (SA-SAGD) Process. *Energy & Fuels* **24**(12): 6327-6345. http://pubs.acs.org/doi/abs/10.1021/ef100621s

Mojelsky, T. W., Ignasiak, T. M., Frakman, Z., McIntyre, D. D., Lown, E. M., Montgomery, D. S., Strausz, O. P. 1992. Structural Features of Alberta Oil Sand Bitumen and Heavy Oil Asphaltenes. *Energy & Fuels* **6**(01): 83-96. http://pubs.acs.org/doi/abs/10.1021/ef00031a013

Morris, K. A., Shepperd, C. M. 1982. The Role of Clay Minerals in Influencing Porosity and Permeability Characteristics in the Bridport Sands of Wytch Farm, Dorset. *Clay Minerals* **17**(01): 41-54. http://www.minersoc.org/pages/Archive-CM/Volume_17/17-1-41.pdf

Mukhametshina, A., Hascakir, B. 2014. Bitumen Extraction by Expanding Solvent-Steam Assisted Gravity Drainage (ES-SAGD) with Asphaltene Solvents and Non-Solvents. Presented in SPE Heavy Oil Conference-Canada. Society of Petroleum Engineers. SPE 170013-MS. http://dx.doi.org/10.2118/170013-MS

Mukhametshina, A., Kar, T., Hascakir, B. 2016. Asphaltene Precipitation during Bitumen Extraction with Expanding-Solvent Steam-Assisted Gravity Drainage: Effects on Pore-Scale Displacement. *SPE Journal* **21**(02): 380-392., SPE-170013-PA. http://dx.doi.org/10.2118/170013-PA

Mullins, O. C. 2008. Review of the Molecular Structure and Aggregation of Asphaltenes and Petroleomics. *SPE Journal* **13**(01): 48-57. https://doi.org/10.2118/95801-PA

Nadeau, P. H. 1998. An Experimental Study of the Effects of Diagenetic Clay Minerals on Reservoir Sands. *Clays and Clay Minerals* **46**: 18-26. http://www.clays.org/journal/archive/volume%2046/46-1-18.pdf

Nasr, T. N., Kimber, K. D., Vendrinsky, D. A., Jha, K. N. 1991. Process Enhancement in Horizontal Wells through the use of Vertical Drainage Channels and Hydrocarbon Additives. SPE Western Regional Meeting, Society of Petroleum Engineers. SPE 21794-MS. https://doi.org/10.2118/21794-MS

Nasr, T. N., Beaulieu, G., Golbeck, H. 2003. Novel Expanding Solvent-SAGD Process "ES-SAGD". *Journal of Canadian Petroleum Technology* **42**(01). PETSOC-03-01-TN. http://dx.doi.org/10.2118/03-01-TN

Neasham, J. W. 1977. The Morphology of Dispersed Clay in Sandstone Reservoirs and its Effect on Sandstone Shaliness, Pore Space and Fluid Flow Properties. In SPE Annual Fall Technical Conference and Exhibition. SPE-6858-MS. http://dx.doi.org/10.2118/6858-MS

Nejatian Daraei, H., Khodapanah, E., and Sahraei, E. 2015. Experimental Investigation of Steam-CO2-Foam Flooding: Combination of CO2-Foam Flooding and Steam Injection as an Effective Enhanced Oil Recovery (EOR) Method in Heavy Oil Reservoirs. *Asia-Pacific Journal of Chemical Engineering* **10**(03): 377-386. doi/10.1002/apj.1881/full

O'Carroll, J. B. 2000. Factors Affecting Bitumen Recovery from Oil Sands. uO Research, University of Ottawa (Canada). http://dx.doi.org/10.20381/ruor-16142

O'Rourke, J. C., Chambers, J. I., Suggelt, J. C., Good, J. K. 1994. UTF Project Status And Commercial Potential An Update, May 1994. In Annual Technical Meeting. Petroleum Society of Canada. http://dx.doi.org/10.2118/94-40

Ovalles, C., Vallejos, C., Vasquez, T., Martinis, J., Perez-Perez, A., Cotte, E.,.., Rodriguez, H. 2001. Extra-heavy Crude Oil Downhole Upgrading Process using Hydrogen Donors under Steam Injection Conditions. Presented in SPE International Thermal Operations and Heavy Oil Symposium, 12-14 March,

Porlamar, Margarita Island, Venezuela. Society of Petroleum Engineers. SPE-69692-MS. https://doi.org/10.2118/69692-MS

Pallatt, N., Wilson, J., McHardy, B. 1984. The Relationship Between Permeability and the Morphology of Diagenetic Illite in Reservoir Rocks. *Journal of Petroleum Technology* **36**(12). SPE-12798-PA. https://doi.org/10.2118/12798-PA

Pang, Z. X., Liu, H. Q., Liu, X. L. 2010. Characteristics of Formation Damage and Variations of Reservoir Properties during Steam Injection in Heavy Oil Reservoir. *Petroleum Science and Technology* **28**(05): 477-493. http://dx.doi.org/10.1080/10916460902780335

Pickering, S. U. 1907. CXCVI.—Emulsions. Journal of the Chemical Society, Transactions, 91, 2001-2021. http://pubs.rsc.org/-/content/articlepdf/1907/ct/ct9079102001

Prakoso, A., Punase, A., Klock, K., Rogel, E., Ovalles, C., Hascakir, B. 2016. Determination of the Stability of Asphaltenes through Physicochemical Characterization of Asphaltenes. In SPE Western Regional Meeting, 23-26 May, Anchorage, Alaska. SPE-180422-MS. https://doi.org/10.2118/180422-MS

Prats, M. 1982. Thermal Recovery. SPE of AIME, New York, NY. OSTI: 5742984.

Punase, A., Hascakir, B. 2016. Stability Determination of Asphaltenes through Dielectric Constant Measurements of Polar Oil Fractions. *Energy & Fuels* **31**(01): 65-72. http://pubs.acs.org/doi/abs/10.1021/acs.energyfuels.6b01045

Putnam, P.E.; Christensen, S.L. 2004. McMurray Formation SAGD (Steam-Assisted Gravity Drainage) Reservoirs in Northeastern Alberta: Comparative Architecture and Performance. In Proceedings of CSPG- Canadian Heavy Oil Association-CWLS Joint Conf. (ICE2004), Calgary, Alberta, Canada. 31 May – 4 June.

Rivero, J. A., Mamora, D. D. 2005. Production Acceleration and Injectivity Enhancement using Steam-Propane Injection for Hamaca Extra-heavy Oil. *Journal of Canadian Petroleum Technology* **44**(02). PETSOC-05-02-05. https://doi.org/10.2118/05-02-05

Rivero, J. A., Mamora, D. D. 2007. Oil Production Gains for Mature Steamflooded Oil Fields Using Propane as a Steam Additive and a Novel Smart Horizontal Producer. Presented in SPE Annual Technical Conference and Exhibition, 11-14 November, Anaheim, California. Society of Petroleum Engineers. SPE-110538-MS. https://doi.org/10.2118/110538-MS

Sarbar, M., Al-Jaziri, K. M. 1995. Laboratory Investigation of Factors Affecting the Formation and Stability of Tight Oil-in-Water Emulsions in Produced Fluids. In OAPEC Conference on New Technology 01: 261-268.

Saxman, D. 1985. The Atlas of Enhanced Oil Recovery From Heavy Oil and Tar Sand Fields. Business Communications Co., Inc. Stamford, CT 06906.

Sharma, J., Gates, I. D. 2011. Convection at the Edge of a Steam-Assisted-Gravity-Drainage Steam Chamber. *SPE Journal* **16**(03): 503-512. https://doi.org/10.2118/142432-PA

Shkalikov, N. V., Vasil'ev, S. G., Skirda, V. D. 2010. Peculiarities of Asphaltene Precipitation in n-alkane-oil Systems. *Colloid Journal* **72**(01): 133-140. doi:10.1134/S1061933X1001014X

Siffert, B., Jada, A., Wersinger, E. 1992. Anionic Surfactant Adsorption on to Asphalt-Covered Clays. *Colloids and Surfaces* **69**(01): 45-51. https://doi.org/10.1016/0166-6622(92)80237-V

Souraki, Y., Ashrafi, M., Torsaeter, O. 2016. Experimental Investigation and Comparison of Thermal Processes: SAGD, ES-SAGD and SAS. *International Journal of Engineering Trends and Technology* **31**(02). https://doi.org/10.14445/22315381/IJETT-V31P218

Speight, J. G. 1991. The Chemistry and Technology of Petroleum. 2nd ed.; Marcel Dekker, Inc. ISBN 0-8247-8481-2.

Speight, J. G. 1999. The Chemistry and Technology of Petroleum, 3rd ed.; Marcel Dekker: New York, and references therein.

Speight, J. G. 2014. The Chemistry and Technology of Petroleum. 5th ed.; CRC Press, Taylor & Francis Group. ISBN- 13: 978-1-4398-7389-2.

Spiecker, P. M., Gawrys, K. L., Trail, C. B., et al. 2003. Effects of Petroleum Resins on Asphaltene Aggregation and Water-in-Oil Emulsion Formation. *Colloids and Surfaces A: Physicochemical and Engineering Aspects* **220**(01): 9-27. https://doi.org/10.1016/S0927-7757(03)00079-7

Stalder, J. L. 2008. Thermal Efficiency and Acceleration Benefits of Cross SAGD (XSAGD). Presented in International Thermal Operations and Heavy Oil Symposium, 20-23 October, Calgary, Alberta, Canada. Society of Petroleum Engineers. SPE-117244-MS. https://doi.org/10.2118/117244-MS

Stape, P. 2016. Performance Evaluation of Solvent Assisted- Steam Injection Processes With Asphaltene Insoluble Solvents. MSc Thesis, Texas A&M University.

Swartzen-Allen, S. L., Matijevic, E. 1974. Surface and Colloid Chemistry of Clays. *Chemical Reviews* **74**(03): 385-400. http://pubs.acs.org/doi/pdf/10.1021/cr60289a004

Sztukowski, D. M., Yarranton, H. W. 2005. Oilfield Solids and Water-in-Oil Emulsion Stability. *Journal of Colloid and Interface Science* **285**(02): 821-833. https://doi.org/10.1016/j.jcis.2004.12.029

Taber, J. J., Martin, F. D., Seright, R. S. 1997. EOR Screening Criteria Revisited-Part 1: Introduction to Screening Criteria and Enhanced Recovery Field Projects. *SPE Reservoir Engineering* **12**(03): 189-198. SPE-35385-PA. https://doi.org/10.2118/35385-PA

Taber, J. J., Martin, F. D., Seright, R. S. 1997. EOR Screening Criteria Revisited—Part 2: Applications and Impact of Oil Prices. *SPE Reservoir Engineering* **12**(03): 199-206. SPE-39234-PA. https://doi.org/10.2118/39234-PA

Tadros, T. F. (Ed.). 2013. Emulsion Formation and Stability. John Wiley & Sons. ISBN: 978-3-527-31991-6

Tissot, B. P., Welte, D. H. 1984. Petroleum Formation and Occurrence. Springer-Verlag Berlin Heidelberg New York, ISBN: 978-3-642-87815-2.

Unal, Y., Kar, T., Mukhametshina, A., Hascakir, B. 2015. The Impact of Clay Type on the Asphaltene Deposition during Bitumen Extraction with Steam Assisted Gravity Drainage. Presented in SPE International Symposium on Oilfield Chemistry 2015, 13-15 April 2015, The Woodlands, Texas, USA, SPE-173795-MS. https://doi.org/10.2118/173795-MS

Van Olphen, H., Hsu, P. H. 1978. An Introduction to Clay Colloid Chemistry. *Soil Science* **126**(01): 59.

Wallace, D., Tipman, R., Komishke, B., Wallwork, V., Perkins, E. 2004. Fines/Water Interactions and Consequences of the Presence of Degraded Illite on Oil Sands Extractability. *The Canadian Journal of Chemical Engineering* **82**(04): 667-677. doi: 10.1002/cjce.5450820405

Wang, D., Lin, M., Dong, Z., Li, L., Jin, S., Pan, D., Yang, Z. 2016. Mechanism of High Stability of Water-in-Oil Emulsions at High Temperature. *Energy & Fuels* **30**(03): 1947-1957. doi: 10.1021/acs.energyfuels.5b02203

Wiehe, I. A. 2012. Asphaltene Solubility and Fluid Compatibility. *Energy & Fuels* **26**(07): 4004-4016. http://pubs.acs.org/doi/abs/10.1021/ef300276x

Willhite, G. P. 1986. Waterflooding, Volume 3 of SPE Textbook Series. Society of Petroleum Engineers, Richardson, TX.

Wilson, M. D., Pittman, E. D. 1977. Authigenic Clays in Sandstones: Recognition and Influence on Reservoir Properties and Paleoenvironmental Analysis. *Journal of Sedimentary Petrology* **47**: 3-31. http://archives.datapages.com/data/sepm/journals/v47-50/data/047/047001/pdfs/0003.pdf

Yen, T.F. 1984. Characterization of Heavy Oil, in Meyer, R.F., Wynn, J.C., Olson, J.C., eds., The Future of Heavy Crude and Tar Sands, International Conference, 2d, Caracas, 1982: New York, McGraw-Hill, 412^123.

Zhao, B., Becerra, M., Shaw, J. M. 2009. On Asphaltene and Resin Association in Athabasca Bitumen and Maya Crude Oil. *Energy & Fuels* **23**(09): 4431-4437. http://pubs.acs.org/doi/abs/10.1021/ef900309j

Zhdanov, S. A., Amiyan, A. V., Surguchev, L. M., Castanier, L. M., Hanssen, J. E. 1996. Application of Foam for Gas and Water Shut-off: Review of Field Experience. In European Petroleum Conference, 22-24 October, Milan, Italy. Society of Petroleum Engineers. SPE-36914-MS. https://doi.org/10.2118/36914-MS

Zhu, D., Bunio, G., Gates, I. D. 2016. Phased Heating and Solvent Injection to Enhance Recovery of Heavy Oil and Bitumen. In SPE EOR Conference at Oil and Gas West Asia, 21-23 March, Muscat, Oman. Society of Petroleum Engineers. SPE-179761-MS. https://doi.org/10.2118/179761-MS

APPENDIX A

Table A.1 - List of steam recovery projects in Alberta
(Reprinted from Saxman 1985)

Field	Project Type	Number of Projects
Athabasca	Pilot	3+
Surmount	Pilot	1
Marguerite Lake	Commercial	2
Muriel Lake	Inactive	1
Fort Kent	Pilot	1
Lindbergh	Commercial	1+
Lindbergh	Planned	1
Garth	Pilot	1
Blackfoot Pool	Inactive	1
Swimming	Proposed	1
Manatokan	Proposed	1
Resdein	Inactive	1
Viking Kinsella	Inactive	1
Primrose	Pilot	1
Hindville	Planned	1
Sugden	Proposed	1
Silverdale	Commercial	1
Cold Lake	Commercial	5+
Wolf Lake	Commercial	1+
Peace River	Commercial	3+
Fort Kent	Commercial	1+
Lloydminister	Inactive	1+
Lloydminister	Planned	1+
Beaver Crossing	Pilot	1
Wabiskaw	Pilot	1
Ardmore	Pilot	1+
Tucker Lake	Pilot	1
Charlotte Lake	Planned	1

+- indicates more than the given number of projects

Table A.2 - List of hydrocarbon recovery projects in Alberta
(Reprinted from Saxman 1985)

Field	Project Type	Number of Projects
Nisku	Pilot	1
Ante Creek	Commercial	1
Redwater	Pilot	1
W. Pembina Nisku	Pilot	2
Mitsue Gilwood	Pilot	2
Bigoray B Pool	Commercial	1+
Rainbow	Commercial	3+
South Swan Hills	Commercial	1
Pembina	Pilot	2
Brazeau River	Pilot	3+
Elk Point	Planned	1
Judy Creek	Planned	2+
Caroline	Planned	1
Nipisi	Proposed	1
Willesden Green	Inactive	1

+- indicates more than the given number of projects

Table A.3 - List of heavy oil and bitumen fields in Alberta with their API Gravity
(Reprinted from Saxman 1985)

Region	Field	API Gravity (°API)
Athabasca	Resdelm	6-8
	Manatokan	9
	Surmount	6-8
	Athabasca deposit	7-9
	Wabasca	< 10
	Grosmont	< 10
	Muriel Lake	10
	Joli Fou	10
	Ipiatik	10
	McLaren	10
	Sugden	11
	Hazeldine	12
	Fort Kent	12
	Saint Lima	13.5
	Pelican Lake	13.5
	Silverdale	15.6
	Kinsella	20
	Horsefly	23
Battle basin	Wainwright	22
	Wainwright Pool	24
Beaver basin	Cold Lake	< 10
Caribou basin	Marguerite Lake	11
Iron basin	Primrose	8.8
Jasper basin	Brazeau River	10
Peace basin	Peace River	9-13

APPENDIX B

CUMULATIVE OIL PRODUCTION GRAPHS

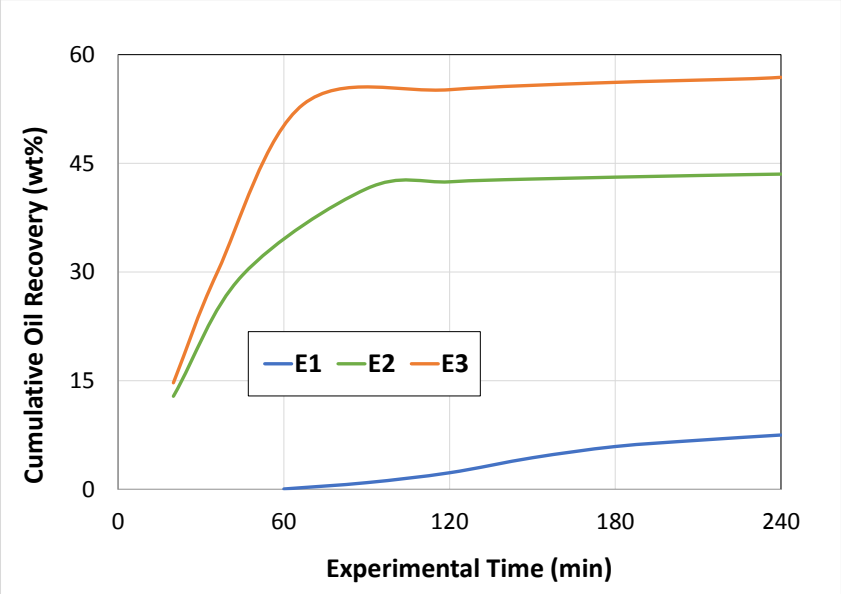

Fig. B.1 - Cumulative oil recovery for flooding experiments (Chapter 1)

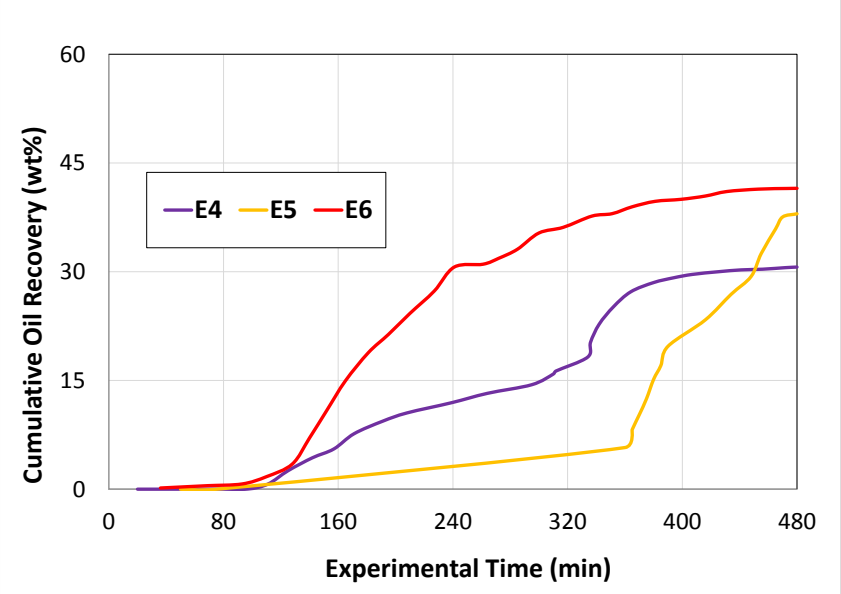

Fig. B.2 - Cumulative oil recovery for SAGD experiments (Chapter 1)

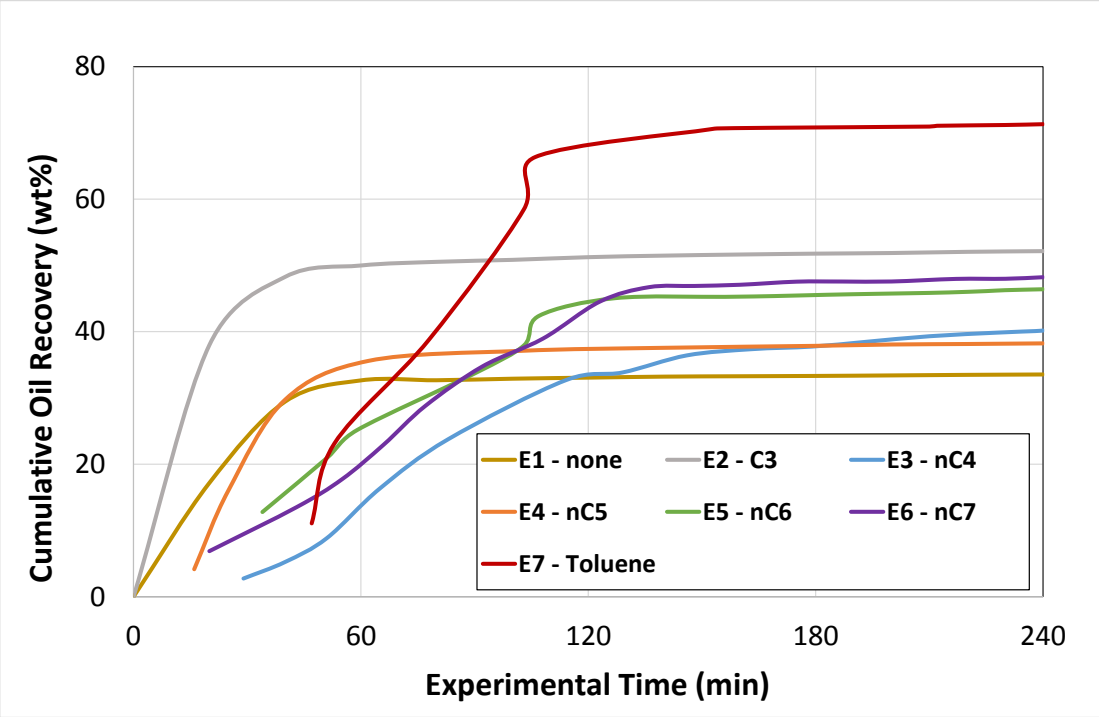

Fig. B.3 - Cumulative oil recovery for Set 1 (No Clay) experiments (Chapter 2)

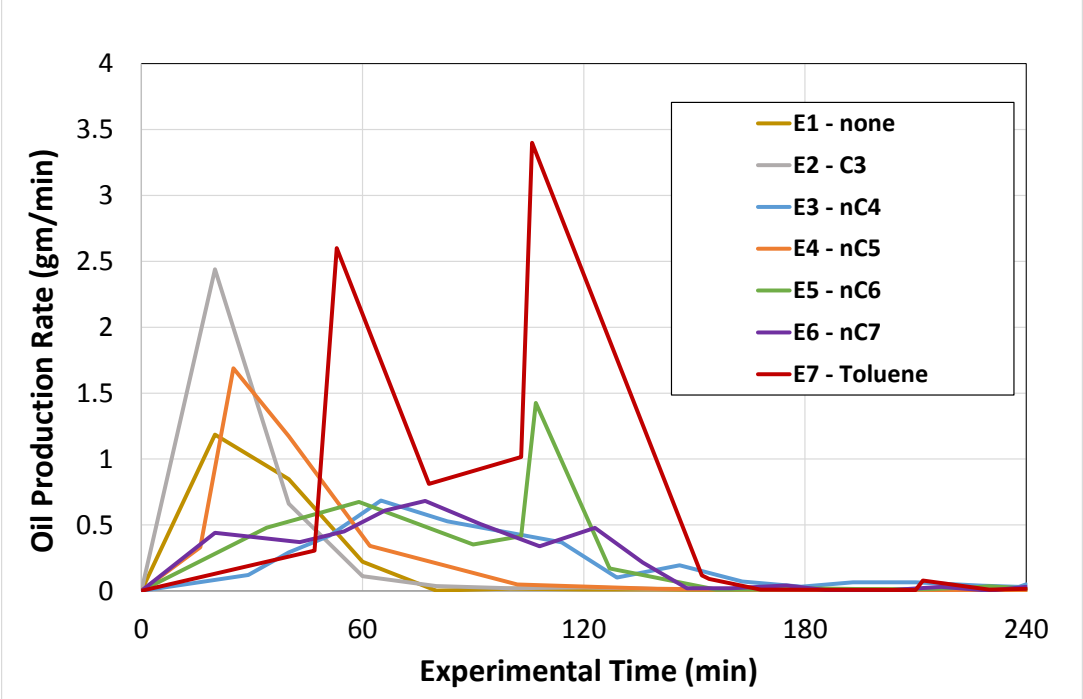

Fig. B.4 - Oil production rate for Set 1 (No Clay) experiments (Chapter 2)

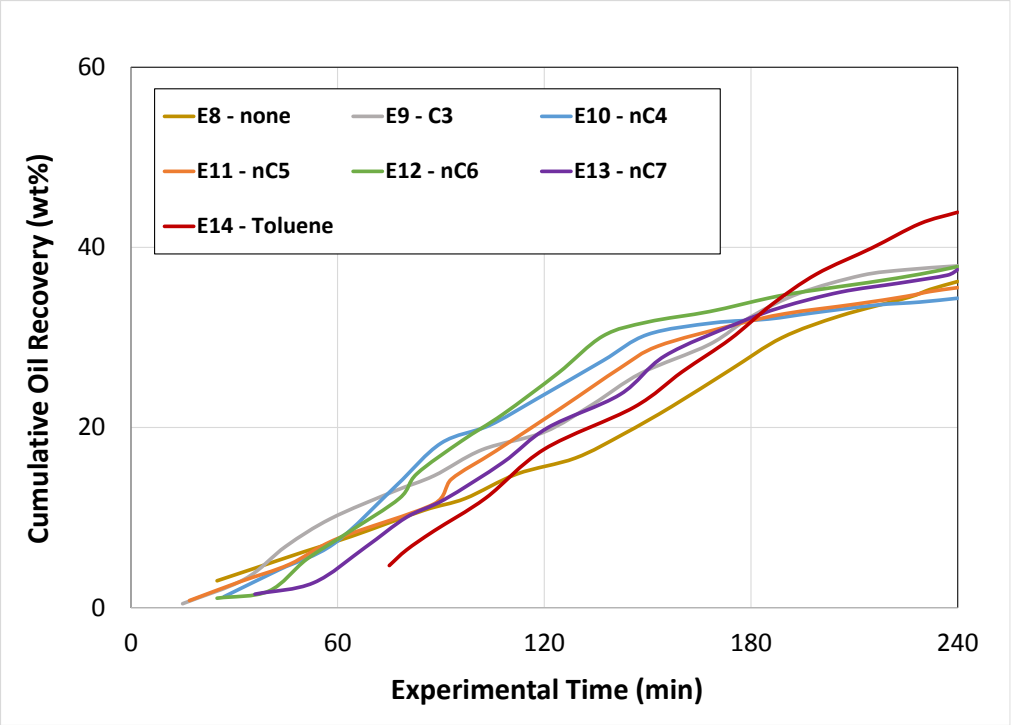

Fig. B.5 - Cumulative oil recovery for Set 2 (Clay1) experiments (Chapter 2)

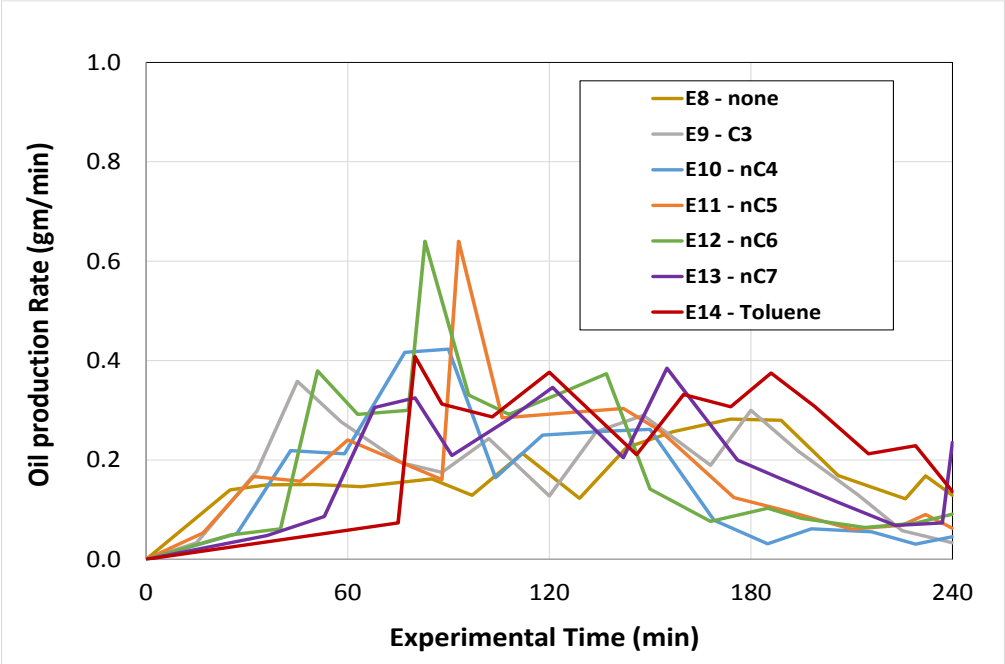

Fig. B.6 - Oil production rate for Set 2 (Clay1) experiments (Chapter 2)

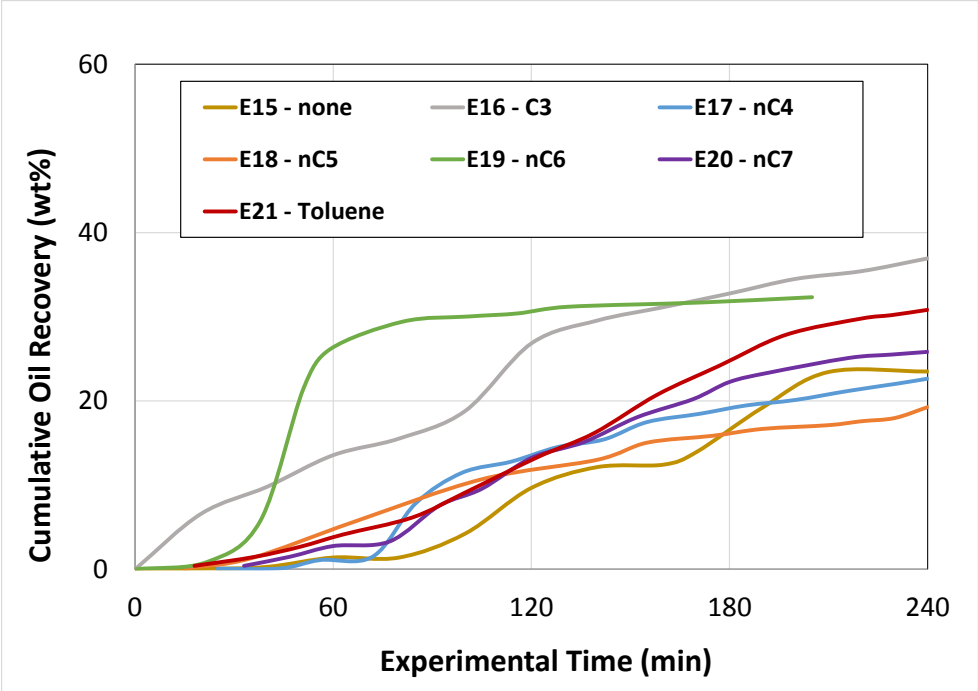

Fig. B.7 - Cumulative oil recovery for Set 3 (Clay2) experiments (Chapter 2)

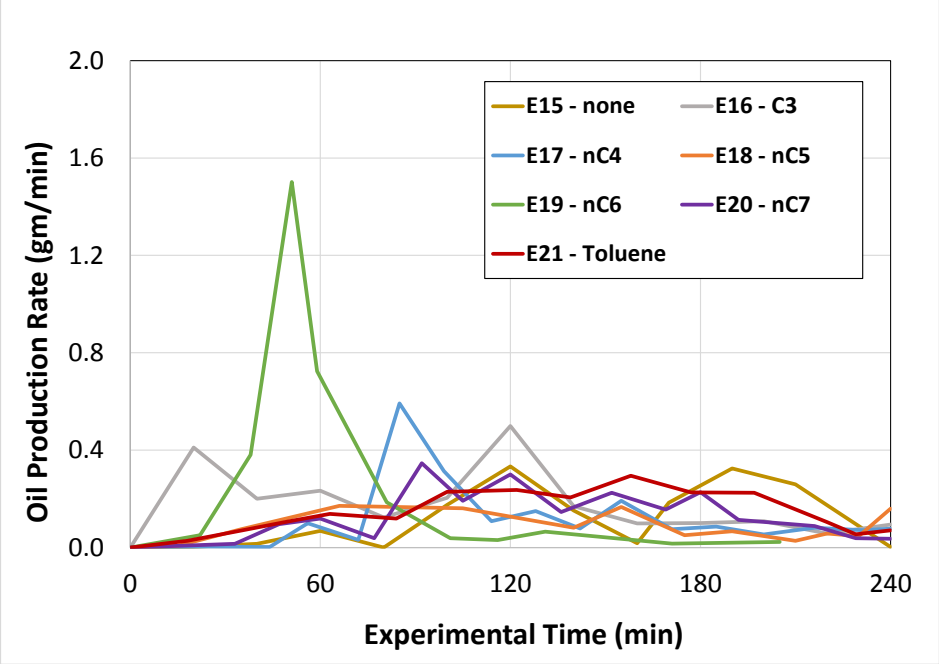

Fig. B.8 - Oil production rate for Set 3 (Clay2) experiments (Chapter 2)

APPENDIX C

TGA-DTA CURVES

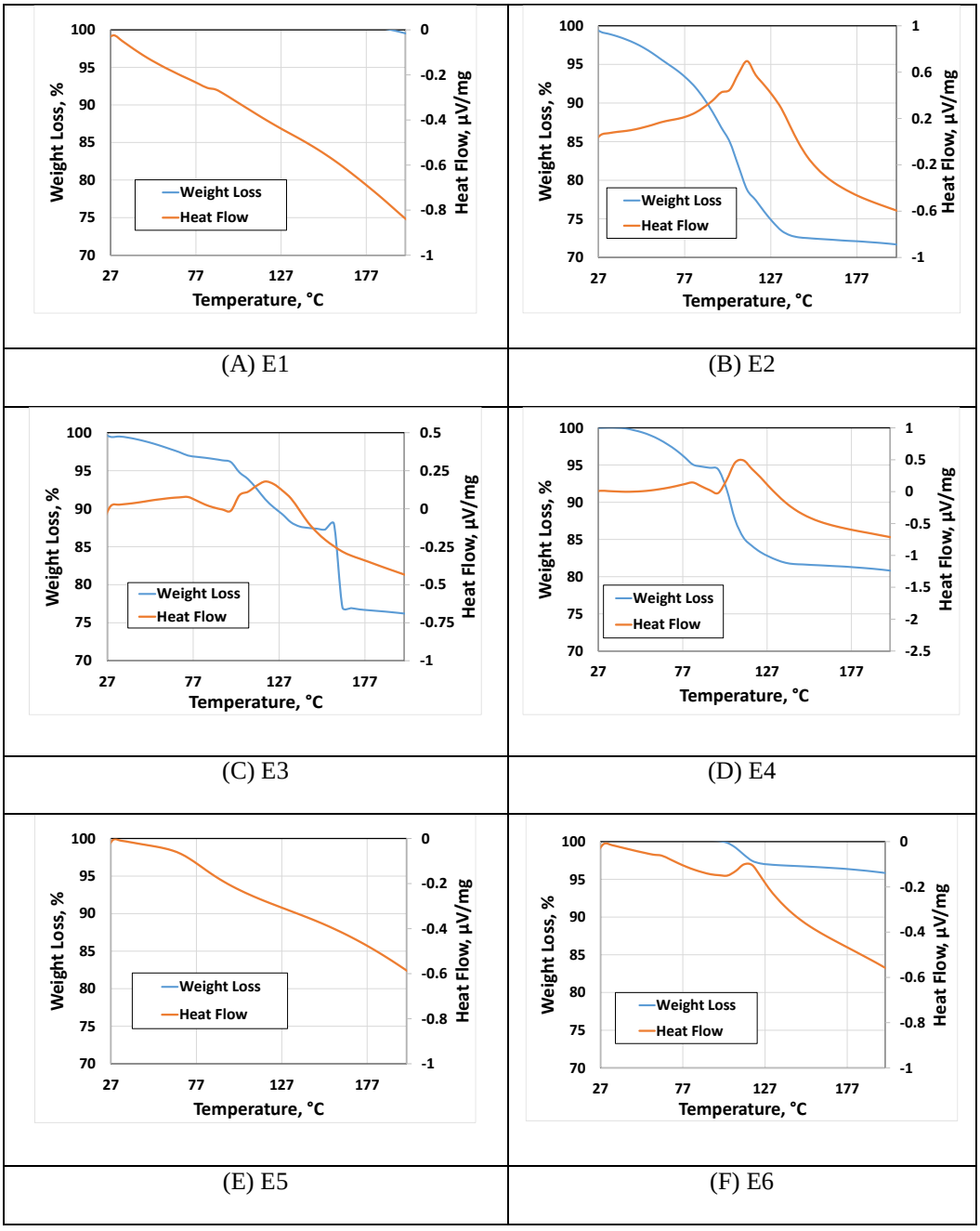

Fig. C.1- TGA-DTA curves for produced oil samples (Chapter1)

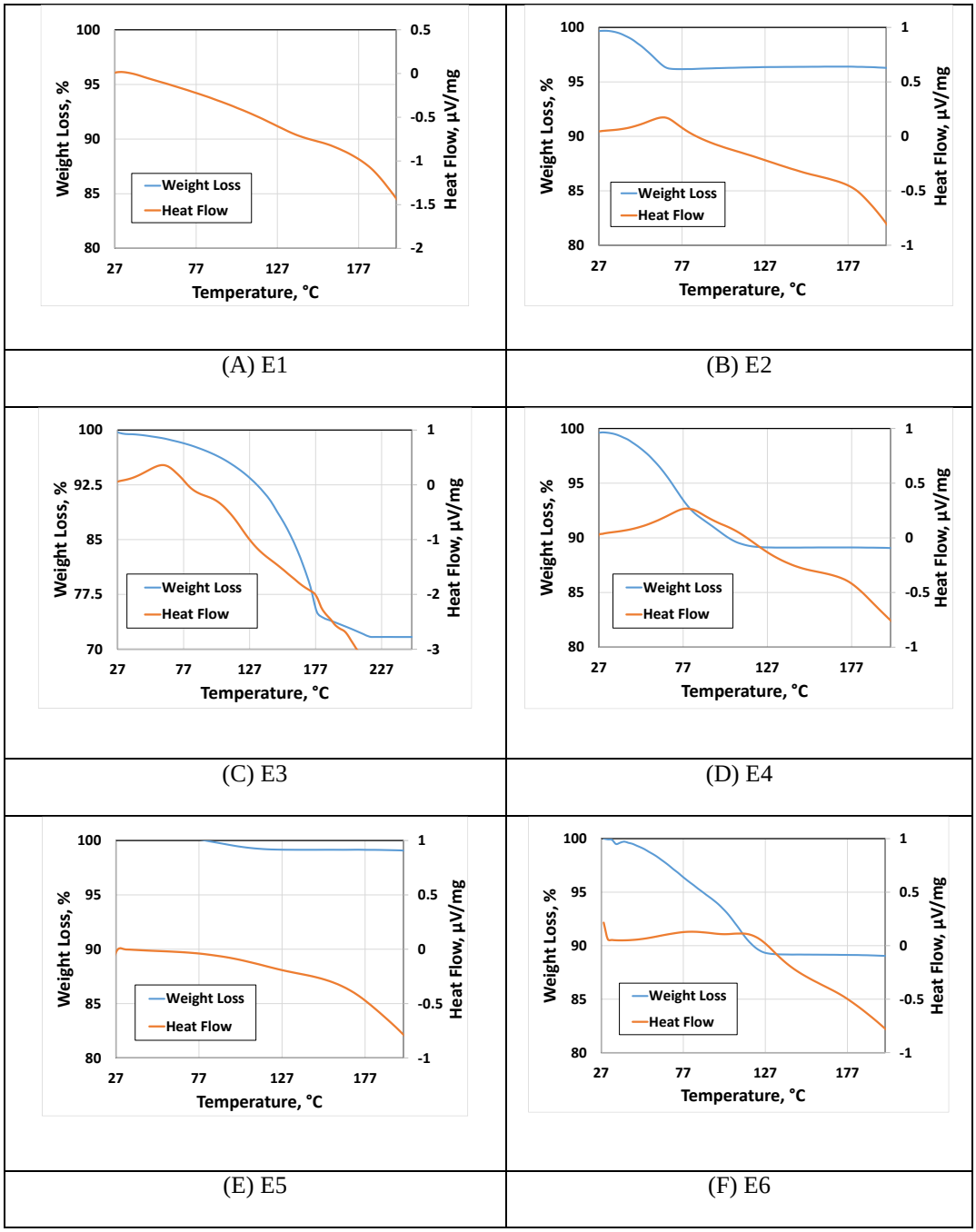

Fig. C.2 - TGA-DTA curves for asphaltenes from produced oil samples (Chapter1)

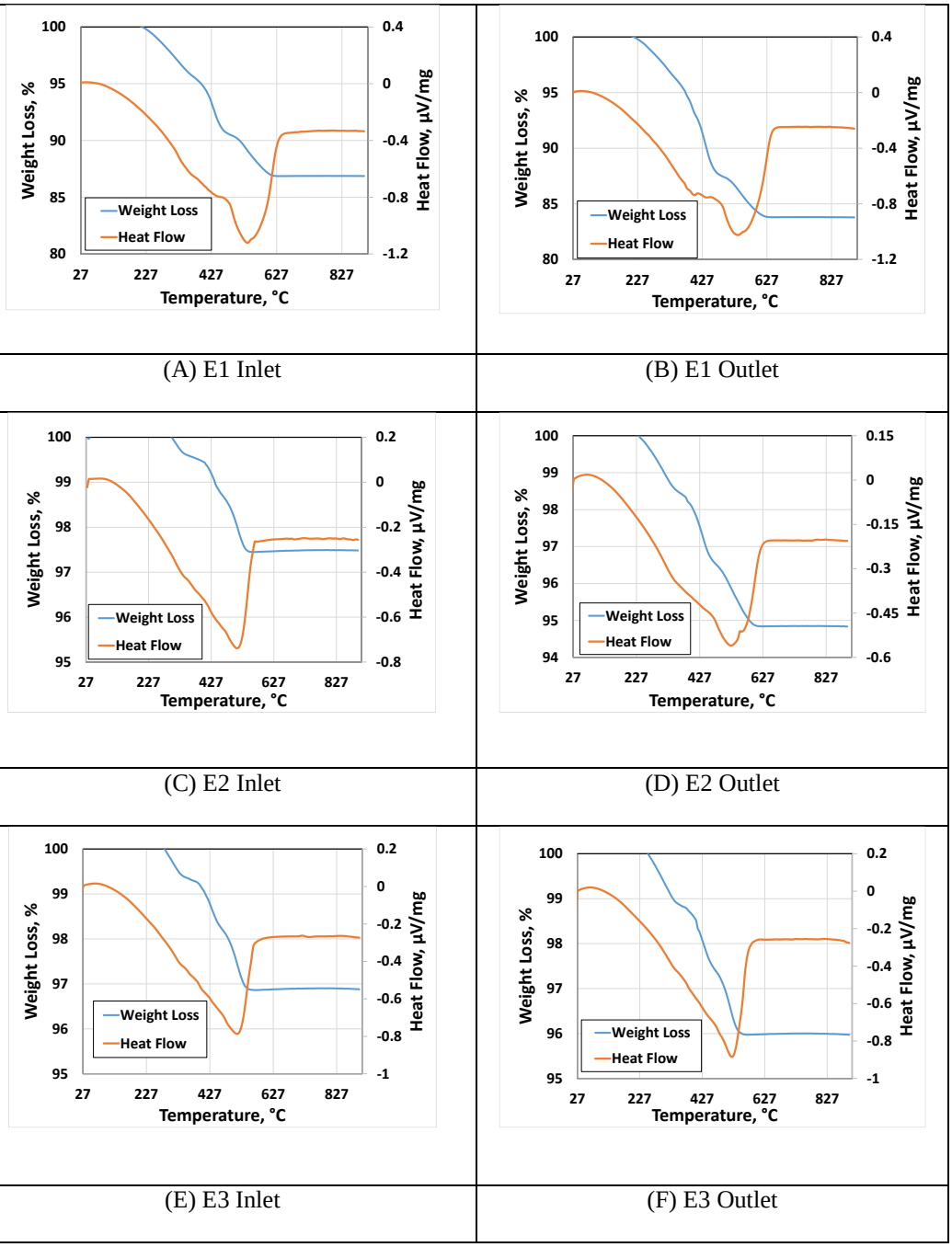

Fig. C.3 - TGA-DTA curves for spent rock samples (Chapter1)

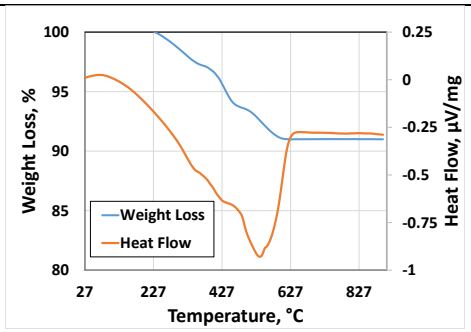

(G) E4(1)

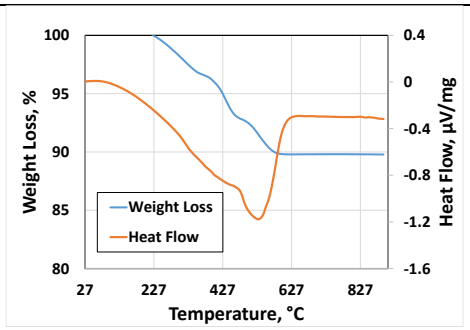

(H) E4(2)

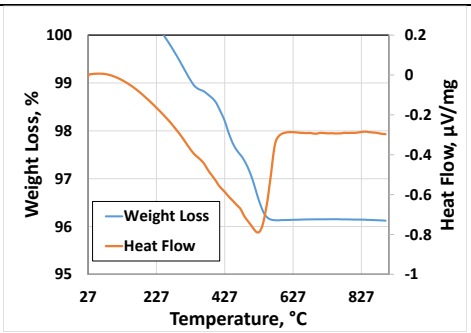

(I) E5(1)

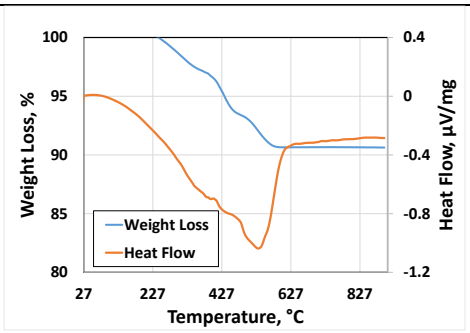

(J) E5(2)

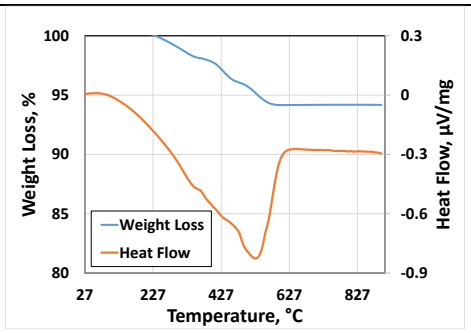

(K) E6(1)

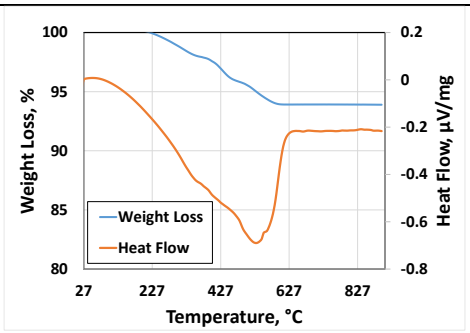

(L) E6(2)

Fig. C.3 Continued - TGA-DTA curves for spent rock samples (Chapter1)

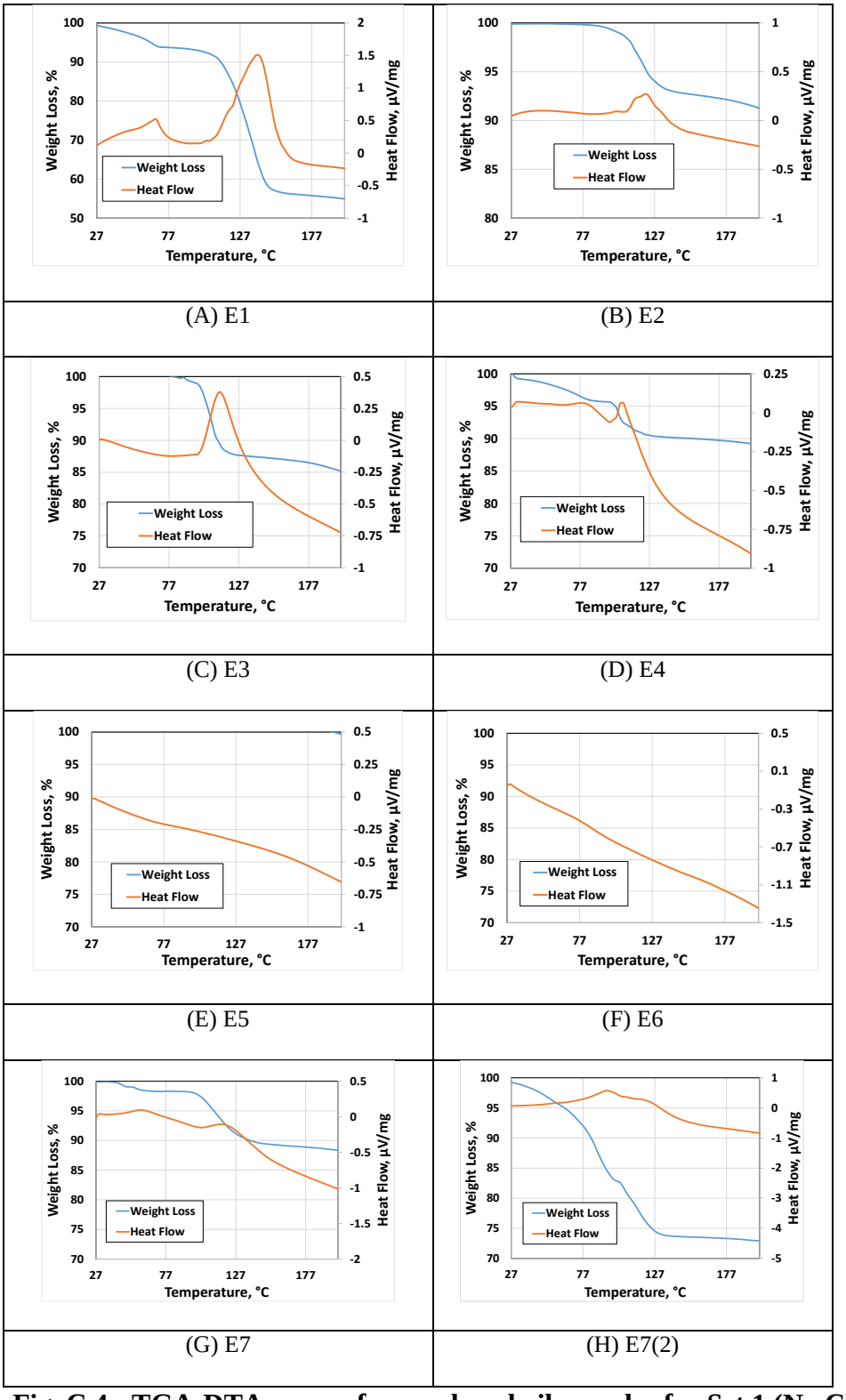

Fig. C.4 - TGA-DTA curves for produced oil samples for Set 1 (No Clay Experiments)

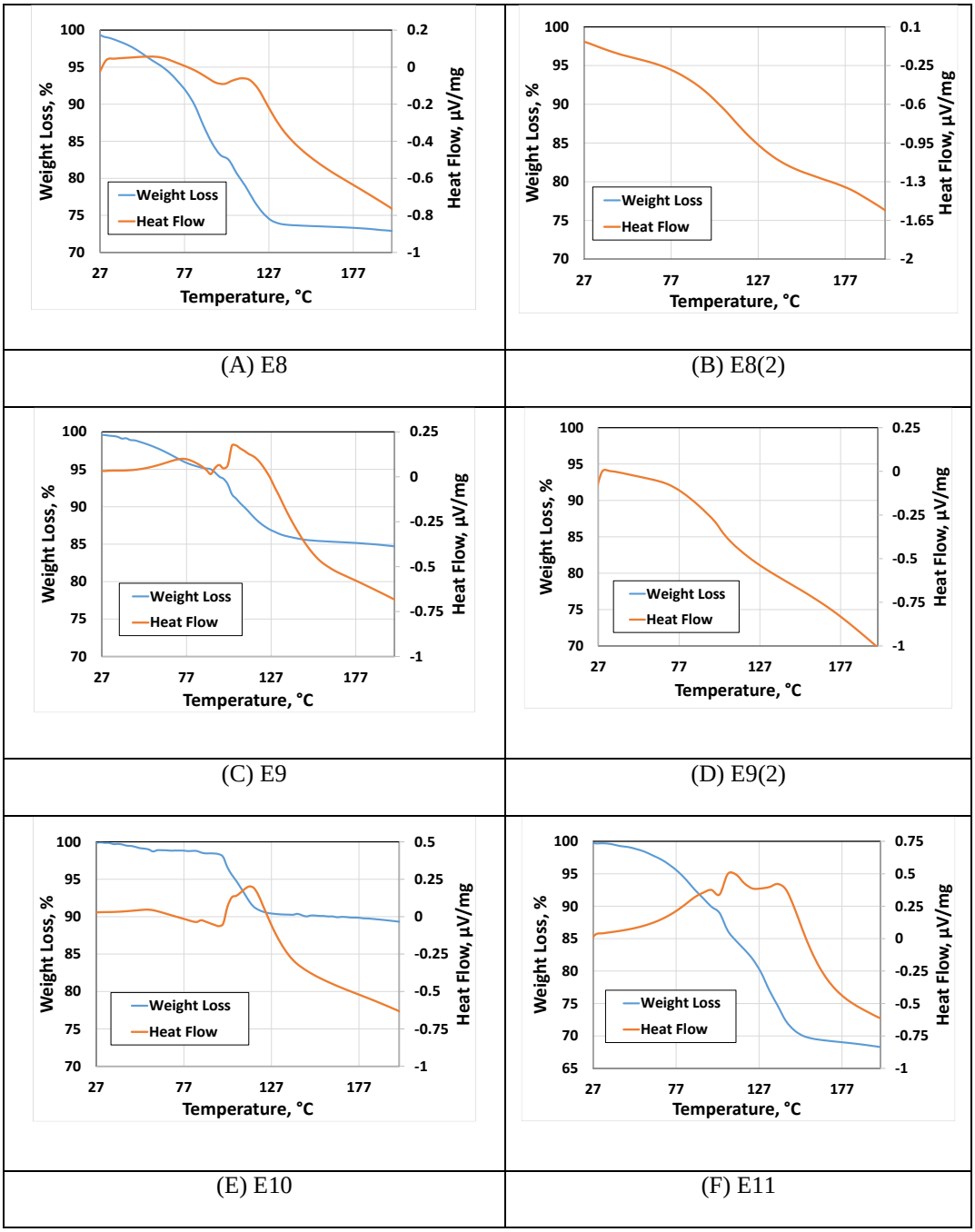

Fig. C.5 - TGA-DTA curves for produced oil samples for Set 2 (Clay1 Experiments)

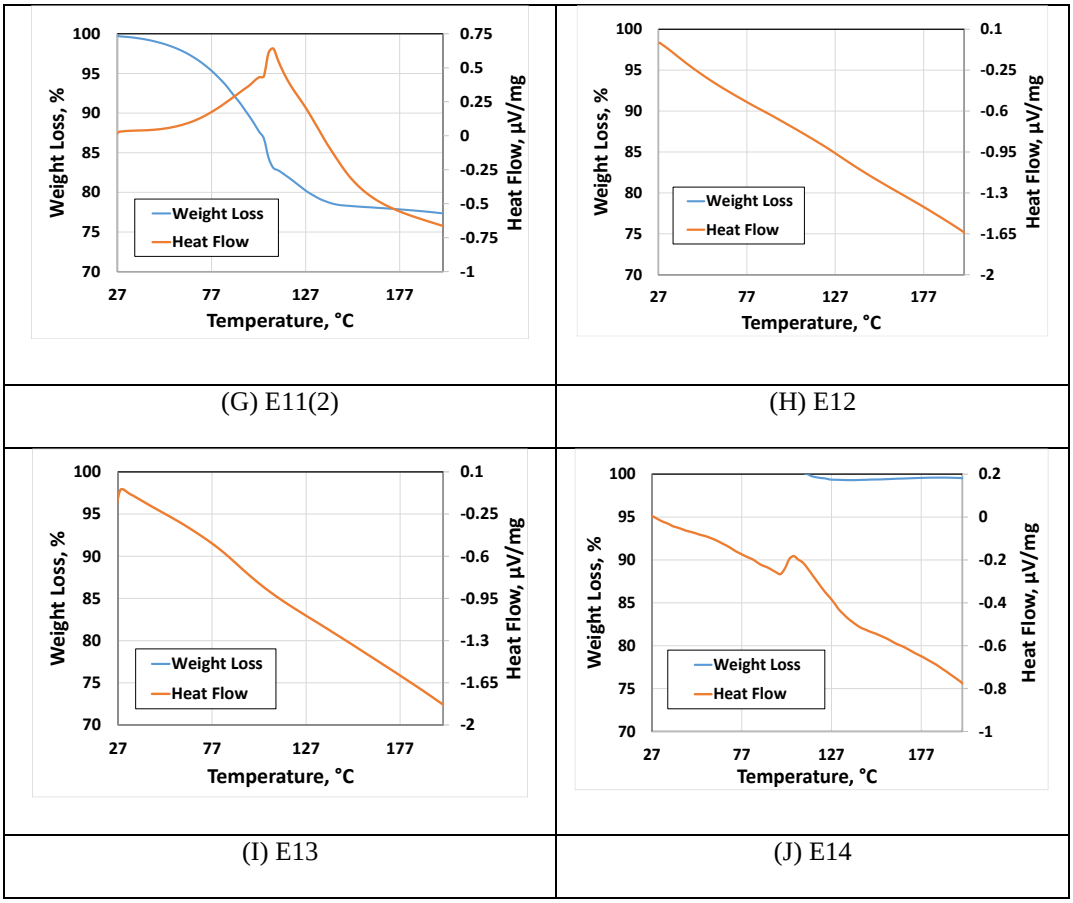

(G) E11(2)

(H) E12

(I) E13

(J) E14

Figure C.5 Continued - TGA-DTA curves for produced oil samples for Set 2 (Clay1 Experiments)

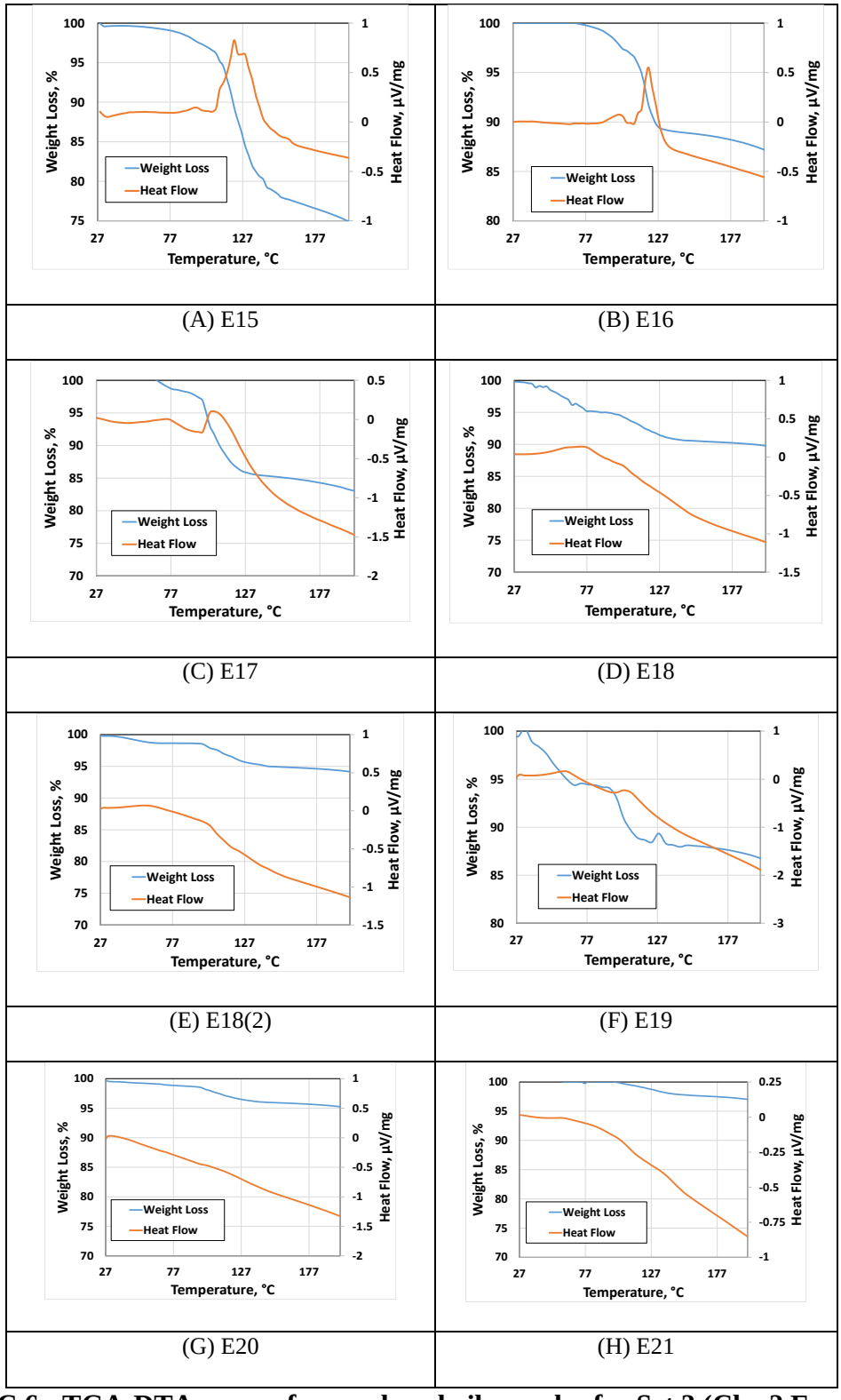

Fig. C.6 - TGA-DTA curves for produced oil samples for Set 3 (Clay2 Experiments)

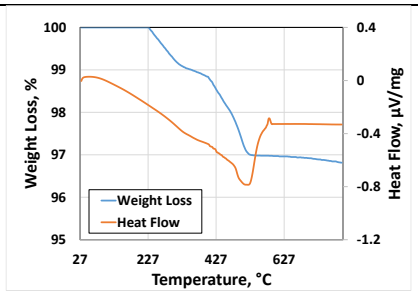

(G) E1 Inlet

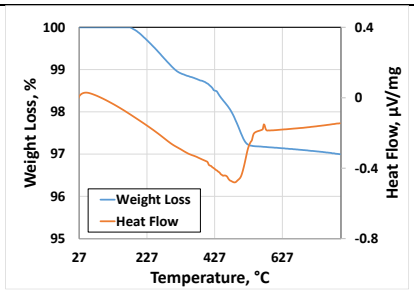

(H) E1 Outlet

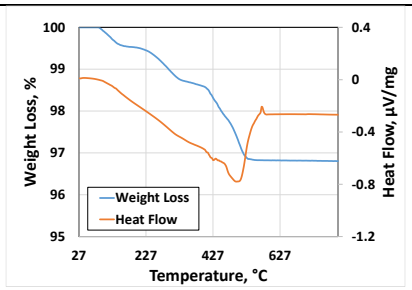

(I) E2 Inlet

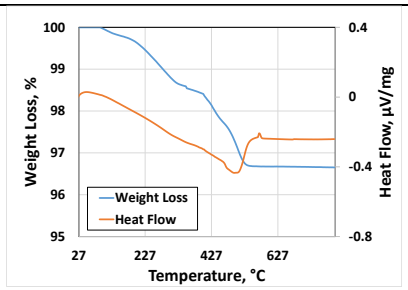

(J) E2 Outlet

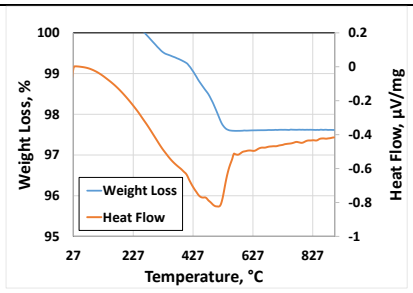

(K) E3 Inlet

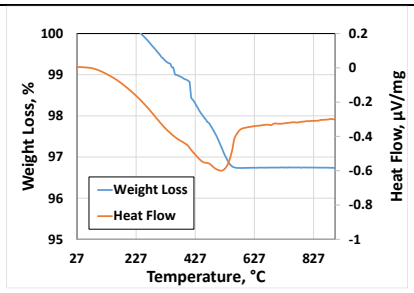

(L) E3 Outlet

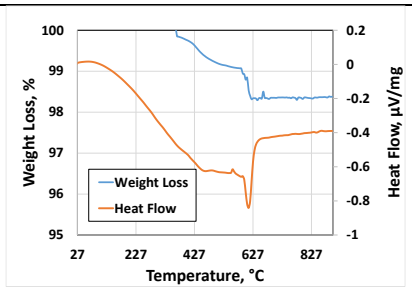

(M) E4 Inlet

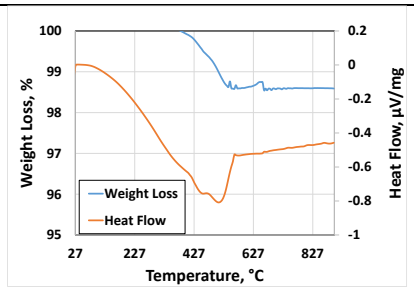

(N) E4 Outlet

Fig. C.7 - TGA-DTA curves for spent rock samples for Set 1 (No Clay Experiments)

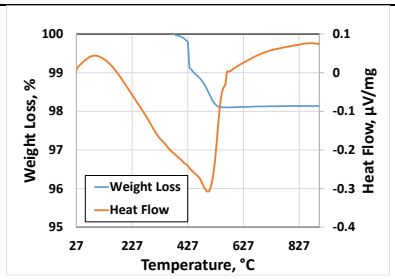

(E) E5 Inlet

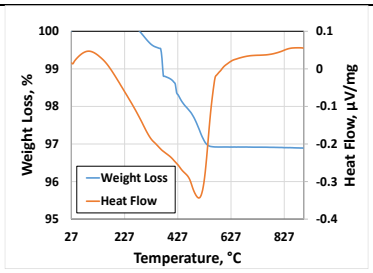

(F) E5 Outlet

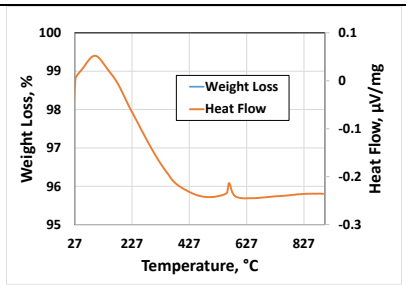

(G) E7 Inlet

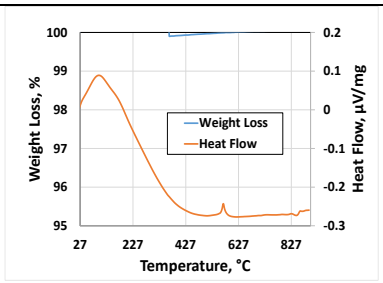

(H) E7 Outlet

Fig. C.7 Continued- TGA-DTA curves for spent rock samples for Set 1 (No Clay Experiments)

For E6, there was an error in the TGA-DTA measurement of the spent rock sample, it is believed that the sand particles were displaced by the injected air flow. Hence, a sudden increase in weight of sample was observed in the TGA analysis of the sample after multiple trials. Hence, for E6, solvent washing method (using n-pentane and toluene) was used to determine residual oil content (Kar et al. 2016). This method can be considered a reasonable alternative to TGA-DTA analysis, as the same procedure was repeated for three other samples and it gave close values, when compared to TGA-DTA method. These are summarized in Table C.1.

Table C.1 - Displacement efficiency comparison for thermal and solvent methods

Experiment	Displacement Efficiency (vol%)					
	Thermal Method (TGA-DTA)			Solvent Method		
	Inlet	Outlet	Avg	Inlet	Outlet	Avg
E3	85.6	80.2	82.90	83.67	82.14	82.91
E4	90.10	91.6	90.85	91.87	90.59	91.23
E5	88.78	81.51	85.14	86.84	83.06	84.95

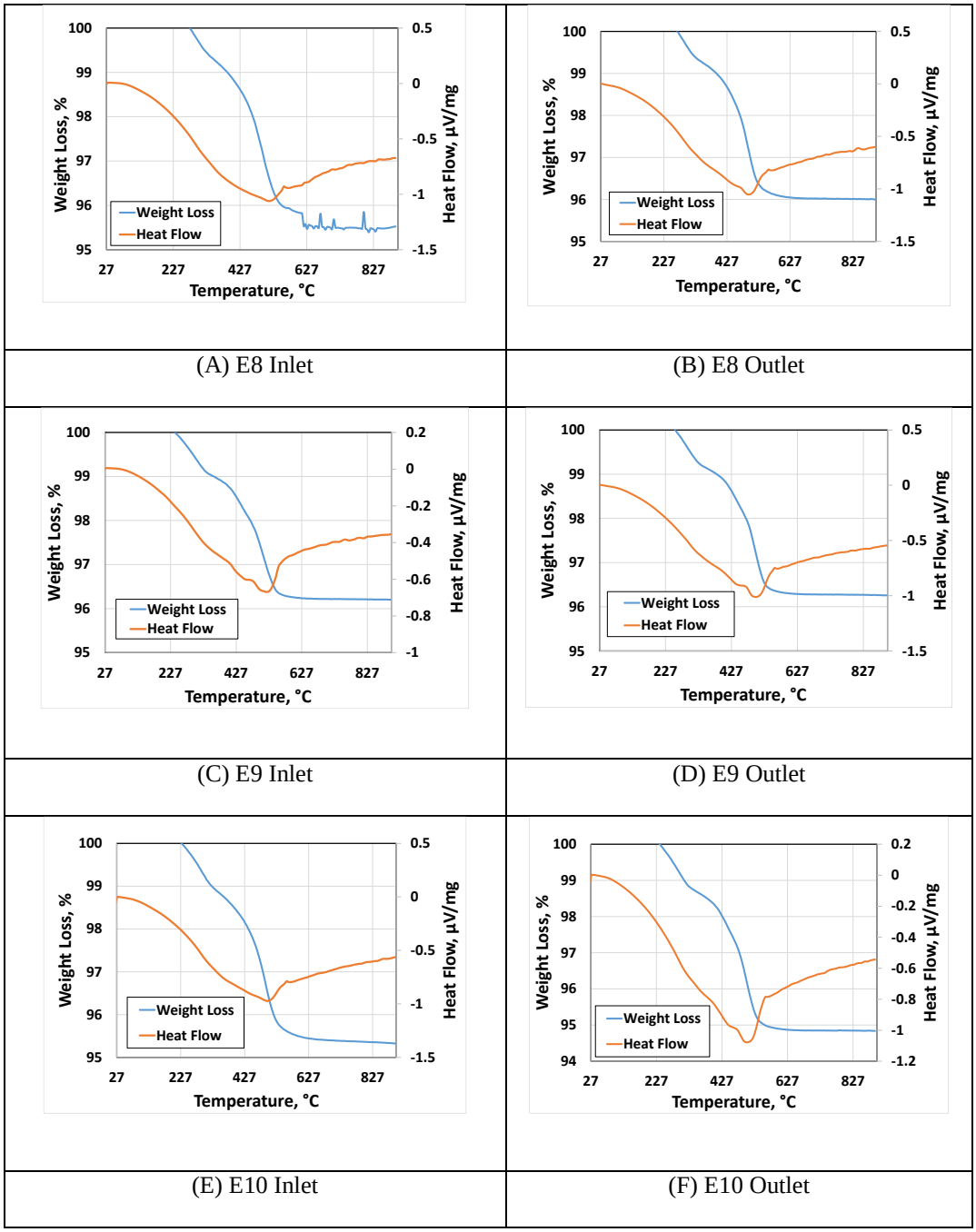

Fig. C.8 - TGA-DTA curves for spent rock samples for Set 2 (Clay1 Experiments)

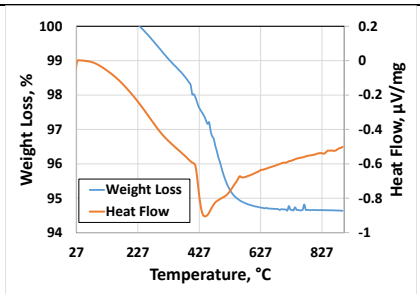

(G) E11 Inlet

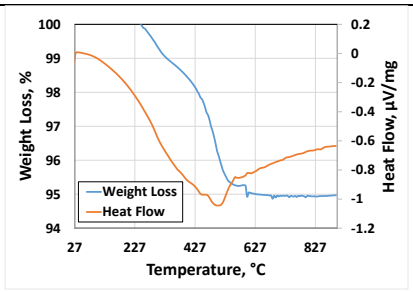

(H) E11 Outlet

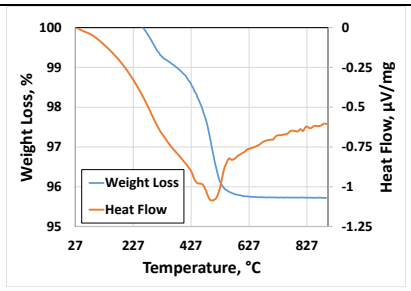

(I) E12 Inlet

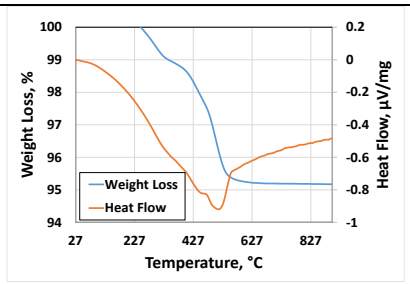

(J) E12 Outlet

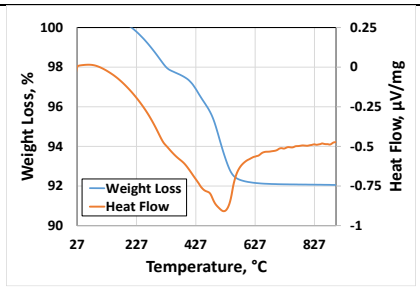

(K) E13 Inlet

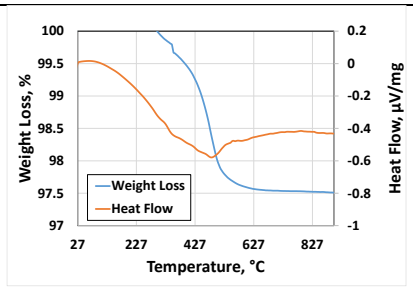

(L) E13 Outlet

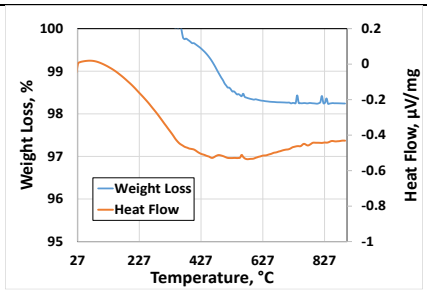

(M) E14 Inlet

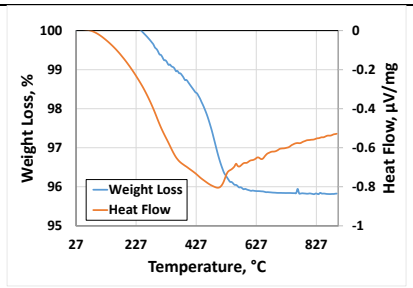

(N) E14 Outlet

Figure C.8 Continued - TGA-DTA curves for spent rock samples for Set 2 (Clay1 Experiments)

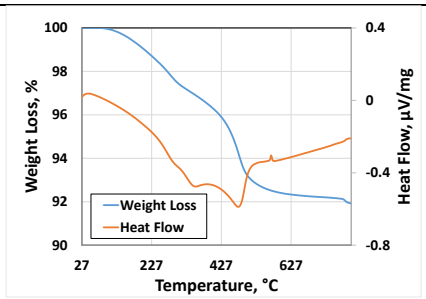

(A) E15 Inlet

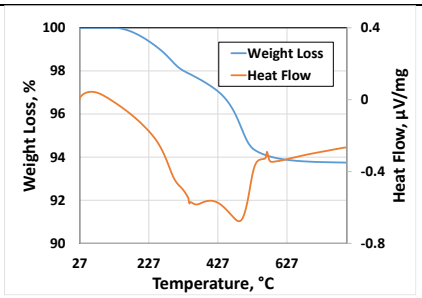

(B) E15 Outlet

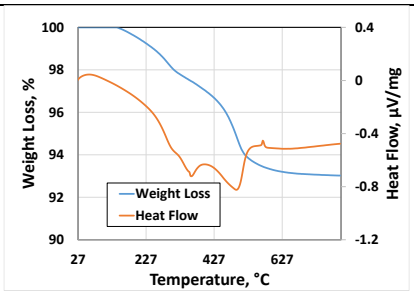

(C) E16 Inlet

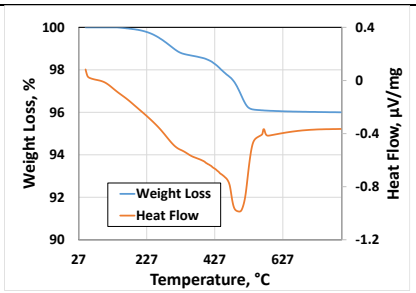

(D) E16 Outlet

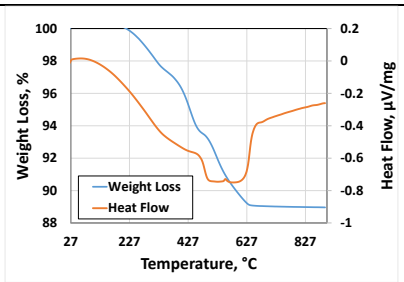

(E) E17 Inlet

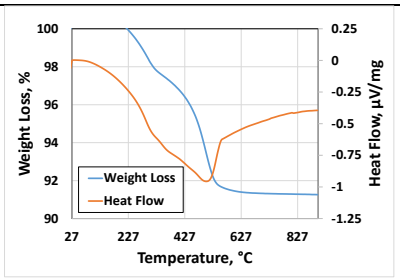

(E) E17 Outlet

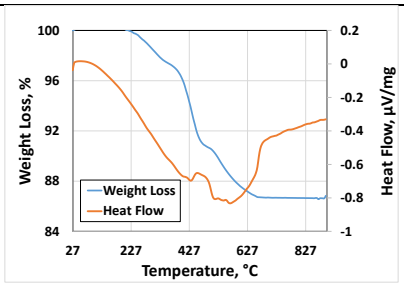

(E) E18 Inlet

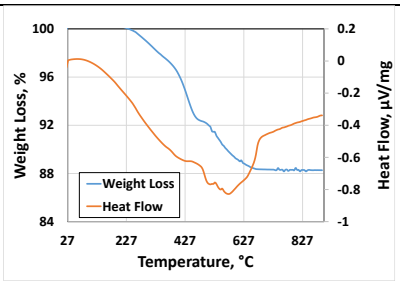

(E) E18 Outlet

Fig. C.9 - TGA-DTA curves for spent rock samples for Set 3 (Clay2 Experiments)

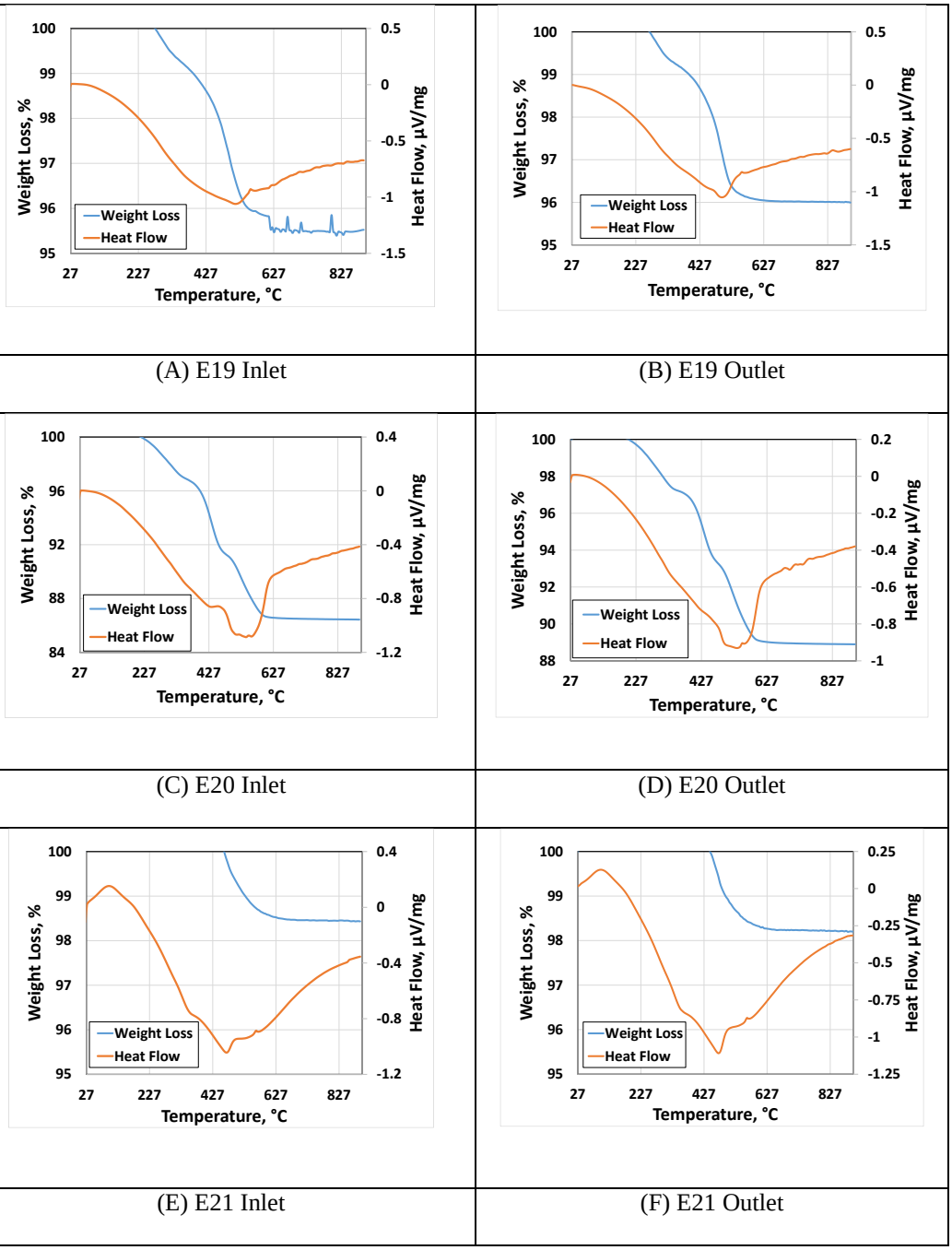

Fig. C.9 Continued - TGA-DTA curves for spent rock samples for Set 3 (Clay2 Experiments)

APPENDIX D

DIELECTRIC CONSTANT CALCULATIONS

Table D.1 - Density and dielectric constant values of individual components

Component	Density (g/cc)	Dielectric Constant (ϵ)
Water	1	80
DAO	1.1	2.52
Asphaltenes	1.42	3.80
n-pentane	0.626	1.76
n-hexane	0.655	1.80
n-heptane	0.684	1.82
Toluene	0.862	2.38

Example Calculation

DAO+ Toluene Mixture

Mass of DAO = 84 mg = 0.076363636 cc

Mass of Toluene = 2178 mg = 2.526096033 cc

Volume fraction of DAO = 0.02934287

Volume fraction of toluene = 0.97065713

ϵ-Theory = 2.384108002

ϵ-Measured = 3.62

% Difference = 51.83875887

APPENDIX E

REPEATABILITY OF SAGD EXPERIMENTS

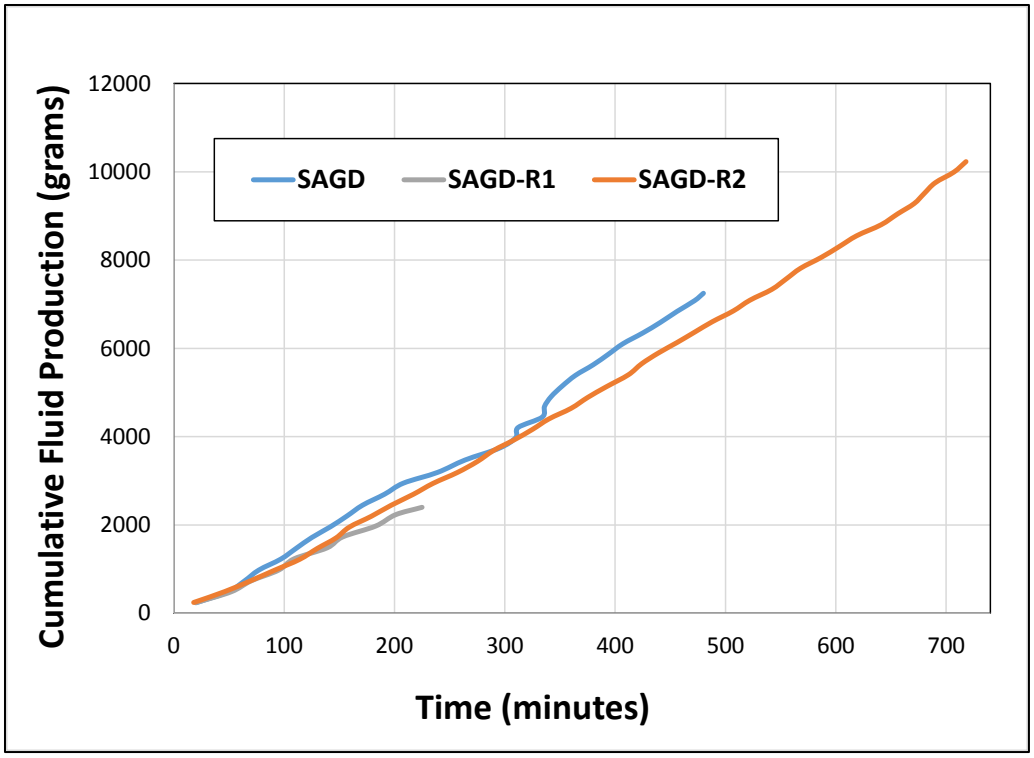

Fig. E.1 - Cumulative fluid production from three SAGD experiments all showing similar increment in production with experimental time